

Sheffield Hallam University

Experiments in human multi-robot systems.

SAEZ-PONS, Joan.

Available from the Sheffield Hallam University Research Archive (SHURA) at:

<http://shura.shu.ac.uk/20309/>

A Sheffield Hallam University thesis

This thesis is protected by copyright which belongs to the author.

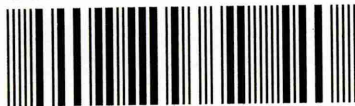
The content must not be changed in any way or sold commercially in any format or medium without the formal permission of the author.

When referring to this work, full bibliographic details including the author, title, awarding institution and date of the thesis must be given.

Please visit <http://shura.shu.ac.uk/20309/> and <http://shura.shu.ac.uk/information.html> for further details about copyright and re-use permissions.

Learning and Information Services
Adsett's Centre, City Campus
Sheffield S1 1WD

102 113 348 5



REFERENCE

ProQuest Number: 10700955

All rights reserved

INFORMATION TO ALL USERS

The quality of this reproduction is dependent upon the quality of the copy submitted.

In the unlikely event that the author did not send a complete manuscript and there are missing pages, these will be noted. Also, if material had to be removed, a note will indicate the deletion.



ProQuest 10700955

Published by ProQuest LLC (2017). Copyright of the Dissertation is held by the Author.

All rights reserved.

This work is protected against unauthorized copying under Title 17, United States Code
Microform Edition © ProQuest LLC.

ProQuest LLC.
789 East Eisenhower Parkway
P.O. Box 1346
Ann Arbor, MI 48106 – 1346

Experiments in Human Multi-Robot Systems

Joan Saez-Pons

A thesis submitted in partial fulfilment of the requirements of
Sheffield Hallam University
for the degree of Doctor of Philosophy

November 2011

Sheffield Hallam University
Centre for Automation & Robotics Research, MERI

The undersigned hereby certify that they have read and recommend to the Faculty of Arts, Computing, Engineering and Sciences for acceptance a thesis entitled “**Experiments in Human Multi-Robot Systems**” by **Joan Saez-Pons** in partial fulfillment of the requirements for the degree of **Doctor of Philosophy**.

Dated: November 2011

Research Supervisors: _____
Dr. Lyuba Alboul

Dr. Jacques Penders

Examining Committee: _____
Dr. Martin Beer

Dr. Alan Winfield

Sheffield Hallam University

Date: **November 2011**

Author: **Joan Saez-Pons**

Title: **Experiments in Human Multi-Robot Systems**

Department: **Centre for Automation & Robotics Research, MERI**

Degree: **Ph.D.** Convocation: **28th November** Year : 2011

Permission is herewith granted to Sheffield Hallam University to circulate and to have copied for non-commercial purposes, at its discretion, the above title upon the request of individuals or institutions.

THE AUTHOR ATTESTS THAT PERMISSION HAS BEEN OBTAINED FOR THE USE OF ANY COPYRIGHTED MATERIAL APPEARING IN THIS THESIS (OTHER THAN BRIEF EXCERPTS REQUIRING ONLY PROPER ACKNOWLEDGEMENT IN SCHOLARLY WRITING) AND THAT ALL SUCH USE IS CLEARLY ACKNOWLEDGED.

Signature of Author

Copyright of the thesis remains with the author. All other intellectual rights embodied in the submission pieces are owned by Sheffield Hallam University. The physical copies of the thesis submitted become the property of Sheffield Hallam University, whilst other artefacts remain the personal property of the author.

Aknowledgements

The work was undertaken as part of the GUARDIANS Project; run by the Centre for Automation and Robotics Research, Materials and Engineering Research Institute, Sheffield Hallam University, Sheffield, UK. A studentship paid the bills.

After a so great experience I obviously have many people to thank. Thanks to my supervisors Lyuba Alboul and Jacques Penders, to Georgios Chliveros and Amir Naghsh for supervision of me and the work, to Leo Nomdedeu who provided a valuable assistance in the dark debugging days, and to Martin Beer and Alan Winfield for their valuable comments on the review.

Thanks to all friends and family in La Ràpita who always challenged me to explain what my research was about in plain words, to Jose, Moh and Willie for the stupid late nights in Sheffield, to the countless friends I left in Slovenija, and to everybody who I will hardly see again but I won't ever forget.

Last and most thanks goes to Polona for everything.

Joan Saez-Pons, La Ràpita, November 2011.

Abstract

This thesis seeks to determine the constraints on the possible coordination control for systems composed of a human and group of mobile robots. In particular the constraints imposed by real-time action, robustness and human safety. We intend to put forward the findings on the first (to the best of the author's knowledge) real-world human / multi-robot system that achieves a complex navigation task.

The focus is on the development of an autonomous robotic system to create a flexible formation of a group of mobile robots around a human in an unconstrained environment. A suitable environment, robot platforms, control architecture and experimental set-up are described.

The robots are virtually linked to each other by application of artificial potential forces that create and maintain a flexible formation. The robots accompany a human, who is an integral part of the team, through a known environment which may contain obstacles. Each robot is capable to detect the position of the robot peers, the human, and obstacles within the sensor range. All robots attempt to maintain specified distances to the human and to every other member of the group, as a result of attractive / repulsive forces. The procedure guarantees cohesion of formation whilst avoiding collisions among participating components.

The control procedure is achieved by generating a minimal generic control model and next devising the required robot controller. By virtue of our methodology, we first test and refine our controller through simulation, followed by a set of experiments carried out in real-world environments to quantify the performance and reliability of the method. We provide performance metrics that illustrate: (a) comparison of the utility of different control methods, (b) examination of trade-offs between different metrics, and (c) details the method of comparison for future research in this area. The refined model / controller, based on these metrics, is shown to be more successful and reliable.

Contents

Aknowledgements	v
Abstract	vi
List of Tables	x
List of Figures	xi
1 Introduction	1
1.1 The Guardians project	1
1.2 Goal	2
1.3 Contribution	2
1.4 Thesis outline	3
2 Related Work	5
2.1 Introduction	5
2.2 Multi-Robot Systems	5
2.2.1 Applications	6
2.2.2 Decentralised vs. centralised	8
2.3 Formation Control	10
2.3.1 Behaviour-based	10
2.3.2 Leader-follower	12
2.3.3 Graph theoretical and geometrical approaches	14
2.3.4 Virtual physics	15
2.4 Approach: HMRS navigation	17
2.5 Conclusions	18
3 Aim and test criteria	20
3.1 Aim	20
3.2 Our formation definition	22
3.3 Performance evaluation	26

3.3.1	Metrics for the formation experiments	26
3.3.2	Common metrics in related work	27
3.3.3	Our formation metrics.	28
4	Experimental Design and Implementation	30
4.1	Experimental design	30
4.1.1	The system	30
4.1.2	Grounded Mobile Robots	32
4.1.3	Simulation	34
4.2	Real-world experiments	44
4.2.1	Distributed software architecture	44
4.2.2	Initial experiments	46
4.2.3	Human follower	48
4.3	Scope and limitations	49
4.4	Summary	51
5	Formation Control I	53
5.1	Hypothesis	54
5.2	Algorithm	55
5.3	Control Model	56
5.4	Simulation trials	58
5.4.1	Procedure	58
5.4.2	Example Simulated Trial	59
5.4.3	Results	60
5.5	Real-world trials	64
5.5.1	Procedure	64
5.5.2	Results	65
5.6	Discussion	68
5.7	Conclusions	69
5.8	Further Work	69
6	Formation Control II	71
6.1	Hypothesis	72
6.2	Algorithm	73
6.3	Control Model	75
6.4	Simulation trials	76
6.4.1	Example Simulated Trial	76
6.4.2	Results	77

6.5	Real-world trials	81
6.5.1	Procedure	81
6.5.2	Results	81
6.6	Discussion	84
6.7	Conclusions	86
7	Discussion	87
7.1	Comparison	87
7.1.1	Simulated vs real-world results	87
7.1.2	FCI vs FCII	88
7.2	What if more obstacles are considered?	89
7.3	What is the suitable value for the maximal tolerance ε_d ?	92
7.4	Considerations about HMRS behaviour	95
7.4.1	What is the influence of the sensor boundary size?	95
8	Conclusions	101
A	Parameters selection	104
A.1	FCI	104
A.2	FCII	107
B	Figure trials for FCI	110
C	Figure trials for FCII	121
	References	132

List of Tables

- 4.1 Base Characteristics of the ERA-MOBI robot. 34
- 4.2 URG-04LX laser range finder specifications. 38
- 4.3 Typical parameters of the human model. 40

- 5.1 Terminology. 54
- 5.2 Values of the parameters for FCI. 58
- 5.3 Summary of results for FCI simulation trials. 61
- 5.4 Summary of results of the FCI trials in real-world. 68

- 6.1 Terminology. 71
- 6.2 Values of the parameters for FCII. 76
- 6.3 Summary of results for FCII simulation trials. 78
- 6.4 Summary of results of the FCII trials in real-world. 84

- 7.1 Performance metrics: mean (standard deviation). 88

List of Figures

2.1	Examples of experiments with MRS.	7
3.1	Overall system.	21
3.2	General distributed control framework	21
3.3	Formations examples.	25
4.1	General situation.	31
4.2	Multi-Robot 2D overhead tracking system.	32
4.3	ERA-MOBI robot carrying a PC and URG-04LX.	33
4.4	Simulations using NetLogo.	35
4.5	Player Stage Hardware Abstraction.	37
4.6	Conventions for describing robot pose.	38
4.7	Model of human.	39
4.8	View of the simulation software.	40
4.9	Scheme for static obstacles' classification.	41
4.10	Fiducial interface.	42
4.11	Segmentation of the laser information.	42
4.12	Occlusion of an element by another element.	43
4.13	Coordinator agent communication scheme.	45
4.14	Initial implementation of the distributed system architecture.	46
4.15	Initial obstacle avoidance trials.	48
4.16	First step: finding the human.	49
4.17	Second step: Sequence of the human tracking.	50
5.1	Convention for differentiating repulsive and attractive forces.	57
5.2	Example of the FCI in a simulated trial.	59
5.3	Trial 5 of the FCI in simulation (highest <i>%tif</i>).	62
5.4	Trial 9 of the FCI in simulation (lowest <i>%tif</i>).	63
5.5	Real-world trial.	65
5.6	Trial 5 of the FCI in the real-world.	66

5.7	Trial 9 of the FCI in the real-world.	67
6.1	Robots acting under FCI.	72
6.2	Example of the FCII in a simulated trial.	77
6.3	Best case. Trial 5 of the FCII in simulation.	79
6.4	Worst case. Trial 9 of the FCII in simulation.	80
6.5	Best case. Trial 5 of the FCII in the real-world.	82
6.6	Worst case. Trial 4 of the FCII in the real-world.	83
7.1	Simulation versus Real-world trials performance metrics in FCI.	88
7.2	Simulation versus Real-world trials performance metrics in FCII.	89
7.3	The performance metrics of FCI versus FCII for Simulation trials.	90
7.4	The performance metrics of FCI versus FCII for Real-World trials.	90
7.5	Distance measurements with the laser range finder.	91
7.6	Maximal tolerance for Simulation trials in FCI.	93
7.7	Maximal tolerance for Real-world trials in FCI.	94
7.8	Maximal tolerance for Simulation trials in FCII.	94
7.9	Maximal tolerance for Real-world trials in FCII.	95
7.10	Behaviour pattern of a group of robots without a human and obstacles.	97
7.11	Behaviour pattern of the human multi-robot system.	97
7.12	Behaviour pattern in the presence of an obstacle.	98
7.13	Clustering of robots with limited sensor boundary.	98
7.14	A connected group with limited sensor boundary.	99
7.15	Robots ‘escape’ the trap of the C -concave obstacle.	100
A.1	Robot-obstacle artificial force.	105
A.2	Robot-peer artificial force.	106
A.3	Robot-robot artificial force.	107
A.4	Robot-human artificial force.	108
B.1	Trial 1 of the FCI in simulation.	110
B.2	Trial 2 of the FCI in simulation.	111
B.3	Trial 3 of the FCI in simulation.	111
B.4	Trial 4 of the FCI in simulation.	112
B.5	Trial 5 of the FCI in simulation.	112
B.6	Trial 6 of the FCI in simulation.	113
B.7	Trial 7 of the FCI in simulation.	113
B.8	Trial 8 of the FCI in simulation.	114
B.9	Trial 9 of the FCI in simulation.	114

B.10	Trial 10 of the FCI in simulation.	115
B.11	Trial 1 of the FCI in real-world.	115
B.12	Trial 2 of the FCI in real-world.	116
B.13	Trial 3 of the FCI in real-world.	116
B.14	Trial 4 of the FCI in real-world.	117
B.15	Trial 5 of the FCI in real-world.	117
B.16	Trial 6 of the FCI in real-world.	118
B.17	Trial 7 of the FCI in real-world.	118
B.18	Trial 8 of the FCI in real-world.	119
B.19	Trial 9 of the FCI in real-world.	119
B.20	Trial 10 of the FCI in real-world.	120
C.1	Trial 1 of the FCII in simulation.	121
C.2	Trial 2 of the FCII in simulation.	122
C.3	Trial 3 of the FCII in simulation.	122
C.4	Trial 4 of the FCII in simulation.	123
C.5	Trial 5 of the FCII in simulation.	123
C.6	Trial 6 of the FCII in simulation.	124
C.7	Trial 7 of the FCII in simulation.	124
C.8	Trial 8 of the FCII in simulation.	125
C.9	Trial 9 of the FCII in simulation.	125
C.10	Trial 10 of the FCII in simulation.	126
C.11	Trial 1 of the FCII in real-world.	126
C.12	Trial 2 of the FCII in real-world.	127
C.13	Trial 3 of the FCII in real-world.	127
C.14	Trial 4 of the FCII in real-world.	128
C.15	Trial 5 of the FCII in real-world.	128
C.16	Trial 6 of the FCII in real-world.	129
C.17	Trial 7 of the FCII in real-world.	129
C.18	Trial 8 of the FCII in real-world.	130
C.19	Trial 9 of the FCII in real-world.	130
C.20	Trial 10 of the FCII in real-world.	131

Chapter 1

Introduction

1.1 The Guardians project

Industrial warehouses in the emergency of a fire are a major concern for fire fighters. In the warehouse fire of 1991 in Gillender Street London (UK) ¹, two fire fighters died and in the 1999 warehouse fire in Worcester (USA), six fire fighters lost their lives ². And recently in November 2007 a tragedy happened in Warwickshire (UK), when four fire fighters were killed in a vegetable warehouse blaze.

As pointed out by the South Yorkshire Fire and Rescue (Penders et al., 2007) in the UK, searching for victims or for the fire source in an industrial warehouse represents a major challenge due to the large dimensions of the area to explore combined with the development of dense smoke. The Guardians³ (Group of Unmanned Assistant Robots Deployed In Aggregative Navigation by Scent) is an FP6, EU funded project developing a group of autonomous mobile robots designed to assist fire fighter in searching a large warehouse as the central application ⁴. A major role of the autonomous mobile robots in the aforementioned situation is to support fire fighters searching the warehouse by enhancing the human's navigation. The user requirements are diverse but basically in order to support fire fighters the mobile robots have to provide and maintain mobile communication links, detect and warn for toxic chemicals, and assist in searching.

¹www.yorkshirepost.co.uk/news/around-yorkshire/local-stories/hi_tech_miniature_robots_set_to_be_latest_firefighting_recruits_1_2419969

²en.wikipedia.org/wiki/Worcester_Cold_Storage_Warehouse_fire

³www.shu.ac.uk/research/meri/research/guardians-project

⁴www.sciencemuseum.org.uk/antenna/firefightingrobots/

1.2 Goal

The research described in this thesis concerns the coordination control of robotic systems composed by a human and a group of robots, Human Multi-Robot Systems (HMRS). In particular, the research aims to develop a real-world robotic system to control a group of autonomous robots to navigate with a human in an unconstrained environment.

During the proposal stage of this thesis it was observed that practically no research had been done in the field of HMRS. However, Multi-Robot Systems (MRS) are widely studied and the literature in this field is extensive (Parker, 2000). Hence previous research in MRS will help us to gain an insight into HMRS. Therefore, when considering a group of robots to navigate with a human, some *research questions* arise.

1. Seeking simplicity yet reliability through local sensing, *what distributed control framework for human multi-robot navigation can be employed?*
2. In order to compare among methods and algorithms, *what sort of exemplary metrics can be utilised?*
3. For being capable of making use of the aforementioned metrics, *what systematic and practical definition of formation can be laid out?.*

1.3 Contribution

This section enumerates the published papers in journals and conferences that report aspects of the work and includes a short description of the contribution to each.

- In (Saez-Pons et al., 2010) the formation of a group of robots and human for the GUARDIANS projects is introduced. The contribution to this paper includes aspects of the formation control and generation, the control model using artificial potential functions, stability considerations, implementation in simulation and real-world experiments and presents some preliminary results.
- The contribution in (Saez-Pons et al., 2011a) is to solve the key problem of including a human in a real multi-robot system and consequently the multiple robot motion coordination. This paper also presents the set of performance metrics used in this thesis (system efficiency and percentage of time in formation) and the novel flexible formation definition. Some results are as well presented whereby the formation control proposed is stable and effective by means of its uniform dispersion, cohesion and flexibility.
- In (Saez-Pons et al., 2011b) the human multi-robot system is integrated with a real-world application where the group of autonomous mobile robots is used to guide a real fire fighter using a centered designed human-robot interaction. The contribution to this work includes

aspects of the formation control of the robots, the implementation and testing of the real-world application.

- (Penders et al., 2011) reports a robot swarm assisting a human fire fighter. The contribution in this work concerns findings in the non communicative swarming behaviours, including the formation control model, human-swarm formation and real-world implementations.
- I contributed as well in (Naghsh et al., 2010) that describes a real-world demonstration involving in-situ interaction between a team of robots and a fire fighter, and interaction between a remote operator and the whole system from a base station. The contribution includes the software system architecture, the formation control of the robot team and the real-world implementation of the experiments.
- The contributions in the early works in (Saez-Pons et al., 2009, 2008; Alboul et al., 2008, 2009, 2010b) include the general problem statement, definitions of the artificial potential functions equations, qualitative remarks on stability, early simulations results and analysis of different possible formation situations.

1.4 Thesis outline

Chapter 2: Related work

Material from many fields will provide a solid starting point for this research, including work from biology-inspired, graph theoretical and geometrical approaches, and both physics-based and behavioural robotics research. Among the formation control strategies reviewed in this chapter, the Social Potential Fields method has been chosen as the initial control framework for the navigation of the HMRS, due to its simplicity yet reliability. Nevertheless, other methodologies are very useful and provide valuable insights when discussing our work on formation control.

Chapter 3: Aim and Test Criteria

This chapter provides an overview of the framework for distributed formation control of a group of robots to navigate with a human, the Social Potential Field method, which belongs to the group of “virtual physics”. A suitable formation definition will be presented, where in our case, formation can be defined as a group of agents establishing and maintaining a certain *flexible configuration*. The configuration does not have a predefined shape but the robots have to stay close to each other and adapt to the geometrical constraints of the environment. Thereafter, in order to compare the performance of different experiments and methods, exemplary metrics are selected in this chapter considering the common metrics used in related works.

Chapter 4: Experimental design and implementation

This chapter describes the experimental set-up: the distributed robotic system, the hardware employed during the experiments and the software architecture developed to enable the real-world implementation. Moreover, in this chapter a description of the simulation software is provided, including the mobile robots and human models, the method to detect the surrounding obstacles, the simulation environment and the description of the control model employed for the simulation experiments.

Chapter 5 & 6 : Experiments

In Chapter 5 a simple social potential field method is proposed as the robot control strategy. It is found that this method generates a formation in both simulation and real-world experiments, and the formation is maintained with the human in movement. Results of several trials are presented and metrics are devised to assess performance. The identical controller is run on the real robots and tested in a real-world environment. Performance metrics showed that in the real world this method is less reliable than in simulation, but does demonstrate a multi-robot control to navigate with a human. In chapter 6, consideration of these results leads to an improved strategy based on combining the social potential fields method with the behavior-based approach. This improved method is found to be superior in simulation and real-world experiments prove to be far more successful and reliable than with the original.

Chapter 7: Discussion and open problems

This chapter further examines the results from the previous experimental chapters making some comparisons between simulations and real-world trials and among methods. The abilities and limitations of the algorithms and experiments are discussed, and some questions and criticisms encountered in the course of the work are addressed.

Chapter 8: Conclusions

Finally, the conclusion compares the stated goals to the results. It is confirmed that the stated hypotheses are proven, and that this work does indeed demonstrate the effective control of a group of robots generating and maintaining a formation with a human. This thesis provides a methodology, an appropriate multi-robot and control architecture for experiments in human multi-robot systems. We propose different strategies for the control of the navigation of a group of robots to move accordingly with a human's movement. Opportunities for extending the abilities of this multi-robot system are discussed, along with suggestions for future human multi-robot projects.

Chapter 2

Related Work

2.1 Introduction

In the recent years, considerable research efforts have been conducted towards *Multi-Robot Systems* (MRS). The appeal for this discipline is sufficiently supported by the plethora of advantages that these systems present with respect to single autonomous robots and well backed up by the advancements in robot technologies. A human could as well broadly benefit in several applications (e.g. search and rescue missions, exploration, guidance, object transportation, etc.) by *cooperating* with a group of autonomous robots, but practically no research has been done in this field. However, MRS are being widely studied and the literature in this field is extensive, hence previous research in MRS will help to gain an insight into Human Multi-Robot Systems (HMRS). The literature in MRS includes many aspects that makes it difficult to provide a comprehensive description; nonetheless, in this chapter we will present a selection based on what is useful for us. We will present an overview of the main issues and applications for MRS followed by the state of the art of the existing formation control methodologies. Finally, based on the existing literature on formation control of MRS, this chapter selects a suitable formation control approach for HMRS.

2.2 Multi-Robot Systems

Generally speaking, the term *Multi-Robot System* (MRS) (Parker, 2000) embraces distinct typologies of robotic systems, e.g., mobile robots with on board robot arms, multiple industrial manipulators, or a team of autonomous robots. In this thesis, MRS will be employed referring to *a team of cooperative autonomous ground mobile robots*. The word *cooperative* in the MRS literature emphasises the interaction of a group of robots, in terms of communication, information exchange to execute a global mission. The meaning of cooperation has been broadly discussed in the scientific community and different definitions have been proposed (Cao et al., 1995). In (Barnes and Gray,

1991) cooperation has been defined as “a joint collaborative behaviour that is directed towards some goal”. In (Mataric, 1997) cooperation is defined as “a form of interaction, usually based on communication” and in (Pomet et al., 1992) is described as “joining together for doing something that creates a progressive result”. The first definition underlines the study of task decomposition, task allocation (Gerkey and Mataric, 2003), and other distributed artificial intelligence issues; the second leads to the requirements of communication or other common resources; the third is related to the performance measurements of cooperation (e.g. time to complete the task, flexibility, robustness, etc.), the latter definition is further worked out and used in this thesis.

The reasons for employing MRS widely vary (Parker, 2003); nonetheless, the main reason for using MRS is to improve system effectiveness. Particularly, concerning with a single autonomous robot or with a team of non collaborating robots, a MRS can improve mission performance in terms of time and quality, can perform tasks not achievable by a single robot (e.g., moving a large object) or can benefit from distributed sensing and actuation. Furthermore, the components of a multi-robot system can be robots with simpler functionalities, and therefore cheaper robots, can provide flexibility to mission execution and introduce redundancy making the solution more fault-tolerant (Winfield and Nembrini, 2006) than having and using a single powerful and expensive robot.

MRS are characterised by multiple aspects in terms of control architectures, algorithms, communication structures, resource conflicts, mechanisms of cooperation, learning or differentiation among robots of the team. Hence, the progress of the research in cooperative robotics has concerned most of these aspects simultaneously, frequently proposed by the scientific community in an combined form. Despite that this strong correlation makes difficult to classify MRS based on individual aspects, several works have been developed only to present a taxonomy valid for the field. In (Dudek et al., 1996) a taxonomy for multi-agent robotic systems is proposed depending on the size of the team (how many robots compose the team), the communication parameters (communication range, topology and bandwidth) and the reconfigurability of the team (homogeneous vs. heterogeneous robots). A more recent work (Farinelli et al., 2004) presents a classification based on different levels of coordination (unaware, aware but not coordinated, weakly coordinated, strongly coordinated systems) and introduces a classification based on the so-called *coordination dimensions* (cooperation, knowledge, coordination, organization) and *system dimensions* (communication, team composition, system architecture and team size). Finally, the work in (Gerkey and Mataric, 2003) presents a taxonomy based on multi-robot coordination mechanisms and on task allocation.

2.2.1 Applications Considerable work in cooperative mobile robotics has biological inspirations, imitating social characteristics of insects and animals, upon the pioneering work by (Reynolds,

1987), who simulated a flock of birds in flight (using a behavioural model based on a few simple rules and only local interactions). In parallel the robotics paradigm of behaviour-based control (Arkin, 1987; Brooks, 1986) was introduced. This paradigm has been useful for robotics researchers to examine the social characteristics of insects and animals, and to apply these findings to the design of multi-robot systems. The most common application is the use of elementary control rules of various biological animals (Reynolds, 1987; Holland and Melhuish, 1999)(e.g., ants, bees, birds and fishes) to reproduce a similar behaviour (Balch and Arkin, 1998) (e.g., foraging, flocking, homing, dispersing) in cooperative robotic systems. However, the main behaviour-based approaches applied to formation control will be discussed in the next section.

The applications of MRS are diverse. There are MRS made up of grounded mobile robots, autonomous robots with wheels or crawlers, built both for indoor environments, i.e., museums, laboratories and buildings (Howard et al., 2006; Parker et al., 2004) or outdoor environments, i.e., open space, grass or bulky floor (Carpin and Parker, 2002; Maxim et al., 2008). In the recent years, applications with different sorts of vehicles have been developed, e.g., different MRS composed of Underwater Autonomous Vehicles (Fiorelli et al., 2004; Stilwell and Bishop, 2000), experiments and control methods with Unmanned Aerial Vehicles (Beard et al., 2006; Gurfil and Kivelevitch, 2007; Ben-Asher et al., 2008; Liu and Passino, 2006) and formation control of marine crafts (Ihle et al., 2004).

MRS applications have been developed in different fields (e.g., military, service and industrial robotics, or study of biological systems) and have been involved in many different applications (Figure 2.1) (e.g., box-pushing, exploration, navigation, traffic control, entertainment and area coverage).



(a) A group of robots pushing a box (Gerkey and Mataric, 2002)



(b) A robot team in square formation (Lee and Chong, 2006)

Figure 2.1: Examples of experiments with MRS.

Several industrial applications, for example, refer to the possibility of moving large objects

using a number of robots (with or without manipulators). Actually, a single robot, may not be capable to move by itself a heavy large object but a MRS may be used, hence, sharing the power requirements among different robots and using multiple contact points. On the other hand, a multi-robot solution may need an accurate robot coordination, e.g., sharing information about their relative positions and the shape and position of the object. Different MRS have been presented to achieve this sort of mission, e.g., in (Mataric et al., 1995) some experimental results of box pushing using two mobile robots are developed (Figure 2.1a), in (Yamada and Saito, 2001) a team of differential-drive mobile robots execute the box-pushing mission without explicit communication, and the work in (Wang et al., 2003a) presents a cooperative object handling with multiple mobile robots based on function distribution and behaviour design.

Exploration and map building is another type of application for a team of cooperating robots. To perform this mission cooperatively, the group of robots have to explore different parts of the environment with some sort of coordination and share the obtained partial maps by each single robot for being able to build a global map; consequently a group of robots can explore and build a map of the environment much faster than a single robot. Simultaneously, each robot has to localise itself in the environment and merge the partial maps obtained. This sort of application, know as *Simultaneous Localization and Mapping* (SLAM), has been extensively researched and different solutions have been proposed, e.g., in (Burgard et al., 2005), a group of three heterogeneous robots is used to reduce exploration time in a situation where the communication ranges of the robots are limited. In (Rekleitis et al., 2000), a two robot team collaborate to explore and map a large area whereas sensing each other reduce odometry errors and avoid obstacles with low reflectance characteristics.

Other applications where a group of robots have been applied include military operation solutions (e.g., surveillance and rescue missions (Balch and Arkin, 1998; Chaimowicz et al., 2004), land mine detection (Santana et al., 2005)), chemical or biological plume source tracing (Zarzhitsky et al., 2005), soccer robots for the popular robocup (Vail and Veloso, 2003; Laue and Rofer, 2004), the well-known robocup rescue applications ¹ and network coverage (Das et al., 2002a; Sibley et al., 2002; Wang et al., 2003b).

Among the whole plethora of applications the most relevant to our work are those related to social based robotics and multi-robot navigation.

2.2.2 Decentralised vs. centralised In the literature the main distinction in MRS is made between centralised and decentralised systems (Cao et al., 1997). In centralised systems, a central unit gathers and manages environmental information to coordinate and control the robot's motion

¹<http://www.robocuprescue.org/>

and to guarantee the mission's success. In these systems, the central unit plays a crucial role because it governs the whole system, i.e., it has to coordinate the obtained information by the distributed sensors or to manage global environmental information, to make all the decisions and to communicate with all the robots of the team; thus, it should be powerful enough to satisfy all the technological requirement. In decentralised systems, instead, the resources are distributed among all the robots. Each vehicle uses its own sensors to extrapolate local information of the environment and the relative positions of close by robots to take its own decisions; moreover, each robot can communicate and share information only with nearby robots and it is aimed at achieving only a part of the global mission.

Advantages and disadvantages of centralised and decentralised systems have been widely discussed in the scientific community. Centralised systems, for example, can manage global environmental information and optimise the coordination among the robots or the mission's achievement; moreover, they are robust to faults of some of the vehicles. On the other hand, the central unit may represent the weak point of the system, actually, the central unit might be the bottle-neck of the system both for computational and communication time requirements; additionally, its eventual flaw puts in jeopardy the whole system. Decentralised systems, instead, permit to exploit distributed sensing and actuation, i.e., to utilise less powerful robots or to employ more, cheaper sensors; they allow to optimise the allocation of the resources and to equip the robots of the team with different actuation and sensor systems; moreover, decentralised systems are tolerant to possible robot faults (Winfield and Nembrini, 2006). On the other hand, within decentralised systems it is complex to coordinate the robots and optimise the execution of the mission, and issues like global localization and mapping, and communication bandwidth represent limits of this system.

In practice, there are many systems that are not strictly centralised or decentralised. In fact, different hybrid centralised/decentralised architectures have been provided to take partial advantages of both the typologies (e.g., the hybrid architectures in (Beard et al., 2001; Desai et al., 1998; Das et al., 2002b) have central planners that perform an high-level control over mostly autonomous robots).

As a result, we have learnt that the usage of MRS is motivated (among others) mainly to improve system effectiveness. A human could broadly benefit from cooperating with a group of autonomous robots in a variety of applications, however for that to happen an architecture must be properly selected and laid out. When considering a robotics system composed of a human and group of robots it is straightforward to conclude that the selected method must not be centralised (Saez-Pons et al., 2010). Moreover, it is fundamental to decide the sort of control mechanism for the system, that will be discussed in the following section.

2.3 Formation Control

“Formation control is the initial step toward real world implementation of cooperative robotics” (Lee and Chong, 2006). The problem of formation control for groups of robots presents many issues which must be taken into consideration such as formation definition, generation, keeping, scalability, robustness and environmental constraints. In previous works, to generate a specific formation by a team of robots many methodologies have been developed. They can be divided mainly in behaviour-based approach, leader-follower strategy, graph theoretical and geometrical approaches, and control based on virtual physics. Next we will describe in more detail each method.

2.3.1 Behaviour-based Initially behaviour-based control was employed to create global behaviours in a group of mobile robots from the combination of simple behaviours. Work has demonstrated the ability for multi-robot teams to flock, disperse, forage, and homing (Mataric, 1994). In (Kube and Zhang, 1992), as few as two basic, local behaviours (avoidance and goal seeking) were shown in experiments with five physical robots to be enough to result in a successful collaborative box-pushing behaviour. Similar work is presented in (Ijspeert et al., 2001), where a group of simulated robots were able to cooperatively pull a stick. (Mataric et al., 1995) showed how a set of simple behaviours (avoidance, aggregation, and dispersion), based on local sensing only, can be combined so that a global flocking behaviour emerges, and demonstrated the behaviours on a group of 13 mobile robots. (H. Ando, 1995) presented theoretical work where a large set of robots, represented as points in the plane, congregated at a single position. Moving synchronously in discrete time steps, robots iteratively observed neighbours within some visibility range, and followed simple rules to update their position.

Furthermore, behaviour-based approach has been applied to the robot deployment problem or coverage (Gage, 1992), in some respects similar to the formation problem described in this thesis, in that the robots will attempt to achieve a static arrangement of nodes that maximises the total detection area (Werger and Matarić, 2001). The work in (Laue and Rofer, 2004) describes a behaviour-based architecture which integrates existing potential field approaches concerning motion planning as well as the evaluation and selection of actions into a single architecture. This combination allows, together with the concept of competing behaviours, the specification of more complex behaviours than the usual approach which is focusing on behaviour superposition and is mostly dependent on additional external mechanisms. A more recent work (Axelsson et al., 2006) presents an optimal solution for the problem of avoiding obstacles whilst progressing towards a goal for a simulated single robot. In particular, the solution is obtained by allowing the robot to switch between a fixed number of behaviours and optimizing over what behaviours to use and

when to switch between them.

In contrast to all these demonstrations, to generate a specific formation by a group of robots using a behaviour-based approach requires a more precise and reliable spatial structure. In (Sugihara and Suzuki, 1990), distributed algorithms: namely circle, contraction, and fillpolygon, were proposed. These algorithms are used to drive simulated robots to form a circle, a line segment, and evenly distributed in a convex polygon. In (Sugihara and Suzuki, 1998), a group of simulated robots formed approximations to circles and simple polygons, using global knowledge of all robots' positions. Each robot oriented itself to, e.g., the furthest and nearest robot. In (Chen and Luh, 1994), a similar setup was presented, but group motion was also considered, e.g., a matrix formation performing a right turn. Some researchers then developed specific algorithms to let robots form a specific geometric pattern (Lee et al., 2004), where three algorithms named Algorithm L, Algorithm C, and Algorithm P/n were proposed to generate formations of line, circle, and regular polygon with n edges.

In (Balch and Arkin, 1998) a behaviour-based control law was proposed to regulate the movement of a team of robots. Several basic behaviours were defined and integrated by different weightings. Robots superposing these behaviours then formed formations like column, wedge, and line. The work was demonstrated in experiments using physical robots with odometry, GPS, and global broadcast of the robots coordinates. In (Balch and Hybinette, 2000) the authors describe a behaviour-based approach to formations using simulated robots. The separate motor schema defined compute a vector for moving to the proper formation position, avoiding static obstacles, avoiding other robots and maintaining the current formation. Each robot builds a list of potential attachment sites and generates an attraction vector for the closest. In (Fredslund and Mataric, 2002), a general algorithm using local sensing and minimal communication was proposed. The robots were assigned unique IDs and a "friend" is defined to represent the relationship between any pair of robots. By the chain of friendships, robots can form formations like column, wedge, line, diamond, and circle.

A behavioural approach to robot formation control based on growing formations from simpler configurations (i.e single robots, line segments, etc.) into more complicated formations is presented in (Naffin and Sukhatme, 2004). By using simple local broadcast communications, they are able to dynamically reconfigure each robots role in formation as the formation grows. The approach is decentralised and requires only a single local sensor for each robot. In (Lemay et al., 2004) the author tackles the deployment of robot formation using a behaviour-based approach allowing to assign positions for robot having to move in various formation. Using only directional visual perception, the robots can initialize and establish a predetermined formation autonomously and distributively using the proposed hybrid control architecture.

In (Antonelli et al., 2008) a new behaviour-based approach for the control of autonomous robotic systems is proposed. The so-called null-space-based behavioural (NSB) control differs from the other existing methods in the behavioural coordination, i.e., in the way the outputs of the single elementary behaviours are combined to compose a complex behaviour. The proposed approach is compared with the main existing approaches whilst two experimental case studies, performed with a Khepera II mobile robot, are reported to validate its effectiveness.

Summarizing, the behavior-based control is constructed by the combination of simple behaviours to obtain a more complex global behaviour. This method has been shown to be easy to implement in real robots within many different applications. Nonetheless, the drawback of this method is to decide when to switch among a fixed number of behaviours in an optimised way. The behavior-based method is very useful and we will return to it when discussing our work on formation control.

2.3.2 Leader-follower The leader-follower strategy is also widely used for representing relationship between robots and used for generating formations. In (Bicho and Monteiro, 2003; Monteiro et al., 2004), the whole group of robots is decoupled into several pairs of robots. Each pair maintains a leader-follower relationship and each robot can then be a leader or a follower. The follower must track the designated relative velocity and angle from the leader for forming three basic formations: column, oblique, and line. The dynamics of designated relative velocity and angle were modeled as a non-linear system and the equilibrium velocity and angle are designed as attractors. More complex formation like a regular hexagon can be combined by the three basic formations. A dynamic systems approach to modeling and generating low-level behaviors for autonomous agents is presented in (S. Goldenstein and Metaxas, 1999). Such behaviors include real-time target tracking and obstacle avoidance in time-varying environments. The novelty of the method lies on the integration of distinct non-linear dynamic systems to model the agents interaction with the environment. In (Das et al., 2002b,a; Fierro et al., 2001; Tanner et al., 2004), robots identified their neighbour robots and environmental characteristics via computer vision. The whole group of robots was also decomposed into the leader-follower pairs. By maintaining specific separation and bearing between the leader and the follower, a basic leader-follower control can be achieved. In (Hsu and Liu, 2005), the authors used one simple representation combining robot ID and relative angle between robots to define formations. Leader-follower strategy was used in formation generation and keeping. Three agents: namely, user agent, robot agent, and virtual operator, were introduced in the formation control process. In (Alur et al., 2000), as part of the Leader-Following behaviour, each robot was controlled using local information, referencing itself to one neighbouring robot and maintaining a certain distance and angle to it. In an experiment with two physical robots, the follower (using computer vision and colour-blob tracking) kept

a fixed heading and distance to the leader.

Many researches related to formation maintenance have employed the method of leader-followers. Among them, (Gervasi and Prencipe, 2004) proposed a computational solution for the flocking problem with weaker assumptions on scheduling but with the ability of detecting multiplicity. In their study, the team is initially divided into a leader robot and followers. (Carpin and Parker, 2002) introduced a cooperative assistive navigation method in order to flock heterogeneous robot teams around a leader robot with a multitude of sensors.

Virtual leaders were used in (Leonard and Fiorelli, 2001) for coordinated and distributed control of various autonomous vehicles. A virtual leader is a moving reference point that influences vehicles in its neighbourhood by means of additional artificial potentials, whose are designed to enforce a desired inter-vehicle spacing. Virtual leaders can be used to manipulate group geometry and direct the motion of the group. Similarly, a leader-follower strategy was employed in (Parker et al., 2003) for deploying a team of mobile sensor nodes to form a sensor network in indoor environments. They use two types of helper robots one that acts as a leader and a second that: 1) acts as a follower and 2) autonomously teleoperates the mobile sensor nodes. The approach involves the use of line-of-sight formation keeping, which enables the follower robot to use visual markers to move the group along the path executed by the leader robot. Results were presented in simulation and partially on physical robot systems.

A leader-formation navigation strategy for multi-robot formation was employed in (Li and Chen, 2005), where a group of simulated robots have to keep certain shape passing through a special environment, members of the group have to change their relative positions in formation in order to avoid obstacles or to resume a predetermined formation shape after passing by. The local control strategy ensures the formation converges to the predetermined formation pattern even if interaction topologies are dynamic. A virtual leader approach to coordinated control of multiple mobile agents with asymmetric interactions is used in (Shi et al., 2005). They present a set of coordination control laws that enable the group to generate the desired stable flocking motion. By using the control laws, all agent velocities asymptotically approach the desired velocity, collisions are avoided between the agents, and the final tight formation minimises all agent global potentials. Numerical simulations were worked out to illustrate the theoretical results.

As a conclusion, the leader-follower strategy is widely used for generating formations based on establishing relationship between robots. However an important drawback is that the existence of a leader provokes to have robots with different roles among the group. Nonetheless, the leader-follower strategy is helpful and we will come back to it when discussing the work on formation control.

2.3.3 Graph theoretical and geometrical approaches In the related literature, many researchers used graph theory to represent a formation or model the relationship among robots. In (Krishnamurthy and Preis, 2005), the authors used basic concepts of graph theory to define a formation, and introduced the graph Laplacian (a representation of vertex-edge relationship) to analyze the linear dynamics of a group of satellites or vehicles. In (Olfati-Saber and Murray, 2002; Muhammad and Egerstedt, 2005), two special properties: graph rigidity and graph connectivity in graph theory were used to stabilise the dynamics of a multi-vehicle system and model the local interaction of a multi-robot system.

In (Desai et al., 2001) the authors use graph theory to control a team of nonholonomic mobile robots navigating in a terrain with obstacles whilst maintaining a desired formation and changing formations when required. Each robot was controlled using local information, either by referencing itself to one neighbouring robot and maintaining a certain distance and angle to it, the $l - \phi$ control, or to two neighbours and maintaining two fixed distances to those, the $l - l$ control. The algorithm was demonstrated in simulation. In (Lin et al., 2004), using graph-based control, three formation strategies for coordinated control of groups of mobile autonomous agents were studied. The simulated robots were modeled as point masses with no kinematic constraints of motion and had limited field of view.

In (Lewis and Tan, 1997), a formation is defined by a so-called virtual structure. The algorithm assumed that all robots had global knowledge; it iteratively fits the virtual structure to the current robot positions, displaced the virtual structure in some desired direction, and updated the robot positions. In (Tan and Xi, 2003; Tan et al., 2004), based on the relative distance between robots, a Voronoi diagram and its dual graph, Delaunay tessellation, can be constructed as a kind of virtual structure. By the structure of Voronoi diagram, robots can cover a certain area and perform search tasks by moving the whole group or forming specific formations. In (Lawton et al., 2003) a virtual structure approach to formations is described. The approach incorporates formation feedback where by the formation leader receives feedback from its followers allowing for stability guarantee. The robots roles were determined a priori and were static. The approach is validated in simulation as well as on physical robots. In (Ogren et al., 2004), the authors use a theoretical coordination framework based on virtual structure to gradient estimation and optimal formation geometry design and adaptation of a simulated mobile sensor network.

The work in (Chen and Li, 2006) addresses a formation navigation issue for a group of simulated mobile robots passing through an environment with either static or moving obstacles meanwhile keeping a fixed formation shape. Based on the Lyapunov function and graph theory, a NN formation control is proposed, which guarantees to maintain a formation if the formation pattern is C^k , $k \geq 1$. In the process of navigation, the leader can generate a proper trajectory to lead formation and avoid moving obstacles according to the obtained information. Graph theory

in (Mai and Lian, 2006) is used to model the physical relationship and information exchanging topology among robots. Considering effects of different information topologies, two theoretical scenarios with six robots in formation control problem are presented and discussed. Simulation studies of the two scenarios show that motion interaction of robots in formation control is affected by information interaction. Similar work is presented in (Wiegand et al., 2006) where graph-based swarm behaviours by specializing agents and their interactions. The method describes behaviours for multi-agent teams through explicit design decisions pertaining to specialization, heterogeneity, and modularity.

In a more recent work by (Cezayirli and Kerestecioglu, 2008) definitions adopted from the computational geometry are given to characterise the robot group. A local steering strategy is proposed such that when each robot in the group applies this steering scheme, the overall result is that the whole group is displaced without losing its connectivity. This is achieved using only limited-range position sensors and without any communication between the robots. And finally, a distributed control algorithm, based on a geometric approach, for simulated swarm robots is demonstrated in (Xiang et al., 2009). Robots negotiate their environment and dynamically show a collective behaviour such as flocking and obstacle avoidance. For instance to overcome an obstacle robots may, directly, go through or move around the obstacle as a whole whilst maintaining a uniform distance from each other. A geometric approach and simplified virtual physical mechanism for obstacle avoidance is combined.

In our work we will use graph theoretical and geometrical approaches to define our notion of robot formations. The formation is represented by a connected graph, whereas nodes are robots or a human and edges are virtual links between the nodes, with a property that each edge is situated in the intersection of the sensor boundary of nodes which it connects.

2.3.4 Virtual physics Using virtual physics, also known as Physicomimetics (Spears et al., 2005), to control the robot action is an important approach to control multi-robot behaviour. Among the different virtual physics-based approaches that use different physical phenomena (i.e. electrical charges, gravitational forces, spring forces and other virtual force models), the potential field (further referred as PF) approach is particularly attractive because of its mathematical elegance and simplicity.

Initially PF was designed for single autonomous mobile robot path planning and obstacle avoidance (Krogh, 1984; Khatib, 1985; Borenstein and Koren, 1990). The basic concept is to direct a robot as if it was a particle moving in a gradient vector field. Gradients can be intuitively viewed as forces acting on a positively charged particle robot which is attracted to the negatively charged goal. Obstacles also have a positive charge which forms a repulsive force directing the robot away from obstacles. The combination of repulsive and attractive forces hopefully directs

the robot from the start location to the goal location whilst avoiding obstacles.

Eventually, the PF was extended to include inter-agent repulsive and attractive forces as a distributed autonomous control for MRS (Reif and Wang, 1999). Reif and Wang define artificial force laws between pairs of robots or robot groups. The force laws are inverse-power force laws, incorporating both attraction and repulsion. The force laws can be distinct and to some degree reflecting “social relations” among robots, therefore the name “social potential fields” (SPF) method. An individual robot’s motion is controlled by the resultant artificial force imposed by other robots and other components of the system (i.e. obstacles and the goal). The approach is distributed in that the force calculations and motion control can be done in an asynchronous and distributed manner.

The PF approach is a widely used method to control the behaviour of a group of robots. Via suitable design, the PF can generate an artificial force to drive robots and form specific formations. In (Bruemmer et al., 2002), the SPF approach is utilised as a means to coordinate group behaviour and promote the emergence of swarm intelligence for spill finding and perimeter formation. A real-world experiment was implemented and they showed that social potential fields scale well to varying numbers of robots and improves performance in terms of time and reliability. (Song and Kumar, 2002) derived controllers from simple PF to control and coordinate a group of robots for cooperative manipulation tasks. The group of robots approach the object, organise themselves into a formation that will trap the object, and then transport the object to the desired destination. Theoretically, they show results on formation stability, scalability and insensitivity to parameters. In (Schneider and Wildermuth, 2003) a directed potential field approach is presented for motion co-ordination in formations of MRS. Different forces belonging to other robots, obstacles and the aspired shape of the formation are combined and used to move each robot to its desired position inside the formation. Whilst moving in formation, the group of robots avoid obstacles and approach towards a specified target. Results in simulation and with real robots in the presence of obstacles are presented.

PF have been used extensively in the field of deployment and coverage of sensor networks. In (Howard et al., 2002) a mobile sensor network composed of a distributed collection of nodes (each of which has sensing, computation, communication and locomotion capabilities) were able of self-deployment using a PF scalable and distributed approach. Similar work was done in (Popa et al., 2004), where classical robotic team concepts (obstacle avoidance, goal attainment, flight formation, environment mapping and coverage) were combined with traditional sensor network concepts (node energy minimization, optimal data rate and congestion control, routing in ad-hoc networks) to control the behaviour of the simulated mobile sensor nodes.

Inter-agent forces have been employed in different applications. In (Schoenwald et al., 2001) a PF approach was applied to search-and-rescue and other related tasks and in (Vail and Veloso,

2003), an approach for sharing sensed information and effective coordination through the introduction of shared potential fields was applied to robot soccer. In (Ge and Fua, 2005), the use of the artificial potential field was extended to generate queues. Formations like wedge, column, arrow-head, and double column can then be generated by combining the robot queues. In simulation the scalability and flexibility of robot formations was improved when the team size changed, obstacles were present and the local minimum problem appeared. The key limitation to this approach is that robots get often trapped in a local minimum either than the desired goal configuration. (Koren and Borenstein, 1991) identified and criticised inherent limitations of the Potential Field Methods (PFM) for mobile robot navigation.

Some problems are inherent to the Potential Field approach. (Koren and Borenstein, 1991) identified and criticised the limitations of the Potential Field Methods (PFM) for mobile robot navigation, more specifically for obstacle avoidance. The key problem of the PF approach is that robots can get trapped in a local minima either than the desired goal configuration. A trap-situation may occur when the robot runs into a dead end (e.g., inside a U-shaped obstacle). Traps can be created by a variety of different obstacle configurations, and different types of traps can be distinguished.

Summarising, the Social Potential Field control based on virtual physics is the most attractive due to its simplicity and functionality. The design and combination of the appropriated potential functions can lead to different emergent behaviours. These functions are simple and fast to compute and can be done locally in a decentralised mode. Consequently, the Social Potential Field has been chosen as the initial control method for a HRMS.

2.4 Approach: HMRS navigation

As previously mentioned the literature in HMRS is scarce. The only similar work in HRMS is presented in (Hashimoto et al., 2008). This paper proposes a method whereas a human and a swarm robot move cooperatively to maintain and surround the moving human. Hashimoto's work is concerned with the control for maintaining the high stability of the swarm, and proposes a control algorithm for the robotic swarm in obstacle space. In addition, each robot with neighbouring robots forms a local swarm that overlapped the other ones partially, so a robot can belong to some local swarms. The proposed algorithm for overcoming the stability problem is based on the attraction force by the center of gravity of the swarm. The repulsion forces prevent the omnidirectional mobile robots to collide with obstacles and with other robots. They do also present some stability results, whereas the stability of the swarm is maintained through simulations using Open Dynamics Engine.

Although the overall concept of Hashimoto's work is somewhat similar, many characteristics

differs from the work presented in this thesis. The main difference is that they do only present the work in simulation and no experiments in real-world implementations are performed. This is an important issue when considering the relevance of this work. Moreover, Hashimoto's control method is based on two virtual forces, local forces (attraction and repulsion by neighbouring robots) and surrounding forces. The surrounding forces, that as the name suggests are used by the swarm to surround the human, make use of global variables (i.e. center of gravity, position and angle of the goal relative to the robots). These global variables are accessible on the simulation level, however if we are to transfer Hashimoto's control to a real-world implementation, these parameters will be difficult to obtain, due to the decentralised nature of the system.

2.5 Conclusions

A human could broadly benefit from cooperating with a group of autonomous robots in various applications. Among the whole set of applications the most relevant with our work are those related with social based robotics and multi-robot navigation. When considering the required system architecture it is straightforward to conclude that the selected method must not be centralised. Moreover, a fully decentralised system will require each individual robot to possess certain advanced perception or sensory capabilities. To take advantage of both typologies and overcome technological restrictions we have employed a custom designed mixed architecture.

We have reviewed the following control mechanisms for our system:

- the **behavior-based control** is constructed by the combination of simple behaviours to obtain a more complex global behaviour. Ease of implementation in real robots within many different applications. The drawback is to decide when to switch among a fixed number of behaviours in an optimised way. The behavior-based method will provide an important improvement to the formation control of our work.
- the **leader-follower strategy** is widely used for generating formations based on establishing relationship between robots. An important drawback is that the existence of a leader causes to have robots with different roles among the group. The leader-follower strategy will provide a valuable contribution to the formation control of our work.
- the **graph theoretical and geometrical approaches** need to have either a global knowledge or individual labeling of the components of the group (characteristic that our decentralised system does not possess), but even though definitions from these approaches are given to characterise our robot formations.
- the **Social Potential Field control** based on virtual physics is the most attractive due to its simplicity yet reliability. The design and combination of the appropriated potential functions can lead to different emergent behaviours and can overcome the inherent problems of

this method (e.g. local minima). These functions are simple and fast to compute and can be done locally in a decentralised mode. Consequently, the Social Potential Field has been chosen as the initial control method for a HRMS.

As far as the author can see, our work is the first real-world implementation of a multi-robot system that is designed to truly navigate with humans. This distinct research area will be referred to as Human Multi-Robot System (HMRS) navigation.

Chapter 3

Aim and test criteria

This chapter provides an overview of the overall aim of this thesis. We describe here the framework for the distributed formation control of a group of robots to navigate with a human, the Social Potential Field (SPF) method. The SPF is based on the virtual forces exerted upon a robot by other robots, the human and the environment, although robots act as if the forces are real. Thereafter, in order to compare the performance of different experiments and methods, in this chapter we select exemplary metrics considering the common metrics used in related works. Moreover, we present as well a suitable formation definition. In our case, formation can be defined as a group of agents establishing and maintaining a certain *flexible configuration*. The configuration does not have a predefined shape but the components (robots and humans) have to stay close to each other and adapt to the geometrical constraints of the environment.

3.1 Aim

The overall aim of our work is to experimentally demonstrate human multi-robot navigation by developing and implementing a formation control algorithm. In our system the team of robots have to distribute in a flexible formation with the human and maintain such formation when the human is in motion. Figure 3.1 shows the general arrangement of the system.

Focusing on formation navigation tasks the following characteristics of the system have been defined:

1. *Scalability*. There is a variable number of robots.
2. *Local sensing*. The robots' sensing capabilities are limited by the range of their sensors. There is no overall knowledge of other robot's positions or headings.
3. *Heterogeneity*. The robot team is built up of different robots with different capabilities.
4. *Flexibility*. The group of robots have to adapt to different environments.
5. *Robustness* in the sense of tolerance to failure of individual components (fault tolerance).



Figure 3.1: Overall system.

6. *Anonymity*. The robots have no label or identity.

As mentioned in the previous chapter, the Social Potential Fields (SPF) method has been employed in Multi-Robot Systems (MRS) as the distributed control framework for formation navigation tasks. In our work we propose the SPF to be used as control laws for the navigation of our Human Multi-Robot System (HMRS).

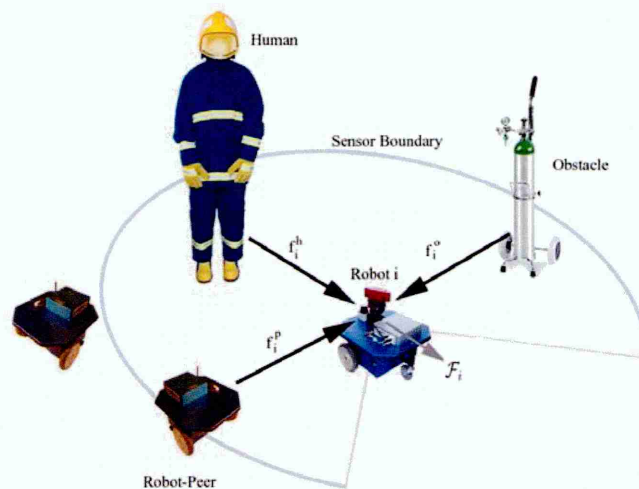


Figure 3.2: General distributed control framework

Let's assume that each robot is equipped with a sensor that allows to detect and distinguish among the components of the system (i.e. robots, obstacles or human) as is shown in Figure 3.2. Naturally, this sensor will have maximum range, that will be referred to as the sensor boundary (SB). Within the SPF framework, the controller is allowed to define pair-wise potential laws for pairs of components of the system. Each robot estimates the resultant potential field from the

relative positions of all other components (at least the components within its SB or neighbouring components) and acts under the resultant force \mathcal{F}_i . Once the force laws are defined, force calculations can be carried out by individual robots in a distributed manner.

At a fixed time, given the number of robots N , the overall artificial force applied by the neighbouring components upon a robot i is

$$\mathcal{F}_i = f_i^h + f_i^o + f_i^p, \quad i = 1 \dots N \quad (3.1.1)$$

where f_i^h represents the force acting between the Robot i and the Human, f_i^o is the force acting between the Robot i and the Obstacle, and f_i^p is the force acting between the Robot i and the Robot-Peer.

The force laws are inverse-power laws similar to those found in molecular dynamics. They are inverse-power laws of distances and can incorporate attraction and/or repulsion. For example, we could define a force law between the human and the robot, where attraction dominates over long distances and repulsion dominates over short distances. As a consequence, when the robot is far away it would come closer, and vice versa. The parameters of the force laws can be chosen arbitrarily. Indeed the parameters are chosen to reflect the relations among robots, e.g., how close together or far apart they should stay. Using and selecting suitable force laws, the resulting system can display “social” behaviors such as clustering, guarding, escorting and so on. To accomplish the navigation of our Human Multi-Robot System in Chapter 5 and Chapter 6 we propose two different strategies, respectively.

3.2 Our formation definition

In order to decide whether a human and a group of robots are in formation or not, a systematic and general definition of formation must be laid out. In the literature there exists different formation definitions, however these definitions are application dependent (according to the environmental conditions, the formation approach and the robot system employed). A formation is generally described in terms of its shape. There are, for example, line, column, diamond and wedge formations (Balch and Arkin, 1998) and others like circle or polygons formations (Sugihara and Suzuki, 1990; Lee et al., 2004).

Some works (Fredslund and Mataric, 2002; Lemay et al., 2004) define a formation as a set of points with specific geometric shape. In both cases, given the position of N robots, an inter-robot distance $d_{desired}$, a desired heading h , and a connected geometric shape (line, column, diamond, and wedge) \mathcal{G} , completely characterizable by a finite set of line segments and the angles between them, the robots are considered to be in formation \mathcal{G} if three criterion hold:

1. *uniform dispersion*, there exists a distance d , such that for all pairs of immediate neighbours (R_{i1}, R_{i2}) with distance $dist(R_{i1}, R_{i2})$, $|d - dist(R_{i1}, R_{i2})| < \varepsilon_{d1}$, and $|d - d_{desired}| < \varepsilon_{d1}$
2. *shape*, exists a “stretching function” f with $f(\mathcal{G}) = \tilde{\mathcal{G}}$, such that for all angles $\theta \in \mathcal{G}$, $|f(\theta) - \theta| < \varepsilon_a$, and such that for all robots R_i , with distance $dist(R_i, \tilde{\mathcal{G}})$ to $\tilde{\mathcal{G}}$, $dist(R_i, \tilde{\mathcal{G}}) < \varepsilon_{d2}$
3. *orientation*, $|f(h) - h| < \varepsilon_a$; for small $\varepsilon_{d1}, \varepsilon_{d2}, \varepsilon_a > 0$

The uniform dispersion criterion states that the same distance is kept between all neighbouring robots with a maximum tolerance of ε_{d1} . The shape criterion states that the robots have to be at the assigned positions depending on the desired formation with a maximal tolerance of ε_{d2} around the desired position. No angle in the original shape must be stretched more than ε_a to make the data points fit. The orientation criterion states that the stretching from shape criterion must not skew the heading more than ε_a .

In a similar way (Naffin et al., 2007) make use of a set of points with specific geometric shape to define a formation. More specifically, they say that given a formation, which is defined as the tuple $\langle \mathcal{G}, h, d \rangle$ where \mathcal{G} is a connected geometrical shape (line, column, diamond, and wedge), h is a desired heading, and d is a desired inter-robot distance, there exist K positions relative to the leader that represent the perfect formation. Given N robots attempting to construct this given formation, where $N \leq K$, they define the formation’s positional error as $P = \frac{1}{N} \sum_{i=1}^N |D(p_i, k_i)|$ where p_i is the i th robot’s position (relative to the leader) and $D(p_i, k_i)$ is the euclidean distance between the two positions. They say that a given set of robots is “in formation” if $P < \varepsilon$, where ε is a user-specified tolerance.

The main drawback of these formation definitions is that a predefined connected geometrical shape (line, column, diamond, and wedge) has to be given to the group of robots. Moreover, one might need to decide when to switch between these geometric shapes. Definitely this formation definitions are not the sort of definitions we are seeking for.

In (Lee and Chong, 2008) a group of robots are considered to be “in formation” when the mean of *inter-robot distance* (d_u) of each robot with the two nearest neighbouring converges into the distance $d_u \pm 1\%$. Some works employed fixed known formation position for the robots, as in the case of (Balch and Arkin, 1998). Some others use graph theory to define a desired formation in terms of either a labeled directed graph (Tanner and Kumar, 2005) or a specific regular formation shape (Mai and Lian, 2006). Similar definition was used in (Hashimoto et al., 2008) where multiple autonomous robots are forming a swarm because $|Ver(\mathcal{G})| = N$, where N is the number of robots, and $|Ver(\mathcal{G})|$ represents the element count of the vertex set of the simple graph \mathcal{G} on adjacent edges.

None of the previous formation definitions include our formation situation; formation can be

defined as a group of components (robots and humans) establishing and maintaining a certain *flexible configuration*, whereas the configuration does not have a predefined shape but the components have to stay close to each other and adapt to the geometrical constraints of the environment.

Before giving a description of our flexible formation definition we must take into account some considerations:

- Each component (robot or human) moves autonomously on a 2-dimensional plane.
- The robots do not rely on centralised directives, nor on any common motion of time and do not share any common coordinate system.
- The components are anonymous, meaning that they do not have any sort of identifiers or labels.
- It is possible to measure the position of close-by components and obstacles relative to the robot within its sensor boundary SB (Figure 3.2).
- The components within the sensor boundary are defined as the neighbouring components.

Taking into account these considerations and the previously mentioned criterion, **flexible formation** can be stated employing the following definition:

Definition: Given the positions of N mobile robots, the group is considered to be in a “flexible formation” if the following two conditions hold:

1. Given the neighbouring components R_j of a robot R_i , there exists a distance d , such that for all pairs of neighbouring components (R_i, R_j) with euclidean distance $dist(R_i, R_j)$, $d - \varepsilon_d < |dist(R_i, R_j)| < d + \varepsilon_d$, where ε_d is defined as the “maximal tolerance” for distance measurements in order to account for perceptual noise and imprecise actuators.
2. Given the following conditions
 - The center of a component is defined as a vertex.
 - The vertex of a component and vertices of neighbouring components are joined by an edge.
 - The resulting simple graph on touching edges is defined as \mathcal{G} .
 - The vertex set of \mathcal{G} is defined as $Ver(\mathcal{G})$.
 - The element count of $Ver(\mathcal{G})$ is defined as $|Ver(\mathcal{G})|$.

the components are considered to be in “flexible formation” only if $|Ver(\mathcal{G})| = N$.

In other words, the group is said to be in *flexible formation* if there is *uniform dispersion* and there exist a *connected graph*. Condition 1 states that the same distance is kept between all neighbouring components within SB with a maximum tolerance of ε_d . In other words, the components are “uniformly dispersed” or the inter-agent distance is kept (Figure 3.3). The case

shown in Figure 3.3a presents a suitable formation when the group has to adapt for example to narrow corridors.

The usage of condition 1 by itself is not sufficient to have a flexible formation, see Figure 3.3b. In this case the components of the group are uniformly dispersed and condition 1 still holds. This is an undesired situation, therefore the necessity of including a second criterion. This condition 2 states that the components of a group are in flexible formation only if $|Ver(\mathcal{G})| = N$. In other words, the element count is equal to the number of components of the group. In graph theory this is also known as a *connected graph*, where nodes are components (robots or human) and edges are virtual links between nodes, called *connectivity graphs* in (Muhammad and Egerstedt, 2003). In the case of Figure 3.3b, $|Ver(\mathcal{G})| < N$, the connected graph does not exist, hence the formation is torn into small groups. Our flexible formation was introduced in our previous publications (Alboul et al., 2008, 2009; Saez-Pons et al., 2010).

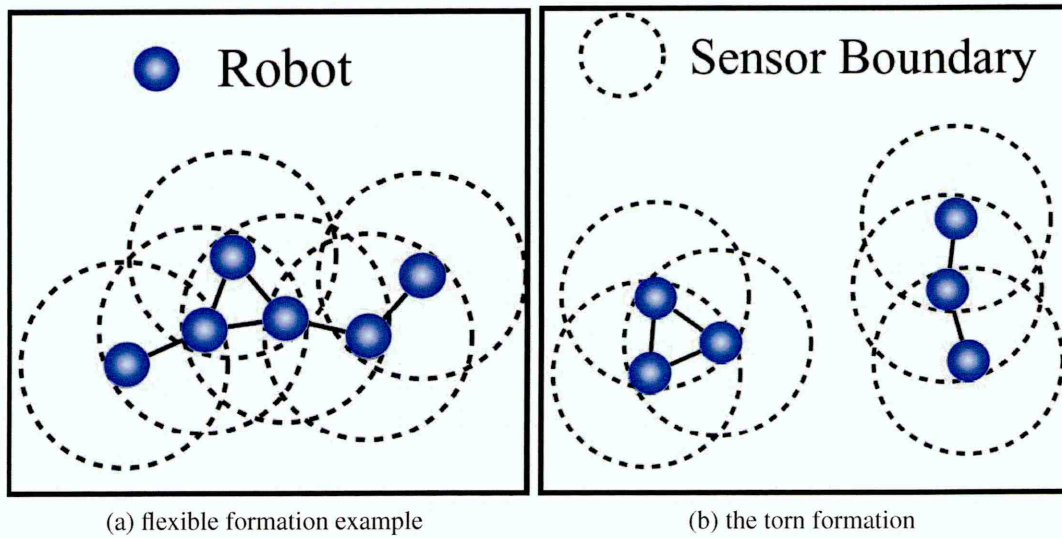


Figure 3.3: Formations examples.

Making use of the criterion 1 for the definition of the flexible formation implies that the value of the “maximum tolerance” for distance measurements, ε_d , has to be properly selected. The value of this parameter directly influences the flexibility of the formation; a low value means to have a strict rigid formation and a high value means to obtain a loose formation. In the literature the selection of this parameter is done empirically according to the sought performance (Fredslund and Mataric, 2002; Lemay et al., 2004; Balch and Arkin, 1998). The evaluation of this parameter will be justified in Section 7.3.

3.3 Performance evaluation

In order to compare among methods and experiments it is crucial to utilise measurements that allow meaningful evaluation of the experimental data. Formation navigation is one of the challenging fields in multi-robot systems research. Surveying the existing literature only sparse discussions of metrics in this field are found. This section gives a short review on the existing metrics and focuses on the problem of developing appropriated metrics for evaluating formation navigation.

3.3.1 Metrics for the formation experiments Selecting the right parameters requires the analysis of the experimental setup carefully. It has a significant influence if the robots operate on an empty warehouse or in a crowded commercial center. However, most metrics are significant when analyzing the effect of a modification (e.g. parameter set) in exactly the same experimental setup and environment.

General parameters for metrics used in the literature are:

1. time
 - traveling time
 - time in / out of formation
 - time for setting up / establishing the formation
 - time for recovering the formation after breaking up
2. position error
 - displacement in distance
 - displacement in angle
3. path
 - overall path length
 - path length for being in/out of formation
 - path length for setting up the formation
 - inter-robot distances
4. others
 - amount of computation
 - communication
 - sensing

Most of these criterion are highly related to the environment. Reviewing the existing works in the field of formation navigation, it is obvious that repeatability and reproducibility for the sake of comparison is very difficult to achieve. Every experimental setup is different even if it is “a typical office environment” or “an empty soccer field”. One solution for the metric problem would be to take into account the influence of the environment and other parameters. This, of

course, implies that a detailed map of the environment and additional information about dynamic objects are available. This is difficult to achieve in unknown real world scenarios.

3.3.2 Common metrics in related work Without going into detail about the application and the methods used we will list the common metrics employed in related existing works.

In (Balch and Arkin, 1998), where a fixed known formation position for the robots is employed, the performance metrics to evaluate the formation experiments are *path length ratio* (average distance traveled by the robots divided by the straight-line distance of the course), *position error* (average displacement from the correct formation position throughout the experiment) and *percentage of time out of formation* (time in which the robots fall out of formation), used to analyze the stability of the system.

In (Fredslund and Mataric, 2002) a behavior-based approach is used to have a number of robots establish and maintain some predetermined geometric shape. The performance metrics used to evaluate their system performance are *formation the first time, ft* (distance traveled by the leader up to the point when the robots established a formation the first time), *percentage of time out of formation* (percentage of time-steps the robots where in formation after ft , used to evaluate the stability of their approach when dealing with empty space and with obstacles) and *robustness* (distance the leader traveled from the point when the formation breaks up, e.g. due to a terminated robot or obstacle, to the point when the formation is repaired).

In (Lemay et al., 2004), which work is mostly related to (Fredslund and Mataric, 2002), only the previously explained *formation the first time* criterion is used as an evaluation measure.

In (Naffin et al., 2007), where a behavior-based approach is used to assemble and maintain robot formations, three metrics to measure the performance of their system are employed: *positional error* (given N robots attempting to construct a given formation, there exist K positions relative to the leader that represent the perfect formation, where $N \leq K$, they define the formation's positional error as $P = \frac{1}{N} \sum_{i=1}^N |D(p_i, k_i)|$ where p_i is the i th robot's position, relative to the leader, and $D(p_i, k_i)$ is the euclidean distance between the two positions), *time to convergence* (duration of time required for a formation to reach a given size N and be in formation for that size is defined as time to convergence $T_c(N)$) and *percentage of time in formation* (defined as $F = \frac{t_{in}}{t_{total}}$ where t_{in} is the time in formation since the formation reached its current size and t_{total} is the time elapsed since the formation reached its current size).

In (Mai and Lian, 2006) graph theory is used to generate a regular hexagon form by six robots. Different factors are used for the evaluation of their performance. The three metrics employed are *system efficiency (SE)* which is similar to the path length ratio (Balch and Arkin, 1998) ($SE = \frac{1}{N} \sum_{t=1}^N \frac{|X_i(t) - X_i(0)|}{l_i(t)}$, where N is the total number of robots, $|X_i(t) - X_i(0)|$ is the straight-line

distance of a robot from the initial position to the position at time t , and $l_i(i)$ is the total traveling distance of each robot at time t), *convergence speed* (time consumed by a robot team from their initial positions to the final positions that form a specific formation) and *robustness* (the ability of a formation to gain back stability after distortion, without considering the case of a robot failure).

In (Lee and Chong, 2008) the fundamental problems and practical issues related to the deployment of a swarm of autonomous mobile robots are discussed. The robots confine themselves into an area with geometrical constraints through local interactions with adjacent neighbouring robots. The only metric used is the *mean inter-robot distance* between two neighbouring robots.

In (Tanner and Kumar, 2005) decentralised cooperative controllers are developed, based on local navigation functions and yielded global asymptotic stability of a group of a mobile agents to a desired formation and simultaneous collision avoidance. They use a similar evaluation metric to (Lee and Chong, 2008) to show their formation generation performance. The only difference is the evaluation of the inter-robot distance between all the members of the team instead.

(Hashimoto et al., 2008) proposes a virtual forces method where a swarm robot moves cooperatively whereas maintaining formation. They evaluate the stability of the swarm using an extent of the whole swarm r described as $r = \sqrt{\frac{1}{N} \sum_{i=1}^N |p^i - g|^2}$, where N is the number of robots, p^i is the position of the i th robot, and g is the center of gravity of the whole swarm. r is the conventional equation of the standard deviation, thus the value of r shows the extent of the whole swarm. It is assumed that the extent of the whole swarm r converges to the constant extent r^* if the stability of the whole swarm is maintained.

3.3.3 Our formation metrics. Based on our formation approach, described in Section 3.2, we choose some suitable metrics, which one can find in the majority of the cited work. Many of the previously seen metrics make use of special characteristics of the formation algorithm. However, since the goal is to compare among different formation methods and experiments this has to be avoided. The metrics we have selected to compare among the forthcoming experiments are:

1. **System efficiency** (Balch and Arkin, 1998; Mai and Lian, 2006). This metric gives a measurement of the distance ratio between the human and the robots.
2. **Percentage of time out of formation** (Balch and Arkin, 1998; Fredslund and Mataric, 2002; Lemay et al., 2004; Naffin et al., 2007). This metrics is used to evaluate the stability performance of the robot system.

One might question the exclusion of the *formation the first time (ft)* metric employed in many of the previously cited work (Fredslund and Mataric, 2002; Lemay et al., 2004), also referred as *convergence speed* (Mai and Lian, 2006; Naffin et al., 2007) when measured in time. This metric gives a systematic measurement of the time/distance required by the group of robots to

generate a formation. f_t requires a defined starting position for the robots, which in our case does not occur. As a result, this metric will not contribute to evaluate the performance of the method being evaluated. Nevertheless, solely for informative purposes, we will show this metric on the evaluation of the methods employed during the experiments.

The rest of the exemplary metrics have been discarded to quantify the results of our experiments. The reason is the fact that they require the knowledge of specific parameters. This is the case of the *formation position error* (Balch and Arkin, 1998; Naffin et al., 2007) which requires to know the final positions of the robots in the formation, data that in our flexible formation approach are not available.

Chapter 4

Experimental Design and Implementation

This chapter describes the experimental set-up: the distributed robotic system, the hardware employed during the experiments and the software architecture developed to enable the real-world implementation. Moreover, we provide in this chapter a description of the simulation software, including the mobile robot and human models, the method to detect the surrounding obstacles, the simulation environment and a description of the control model employed in the simulation experiments.

4.1 Experimental design

The experimental goal of this work, as described and motivated in previous chapters, is to demonstrate human multi-robot navigation by developing and implementing a formation control algorithm. The equipment and procedures described here are designed as the minimum system required to achieve this goal.

Initial design, component selection and acquisition, most low-level C programming, all of the control, communications, modeling, logging and visualization software was completed by the author. System integration and debugging was the most time-consuming and laborious of the author's tasks. Most components went through several iterations and the system took around 20 months to complete.

4.1.1 The system In our scenario three different component classes are envisaged: autonomous mobile robots, humans and obstacles (i.e. walls, doors, objects, etc.). In general the mobile robots do not have a global view of the situation (due to limited sensing capabilities) and do not have knowledge of the goal state. They can “sense” and “detect” the surrounding neighbours within

their sensor boundary (SB) and react according to their positions. I will explain in the forthcoming chapters how the mobile robots perceive the environment and what sensors are used. The bounding environment and objects of the scene are considered as obstacles. Figure 4.1 shows an general situation of the human multi-robot system.



Figure 4.1: General situation.

This general arrangement is reproduced in a robot system, subject to the limitations explained below in Section 4.3. This system is used as a platform for the experiments in HMRS formation control described in this chapter.

The following elements have been identified to be required for a human multi-robot system.

1. a number of grounded mobile robots to navigate with the human,
2. a suitable experimental environment,
3. means of determining the positions of the robots and the human,
4. software architecture,
5. an algorithm to control the robot formation and effectively navigate with the human.

The rest of this chapter describes each of the first four elements in turn, whereas in Chapter 5 and Chapter 6 we introduce a different candidate formation control algorithm, respectively.

4.1.2 Grounded Mobile Robots This section presents the selection process of the grounded mobile robotic platforms. Afterwards the characteristics, components, configuration and interfaces of the selected platform are documented.

Selection process

Initially small-size mobile robots were selected, more specifically the Khepera III mobile robots produced by K-Team¹, which come with an embedded complete standard Linux Operating System. The Khepera's sensors are basically short distance IR array sensors and five sonar sensors, although recently laser range finder has been added to this platform (Alboul et al., 2010a). Due to its low computational power, basic navigational algorithms such as localisation or map building were difficult to add on, therefore a full tracking system with an overhead camera had to be developed. Some time and resources were given to find a proper solution to be used with Khepera III (Figure 4.2a) and a working system was built up (Prieto, 2009).

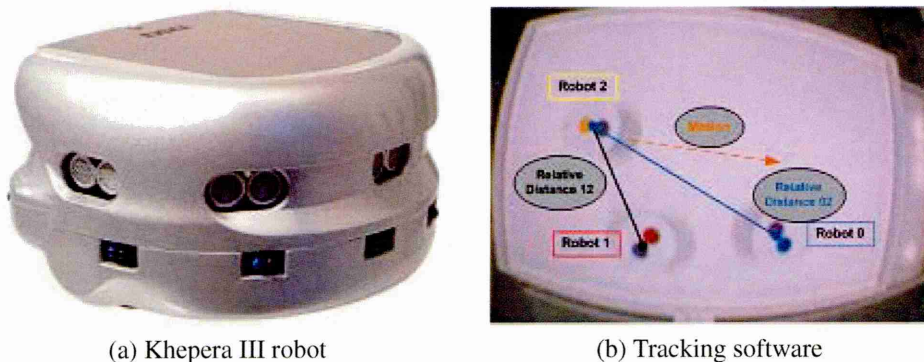


Figure 4.2: Multi-Robot 2D overhead tracking system.

The overall design consisted of an overhead fire-wire camera connected to a linux-based computer, a set of Khepera robots provided with a top-placed marker and a color-based tracking algorithm to detect robot's positions (Figure 4.2b). The system basically consisted in detecting the color markers of each Khepera robot and extracting its absolute position, similar to the SwisTrack tracking software (Lochmatter et al., 2008). The results obtained were acceptable, however very sensitive to changes in illumination, radial and perspective distortion, and more important, the system needed a long time to be initialised and tuned. Additionally, the set-up did not allow the inclusion of a human, small-size mobile robots could be crushed under human's feet and the set-up could not be easily transported and adapted. Although the systems was sufficient to validate and test the control formation algorithms, the overhead tracking system and the small-size robots were

¹www.k-team.com

discarded due the multiple mentioned inconvenients.

ERA-MOBI platform

The most important requirement for the mobile platform was that it had to be capable of dealing with human movements. It came out that in order to match the system requirements the most suitable robotic platform would be a commercial medium-size one. The Pioneer, produced by Mobile Robots², is a durable and the most popular differential drive mobile robot in academic research. The base Pioneer 3 DX platform comes fully assembled with 500-tick encoders motors, 19cm wheels, tough aluminum body, 8 forward-facing ultrasonic (sonar) sensors, 8 optional rear-facing sonar, hot-swappable batteries, and a complete software development kit. However, the Pioneers high versatility, reliability and durability comes with a high drawback too, its price. Consequently, the autonomous mobile robots selected were the ERA-MOBI mobile robot (Erratic) provided by Videre Design³, a compact and powerful platform carrying an integrated PC and a laser range finder (URG-04LX) by Hokuyo⁴ (Figure 4.3). It is useful to mention, that for the price of a single Pioneer a whole set of fully equipped Erratic robots was acquired.

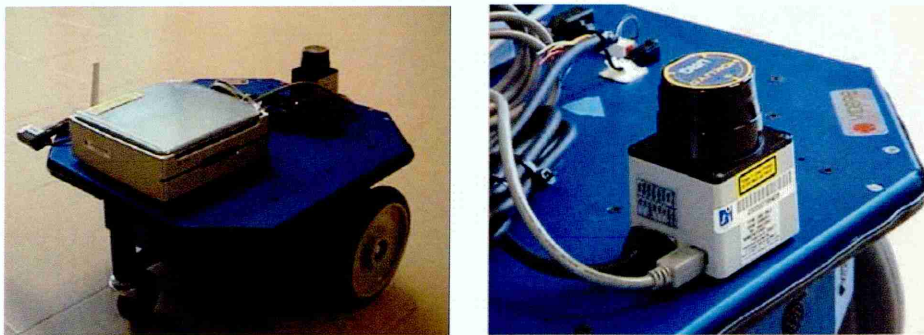


Figure 4.3: ERA-MOBI robot carrying a PC and URG-04LX.

The Erratic (ERA) mobile robot is a full-featured commercially available mobile robot base. ERA is a compact and powerful platform, and capable of carrying a full load of robotics equipment, including an integrated PC, laser range finder, and stereo cameras. Table 4.1 shows the base characteristics of the ERA robot.

The robot controller connects to several sensors and actuators on the robot. Through the USB connection, the controller accepts commands to control the actuators, and sends the collected information from its sensors. User programs on the PC can communicate directly with the controller. Each sensor or actuator can be thought of as an interface. ERA's software is the

²www.mobilerobots.com

³www.videredesign.com

⁴www.hokuyo-aut.jp/

Table 4.1: Base Characteristics of the ERA-MOBI robot.

ERA-MOBI	Parameter Value
Base platform size	$L = 50$ cm, $W = 44$ cm, $H = 18$ cm
Wheels	15 cm diameter, 6.25 cm diameter (caster), polymer core, soft non-marking rubber
Wheelbase	33 cm
Drive type	Differential, single rear caster
Maximum Speed	2 m/sec, 720 deg/sec
Motors	DC reversible with gear head, 72 W continuous power
Encoder resolution	500 cycles per motor revolution
Controller	16 bit micro controller, integrated controller/motor driver, analog, digital, and servo interfaces
Power	12V, 7AH lead-acid batteries (x3), 5A charger
Weight	4.5Kg (base), 12Kg (base + batteries)
Payload	20Kg

Player/Stage project ⁵, which is an open-source, widely-supported middleware platform. This section documents the interfaces of the ERA platform, as well as the Player driver abstract interfaces that correspond to them.

By means of the Player interface, many of the controller parameters can be changed using the Player driver configuration file for ERA. The configuration file is read by the Player driver on the on board PC, to determine the resources of the robot base. When launching the Player interface it reads the configuration file and starts the driver using its parameters.

The controller drives the robot wheels using an integrated dual H-bridge motor driver. The driver is able to supply up to 30A at 12V to the motors, although in practice the current is limited to less than this. The motors are rated at 75W continuous power, and are able to drive the robot at speeds up to $2m/sec$ and $720deg/sec$. Each wheel is controlled independently, allowing the robot to turn as well as drive forwards or backwards, also referred as differential drive. The motor controller is used employing the TR mode, the controller sets the translational and rotational speeds or positions independently. For example, the forward velocity can be set as $0.3m/sec$, whereas setting the rotational velocity to $20deg/sec$.

4.1.3 Simulation This section describes a simulation model that encapsulates the behaviour of the whole human multi-robot system and the considered environment. The simulation was required to be similar enough to the real system to allow the design of control algorithms which

⁵playerstage.sourceforge.net

would be transferred to the real world, yet be simple enough to (a) be easily understood and (b) run much faster than real time. It was hoped that the process of modeling the system would inform the design of control methods.

NetLogo

At the beginning it was determined that the most convenient would be to use a multi-agent system software, and after a short software survey, the popular software tool named NetLogo⁶ was selected. NetLogo is a programmable modeling environment for simulating natural and social phenomena. NetLogo is particularly well suited for modeling complex systems developing over time. NetLogo was chosen to check the proof of concept for the human multi-robot control methods.

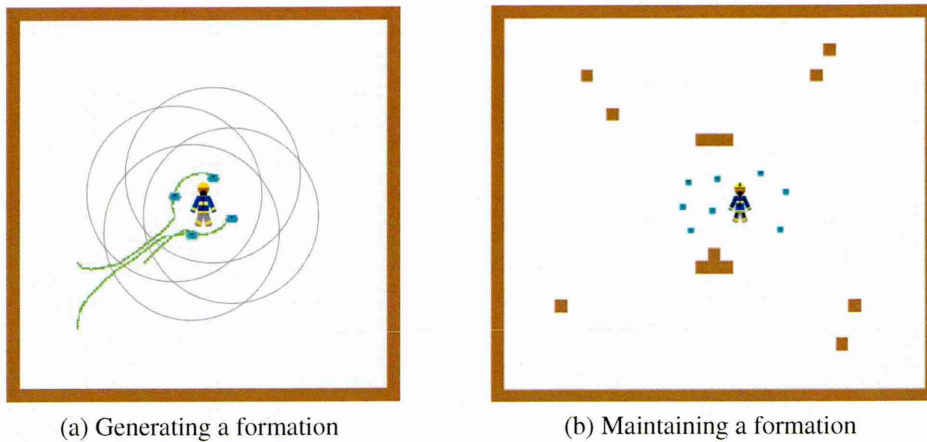


Figure 4.4: Simulations using NetLogo.

Employing solely NetLogo, simulations for the generation and maintenance of human multi-robot formation were performed. This can be seen in Figure 4.4a, where four robots and a human generate a formation (Saez-Pons et al., 2009; Alboul et al., 2010b). Figure 4.4b presents a NetLogo simulation where six robots and a human maintain formation through the environment, while avoiding obstacles represented by brown bricks (Alboul et al., 2008). These two figures show are only qualitative results, though the usage of a NetLogo proved the concept of the distributed formation control of a human multi-robot system.

However, it was required to employ a simulation tool where so few or no changes are required to move between simulation and real hardware. Moreover, the software had to be capable of simulating a population of real robots, sensors and objects with their physical properties. Therefore,

⁶ccl.northwestern.edu/netlogo

it was decided to migrate simulations to “The Player/Stage Project” (Gerkey et al., 2003), a set of free software tools for robot and sensor applications.

Player Stage Project

Player is a network server for robot control. Running on the (physical or simulated) robot, Player provides a clean and simple interface to the robot’s sensors and actuators over the IP network. The client program talks to Player over a TCP socket, reading data from sensors, writing commands to actuators, and configuring devices on the fly. The summarised features of Player are

- Player supports a variety of robot hardware.
- Player is designed to be language and platform independent. The client program can run on any machine that has a network connection to the robot, and it can be written in any language that supports TCP sockets.
- Player allows multiple devices to present the same interface.
- The behaviour of the server itself can also be configured on the fly.
- Player is free software, released under the GNU Public License.

Stage is a robot simulator. It simulates a population of mobile robots, sensors and objects in a two-dimensional bitmapped environment. Stage provides fairly simple, computationally cheap models of many devices, including sonar and infrared rangers, scanning laser range finder, color-blob tracking, fiducial tracking, bumpers, grippers and mobile robot bases equipped with odometry or global localisation.

Stage is often used as a Player plugin module, providing populations of virtual devices for Player. This is the well-known “Player/Stage” system. The robot controllers and sensor algorithms are written as ‘clients’ to the Player ‘server’, see Figure 4.5. Due to this hardware abstraction, typically, clients cannot tell the difference between the real robot devices and their simulated Stage equivalents. It has been found that Player clients developed using Stage will work with little or no modification with the real robots and vice versa. Thus Stage allows rapid prototyping of controllers destined for real robots and experiments with realistic robot devices.

Using Player with Stage requires two configuration files: a Stage ‘.world’ file and a Player ‘.cfg’ file. The .world file defines the simulated ‘world’, composed of ‘models’, i.e., sort of sensors and actuators are to be simulated, which background image to load, etc. On the (physical or simulated) robot a Player configuration file needs to be written, with the extension .cfg, that instantiates the driver(s) needed to control the robot and tell the driver(s) how to access relevant hardware. The job of the configuration file is to map the (physical or simulated) devices to Player devices.

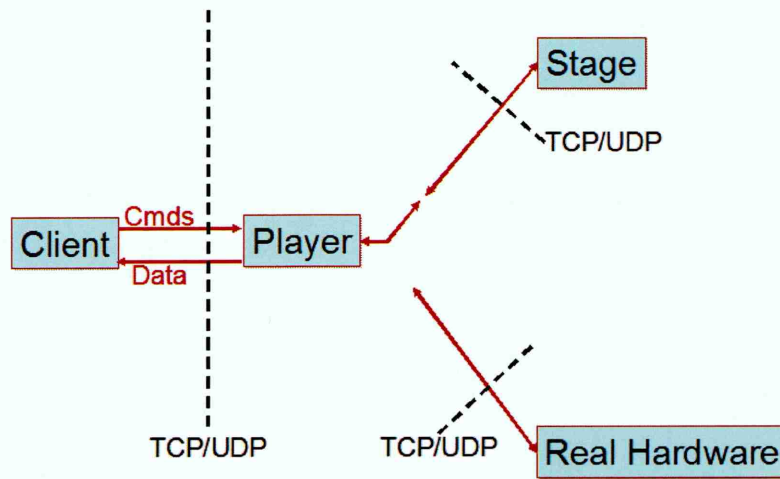


Figure 4.5: Player Stage Hardware Abstraction.

Robot Model

The ERA robot model definition is loosely based on the real robotic platform described in Table 4.1. The location of a particular robot of index i is defined by a position vector R_i and the orientation by a unit vector \hat{u} , which also defines the robot's local reference frame (Figure 4.6). At each time step of duration Δt , a velocity v_i is assigned to each robot and the position subsequently updated thus using the following listing

Listing 4.1 Determine Position $R_i^{(s+1)}$

- 1: **if** $|v_i^{(s)}| \neq 0$ **then**
 - 2: $\hat{u}_i^{(s+1)} = \text{norm}(v_i^{(s)})$
 - 3: **else**
 - 4: $\hat{u}_i^{(s+1)} = \hat{u}_i^{(s)}$
 - 5: **end if**
 - 6: $R_i^{(s+1)} = R_i^{(s)} + \Delta t \cdot v_i^{(s)}$
-

where R_i is the position vector of robot i and \hat{u} the unit vector. At all times the robot's orientation matches the direction in which it travels so conceptually each movement consists of a combination of rotation and translation.

The sensor model is loosely based on the laser range finder URG-04LX (Figure 4.3). The technical specifications of this device are shown in Table 4.2 and further information can be found in the manufacturer's (Hokuyo Automatic Co., LTD.) website ⁷ and in the online document ⁸

⁷www.hokuyo-aut.jp/

⁸www.hokuyo-aut.jp/02sensor/07scanner/download/data/URG-04LX_spec.pdf

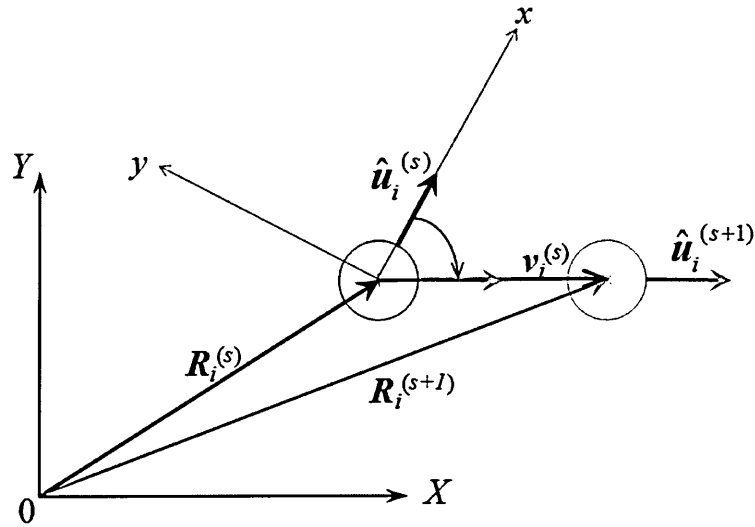


Figure 4.6: Conventions for describing robot pose.

Table 4.2: URG-04LX laser range finder specifications.

URG-04LX	Parameter Value
Power source	5VDC \pm 5%
Current consumption	500mA or less (800mA when start-up)
Measuring area	240 $^\circ$
Accuracy	60 to 1000mm: \pm 10mm 1000 to 4095mm: 1% of measurement
Angular resolution	Step angle: approx. 0.36 $^\circ$ (360 $^\circ$ /1,024 steps)
Scanning time	100msec/scan
Ambient temperature/humidity	-10 to +50 degrees C. 85% or less
Weight	Approx. 160gr.

Human Model

The human is modeled in a very similar way to the robots. His physical extent is approximated by a disk and the sense of touch is modeled as sectors (Figure 4.7). The orientation of the human is defined by the direction is facing and we assume that all movements are in the same direction as this orientation vector. The typical parameters of the human model are drawn together in Table 4.3. The human model includes the mass, standard human size and localisation, that in simulation is based on a simple odometry model.

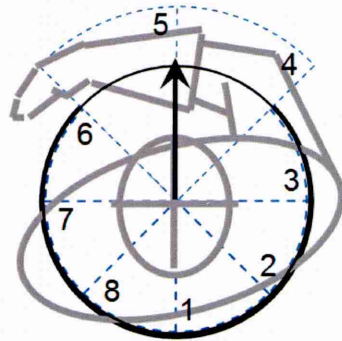


Figure 4.7: Model of human.

The human model was determined by personal observation on real fire fighters training sessions in the United Kingdom. Fire fighters aiming towards the scene of operations advance only at a crawling speed: they progress $12m$ in about one minute, what means $0.2m/sec$ (Penders et al., 2011). If the fire fighter is a squad leader or is operating alone he will sweep his arm up and down in the direction in which he moves to feel for obstacles or wires and also test the ground to check its integrity as well as detecting objects at foot level. To reflect this, the two front facing sensor sectors (4 and 5) have a wider reach than the ones at the back and side, the latter extend only as far as the physical extent of the fire fighters body. The touch ranges are just rough estimates and possibly they could be refined by making a detailed study of the movements of a real fire fighter, however this is out of this thesis scope.

Environment

Figure 4.8a shows an overview of the simulation software. The Stage window consists of a menu bar and a view of the simulated world. The world view shows part of the simulated world. One can zoom the view in and out, and scroll it to see more of the world. Simulated robot devices, obstacles, etc., are rendered as colored polygons. The world view can also show visualizations of the data and configuration of various sensor and actuator models. The View menu has options

Table 4.3: Typical parameters of the human model.

Human model	Parameter Value
Radius	0.30 m
Touch range	0.30 m (sectors 1, 2, 3, 6, 7, 8) 0.45 m (sectors 4, 5)
Max. speed	0.2m/sec

to control which data and configurations are rendered. The description of the robot and human model is part of the simulated world defined in a .world file.

The environment is based on the 2D scenario where the real world experiments take place shown in Figure 4.8b. Stage draws the model by interpreting the lines in a bitmap file. The file is opened and parsed into a set of lines. The lines are scaled to fit inside the rectangle defined by the model's current size.

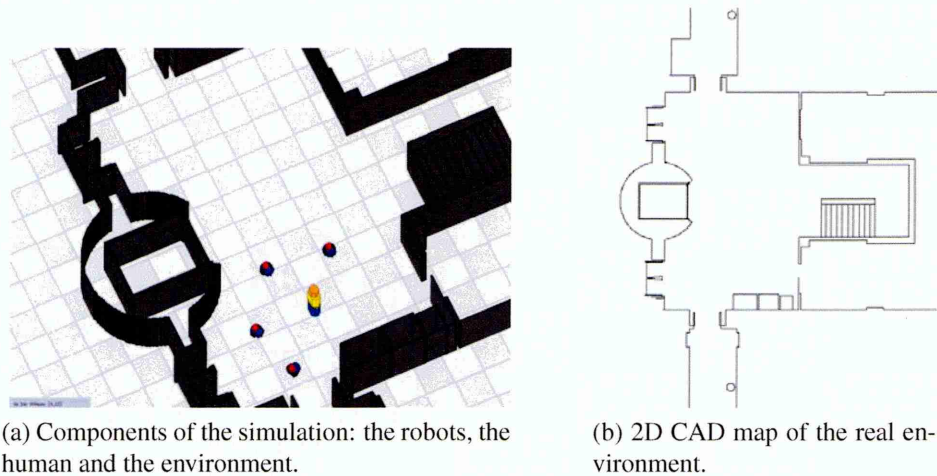


Figure 4.8: View of the simulation software.

The obstacles that the robots or the the human might encounter in the environment vary considerably, however in Figure 4.9 a possible scheme for classifying static obstacles is as follows:

1. can be negotiated by human and robot (e.g. small fragments or debris)
2. block the progress of robot but can be stepped over or moved out of the way by human (e.g. empty wooden crate)
3. block the progress of robot but can be stepped over by human (e.g. steel beam)
4. can be passed under by robot but block the progress of the human (e.g. underneath a storage rack)

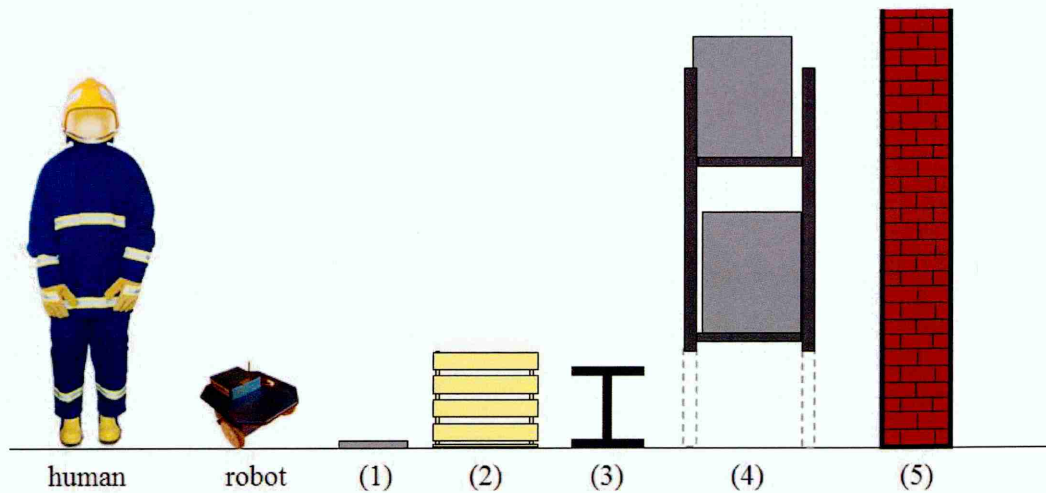


Figure 4.9: Scheme for static obstacles' classification.

5. block the progress of the robot and the human (e.g. brick wall)

The on board sensing of the robots

In order to apply a formation control approach, it is essential that the robots:

1. detect, identify and obtain the relative positions of other robots, problem referred as the “the mutual localisation problem” (Franchi et al., 2009).
2. acquire the human's relative position
3. find the nearest obstacle in the environment and obtain its relative position.

In simulation it is relatively straight forward to solve (1) and (2), since a fiducial (marker) detection is employed. The fiducial interface provides a simulation of devices that detect coded fiducials (markers) placed in the robots and the human through the laser interface. Figure 4.10 illustrates an example in simulation where the robot R_i can detect and identify the human H and the robot peer R_1 within the sensor boundary. In the real-world a fiducial detector example could be a pan-tilt-zoom camera combined with a color blob detector searching for color-coded fiducials or a laser device that searches for retro-reflective targets in the laser range finder data.

In simulation, to find the nearest obstacle in the environment and obtain its relative position, problem (3) requires a more elaborated approach. This case is exemplified by Figure 4.11a. It can be seen that the closest object O_1 to Robot R_i has been wrongly determined, the correct closest object O_1 is placed to the right side of R_i and the laser measurements say that O_1 is on the left side, that in this case corresponds to a peer robot R_1 . This situation is caused by the readings

coming from the laser-range finder since such readings are merely distance measurements. These distance readings provide that the measurements of the closest obstacle corresponds to the shape of R_1 , that is in this case is totally correct. Therefore, we need to find a solution to obtain the closest object position without taking in consideration other robot peers and human shapes.

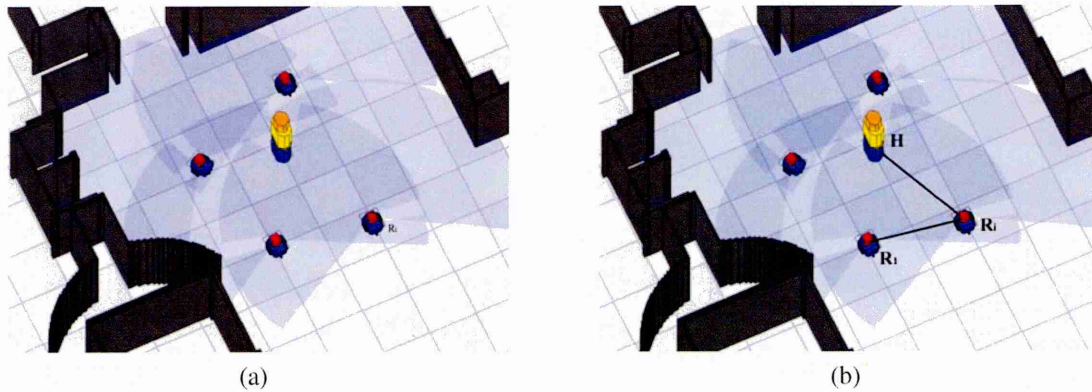


Figure 4.10: Fiducial interface.

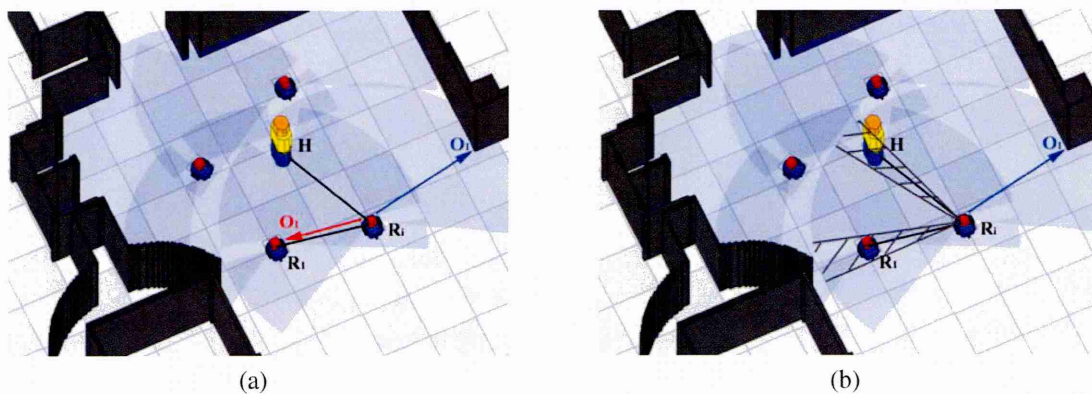


Figure 4.11: Segmentation of the laser information.

The solution adopted is exemplified in Figure 4.11b. It consists of segmenting the laser range-finder information. Within the laser distance information, the positions of the neighbouring robots and the human are omitted, since they do not account for the estimation of the closest obstacle. Naturally, the laser range finder information is segmented according to the set of detected beacons by the fiducial interface. Once the laser information is segmented, those sectors which include the fiducial items are disregarded to detect the nearest obstacle. This simple method provides a reliable and easy to implement solution to detect and localise the closest object. The robust and reliable results of this solution makes it suitable to be applied to the real-world experiments. This issue is addressed with more detail in Section 7.2.

Control model

The velocity of a particular robot R_i is proportional to the resulting 'force' exerted on it by other objects in its environment. The magnitude of these forces is proportional to the values of potential functions which, in most cases, vary according to the distance between the robot and surrounding elements as measured by the model sensors. The surrounding elements considered are other robots, human and obstacles. In the simulations, for most types of forces, each element detected by the sensor measurement contributes a force and only the closest obstacle enters into the force calculation. Section 7.2 provides a discussion about the usage of environmental obstacles. Naturally if there is some element not detected the force contribution from that measurement distance is zero. It should also be added that if the line of sight of robot, R_i , to an element, E_j , within a given measurement distance is obscured by another type of element, E_k , then E_j does not contribute to the forces on R_i . This constraint is applicable to the calculation of all the potential forces.

For the purpose of simulation, the criterion for an object, E_k , being obscured from the view of R_i by an intervening object, E_j , within the sensor boundary SB of the robot R_i , could take three forms as shown in Figure 4.12:

- a The edge of E_k just touches the shadow of E_j .
- b The center of E_k just touches the shadow of E_j .
- c E_k lies completely within the shadow of E_j .

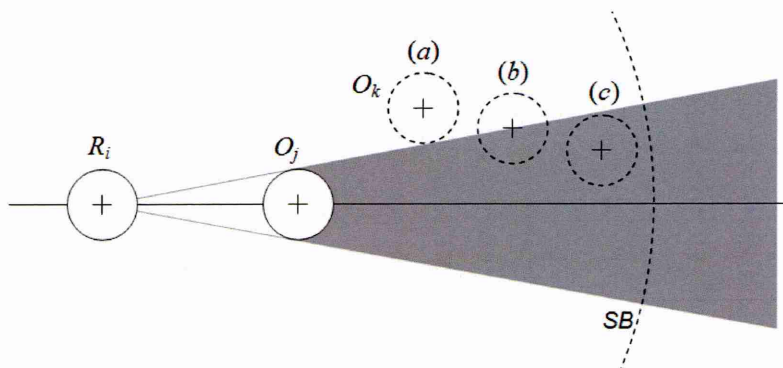


Figure 4.12: Occlusion of an element by another element.

In the real world, ideally an element would be detectable until it is totally occluded, but in our simulation an element is occluded by another element only when its center is occluded, that corresponds to the adopted criterion (b).

To obtain a velocity, all the forces on a particular robot are first added to give the sum of all forces $F(i)$. The velocity is then simply given by

$$v(i) = \text{minimum}(\text{maxspeed}(i), |F(i)|) \quad (4.1.1)$$

Once the robots are equipped with mutual localisations sensors different potential functions can be defined. In this work, we propose two different control methods based on the usage of social potential fields, *Formation Control I* (Chapter 5) and *Formation Control II* (Chapter 6), respectively. The various potential functions used and the forces that are associated with them are described in the respective chapters.

4.2 Real-world experiments

The human multi-robot system comprises adapted commercial mobile platforms with on board integrated PC and a human equipped with a small-size Pentium-based Linux workstation. The robots and the human operate in a known and defined environment, although there might be dynamic and unexpected objects. As previously mentioned, the control model is based on the social potential field framework (Section 3.1). This method considers that a robot of the group equipped with a sensor capable of detecting and identifying within its sensor boundary the relative positions of the human, obstacles and robot peers (Section 4.1.3).

In mostly all of the related work, vision has been employed to identify and detect other robot's positions (Alur et al., 2000; Fierro et al., 2001; Lemay et al., 2004; Howard et al., 2006). In some other cases, to allow robot recognition and identification, vision has been combined with other sensors such as sonar (Lee and Chong, 2006), infrared (Barfoot and Clark, 2004) or laser range finder (Fredslund and Mataric, 2002). Certainly, the usage of a vision system on the robots would make the mutual localisation problem simpler but it is not the case of our robots, since vision was excluded as a solution right at the beginning of this work due to the low-visibility characteristics of scenarios considered for the Guardians project. The mutual detection problem is an ongoing research issue and multiple solutions have been proposed, although all solutions are application-dependent. Therefore, we applied an overall system that can be used to simulate individual robot behaviour as well as that it can be applied on the real robots independent of the solution employed for robot-peer recognition.

4.2.1 Distributed software architecture The solution implied the usage of a distributed software architecture capable of implementing different robot behaviours (formation and following), handling communication, running distinct robot navigation algorithms (localisation and collision avoidance), defining different agent types, interacting with the hardware involved (actuators and sensors), interfacing with the users, and everything combined with different software platforms (Player, Javaclient and JADE). Such architecture was employed within the GUARDIANS

project consortium and a more detailed description can be found in (Saez-Pons et al., 2011b).

Contrary to simulation, in the real-world experiments the robots do not possess mutual localisation sensors, therefore the software architecture for multi-robot formation control was employed for properly designing every functionality of the multi-robot system. The communication scheme of the distributed architecture is shown in Figure 4.13. Using this distributed architecture the system is able to share the robots and human poses within the whole team.

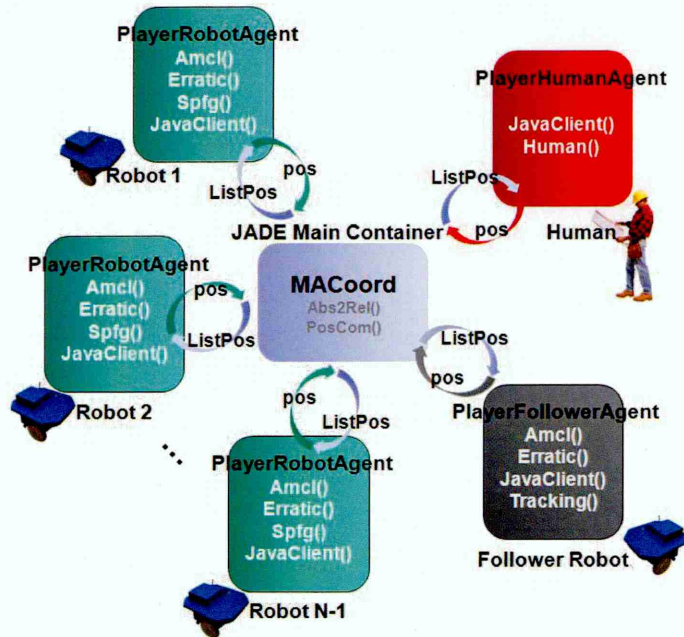


Figure 4.13: Coordinator agent communication scheme.

Each robot is provided with a map of the environment, on which they localise themselves to obtain their absolute pose (x, y, θ) using the Adaptive Monte-Carlo Localisation algorithm (Fox, 2001). The central repository coordinator (MACoord) takes care of collecting the robots' localisation data, store it and distribute it to each agent. Employing this distributed architecture the system is capable to share all the robots and human poses through the whole team, allowing any control method to take advantage of these essential data.

4.2.2 Initial experiments Initial tests of the real-world experiments employing the aforementioned distributed software architecture were conducted during the development of the thesis. The main goal of these tests was to validate in a structured way the main solutions of the software and hardware architecture such as communication, involved hardware, types of agents, localisation algorithms and most importantly the different agent functionalities.



Figure 4.14: Initial implementation of the distributed system architecture.

In order to simplify initial validation, the first trials were done without a real human. Instead, a remote controlled mobile robot mocking the human was employed, further referred as the leader

robot. Figure 4.14⁹ shows the snapshots of the real-world experiments for the formation control I with the snapshots labeled (a) to (f) in time sequence. In this case three robots were employed as robot peers and another one acted as a leader. The lower corner of each snapshot shows the absolute positions of each component of the group in the given 2D map.

The software architecture was launched and the overall performance of the group was qualitatively observed. An operator was able to freely control the leader robot, that can be seen in Figure 4.14a placed in the center and represented with a red circle in the snapshots and in the given map representation. The test started with the robots placed at some random initial positions (Figure 4.14a). Afterwards, the leader robot was remotely moved around the environment and the performance of the robot peers were recorded. The snapshots 4.14b and 4.14c show that as soon as the leader starts moving a robot peer that is within the leader's trajectory moves rapidly away while the other robots follow the leader. In the snapshots 4.14d to 4.14e the leader was moved to maximum speed to observe if the robots could catch up. The leader was stopped at the position shown in Figure 4.14f and the robot peers started to come closer to the leader. At the end of the test the robot peers under the formation control I ended up in a situation similar to the starting one, however in this situation the leader is the one placed on the left side of the formation, as in the initial situation the leader was in the middle.

Another trial was performed in order to observe how the group performed with non-represented obstacles, that is an object that is not present on the given 2D map. For that reason, as seen in Figure 4.15⁹, a tall bin was placed in the middle of the environment. The leader was remotely controlled to move along the wall and the behaviour of the robot peers were observed.

The leader robot, marked as before with a red circle, moves on the right side of the picture above. The three robot peers placed in the center of the snapshot 4.15a under the control of method 1 have to follow the leader, maintain the flexible formation and avoid non-represented obstacles. As the snapshots 4.15b and 4.15c show, the mobile robots do follow the leader and go around the bin while they also avoid colliding the other members of the team. Last snapshot 4.15d show how the group has passed the obstacle and continue maintaining formation with the leader.

At this stage the qualitatively observed results were promising, since the team was able to generate and maintain formation during the experiments. The next step in order to conduct extensive experiments in human multi-robot systems was obviously to include the human into the formation.

⁹Copyright images of the Guardians project mid-term review



Figure 4.15: Initial obstacle avoidance trials.

4.2.3 Human follower Using only the laser range finder information we intended to detect and track a human walking in front of the mobile platform, similar to the work in (Nomdedeu et al., 2008). The image sequence showed in Figure 4.16 represents this process. Given the initial position (Figure 4.16a) of the human within the field of view of the robot, the first step of the method is to search in a specific area (range ϵ and distance δ) for an object of a certain width (Figure 4.16b). This object represents the legs of the human. In this figure it can be seen in red the readings of the laser range finder, where the x-axis represents the bearing and y-axis represents the distance.

The second step consists to track the human. A linear search is performed on both sides of the initial position of the legs to find the object's width. The object dimensions is represented by the blue rectangle in Figure 4.16c. The blue box represents the detected and tracked object, in green the human's legs and in red the walls and obstacles.

Figure 4.17 shows the process of detecting and tracking the human's legs over time. Initially (top) it can be seen how the distance between the human and the robot increases. In this case, the robot is moving deliberately slow to let the human gain some distance. Once the human is at the desired relative distance (Figure 4.17 middle), the robot starts following. The bottom row shows

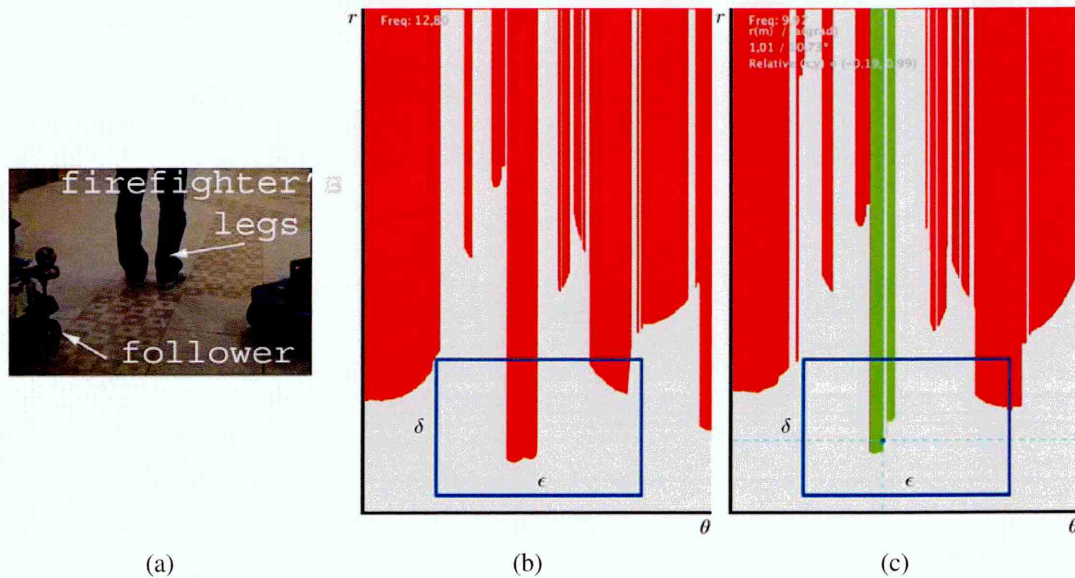


Figure 4.16: First step: finding the human.

the sequence when the human walks near the wall. In a control loop the distance to the human is calculated and the robot maximum velocity and turn rate is set proportional to the distance. An obstacle avoidance routine that uses sonar and laser information is at any time employed to ensure the safety of the human and of the robot itself. Due to the relative low velocity at which a human walks and the high laser scan rate, it is safely assumed that the human will be at the near neighbourhood of the previous detected location. Therefore, the last detected location is used to search for the object's new position and track the human's legs.

4.3 Scope and limitations

At the beginning of the work it was determined that no attempt would be made to simulate the physical and navigational abilities of a real human. In this thesis the human is simply considered as an agent that moves freely throughout the entire environment. This assumption is according to the role of the human in the fire and rescue service manual of working practices.

It is assumed that the problems of moving rapidly over uneven terrain are general, separate engineering issues; likewise issues of long-term autonomy and individual physical robustness. Solutions to these problems would be necessary but not sufficient to allow the construction of a useful human multi-robot team. This work examines the sort of control strategies that must be developed if a group of robots is to gather around a human and navigate accordingly to its motion.

Distinguishing the human from other supporting objects is absolutely fundamental to achieving the aims of the scenario. If the robots cannot distinguish the human they will not be able to

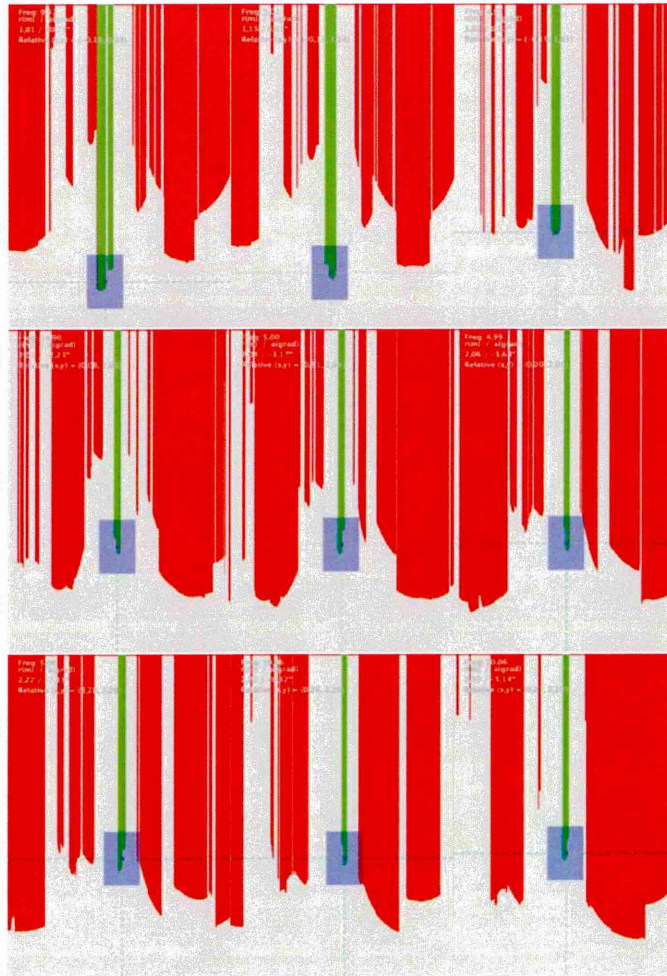


Figure 4.17: Second step: Sequence of the human tracking.

stay close and follow. The solution that has been adopted is for the robots to have a priori knowledge of the initial position of the human and then subsequently track him as he moves away from that position. The advantage of this approach is that it requires no additional hardware - the robots simply use their existing sensors to track the position. However if the robot loses sensor contact with the human for a significant period of time, due to the line of sight being broken by an obstacle or another robot, it might not be possible to re-establish contact. The reason for this is that even if the robot subsequently reacquires a line of sight it might well be unable to positively distinguish among the human and other surrounding objects, particularly moving ones i.e. the other robots. Naturally, a hardware solution could be employed. For example, marking the human with special clothing (RF tags) or employing the kinect sensor would allow the robots to immediately detect the human at the start of the mission as well as giving the robots a much better chance of reacquiring contact should it be subsequently broken. In (Sales et al., 2010) some initial research to person following using a combination of laser range finder, sonar and vision sensors under different low-visibility conditions was researched. Nevertheless this solution requires a study to assess the reliability and accuracy of this method and it was unfortunately beyond the scope of this work.

Moreover, it is recognised that one of the major differences between the real-world and the simulated system is the lack of detection and identification on board (Section 4.1.3). In simulation each robot is capable of detect and distinguish among obstacles, humans and other robots solving the mutual localisation problem. Transferring this ability into the real world would be a significant challenge and was unfortunately beyond the time constraints of this work, although during the first stage of this work it was considered as a problem to solve. The decentralised algorithms used to control the simulated robots with mutual localisation sensors are completely identical to those demonstrated on the real-world system without mutual localisation sensing.

In our experiments a 2D map of the environment is available prior to the trials; such a map should be accurate in its measurements and boundaries, however it may not include some or all possible obstacles. This is due to the localisation algorithm employed by each robot to obtain its absolute pose and the relative positions of all the other agents of the team. One might argue that a 2D map is not always available and represents an important constraint of the system portability. Nevertheless, a simultaneous localisation and mapping algorithm could be used instead, although in our case for the mere fact of having an experimental working setup it was decided to employ an effective localisation technique, as the adaptive Monte-Carlo algorithm, with a given 2D map.

At last but not least, through all the experiments we had available a reliable Wi-fi network and there was reduced or no magnetic interference. This might play an important role to take into account when performing on large open-space scenarios (i.e. large warehouse or commercial center), where the strength of wireless networks might vary considerably. However, this issue was unfortunately out of the scope of this work.

4.4 Summary

In order to conduct a systematic study to investigate the effects of changing the key variables that influence the HMRS navigation behaviour a formalised version of the scenario is proposed for the initial simulations. The team consists of a group of four robots, the human and a confining enclosure or the environment within which to observe the basic behaviour of the robots under the influence of the potential functions.

Although a suitable simulation tool is employed the transfer between simulation and hardware is not straight forward as discussed in Section 4.2. Due to the lack of a robust and efficient technology to solve the mutual detection problem a provisional solution has been employed. This consists in designing a distributed software architecture that would bring an alternative to using mutual detection sensors. After all, the expected output of an on board mutual detection sensor would be a list with the relative positions of the surrounding elements (robot peers, obstacles and human). The usage of central repository instead, to collect each agent absolute pose and publish

the aforementioned list is a transparent and suitable alternative in the context of our research questions, the control strategy and the expected grouping behaviour. However, it contradicts the Guardians aim of a fully decentralised system.

Chapter 5

Formation Control I

The previous chapters have described the experimental setting for a multi-robot system designed to navigate with a human. This chapter presents the simplest yet sufficient control framework to achieve human multi-robot system navigation. The methodology employed during this chapter is the following:

- a** present the hypothesis to be tested
- b** define the algorithm to achieve HMRS navigation
- c** test the algorithm in simulation and in real.

Metrics for examining the success of the simulated and real-world trials devised in Chapter 3 are used in this chapter together with a summary of the results of the simulated and real-world trials. This chapter ends with a discussion and a conclusion about the control Method 1, its advantages, drawbacks and a further work to be developed.

Work presented in this chapter has been published as refereed conference papers (Saez-Pons et al., 2008; Alboul et al., 2008; Saez-Pons et al., 2009; Alboul et al., 2009; Naghsh et al., 2010) and journal papers (Saez-Pons et al., 2010; Penders et al., 2011).

To assist the reading and understanding of this chapter the following Table 5.1 is included in order to summarise the terminology employed.

Table 5.1: Terminology.

Parameter	Description
SB	Sensor boundary
R	Robot
O	Obstacle
Neighbouring components or Peers	Components of the group within SB
Robot-Peer force	Force that acts between robot and peer
Robot-Obstacle force	Force that acts between robot and obstacle
\vec{F}_S	Resulting Social Artificial force
\vec{v}	Velocity vector of each robot
$\ \vec{v}\ $	Velocity vector magnitude or robot speed
V_{max}	Maximum velocity
Δt	Simulation time step
\mathcal{P}_{Peer}	Robot-peer potential function
\mathcal{P}_{Obs}	Robot-obstacle potential function
f_{Peer}	Magnitude of the Robot-peer artificial force
f_{Obs}	Magnitude of the Robot-obstacle artificial force
$d_{R_n}^{R_j}$	Distance between robot R_n and R_j
\hat{U}	Unit vector
f_{max}	Maximum of a potential force
w	Horizontal shift parameter or contact distance
k	Compressing ($k < 1$) or stretching ($k > 1$) parameter
% <i>tif</i>	Percentage of Time In Formation
SE	System efficiency
fft	Formation for first time
SP	Starting position
FP	Final position
RT	Robot trajectory
HT	Human trajectory

5.1 Hypothesis

Our flexible formation Definition 3.2 states that a group of robots and a human are in formation if the agents (human or robots) are uniformly dispersed and if there exist a connected graph covering the group. Keeping in mind this definition, the experiment described in this chapter has been designed and conducted to test the following hypothesis:

1. A flexible formation can be achieved by exploiting the “social relations” among robots, whereby the formation is generated directly from the attraction/repulsion interaction between the components of the team (human and robots) and the repulsion with the obstacles

in the environment.

2. Following from 1, the group of robots will maintain the formation whilst the human is in motion.
3. A simulated formation control can be used to design and test a formation controller that achieves 2. If the control model captures the underlying mechanism of formation, then the same algorithm that controls the model's behaviour should control the real robots.

An algorithm is presented that generates a flexible formation as proposed in hypothesis 1 and moves the mobile robots as suggested in hypothesis 2. This control algorithm will be referred as the Formation Control I (FCI). A set of simulation trials will test the FCI and show that the HMRS generates and maintains a formation. A number of similar real-world trials with the same controller running on the physical robots will be set to test hypothesis 3.

5.2 Algorithm

The basic mechanism is that at each time step the control algorithm must generate a velocity vector \vec{v} for each robot's controller to execute. Each robot's velocity vector is given by the Listing 5.1. A robot is attracted and/or repulsed by all neighbouring components (human and other robots within its sensor boundary, SB). These neighbouring components will be referred as "peers". The resulting force causes the robots to maintain a common distance between them and it will be referred to as the "Robot-Peer force" (line 5). At the same time, each robot avoids the nearest obstacle by means of the repulsive "Robot-Obstacle force" (line 9). A more detailed description of these forces will be given below. The sum of these two forces results in the "Social Artificial force" (line 11).

Using a discrete-time approximation to the continuous behaviour of the robot with time-step Δt and the social artificial force \vec{F}_S , the algorithm determines the velocity vector of each robot $\vec{v} = (v_x, v_y)$ (line 13). The speed of the robot, that is the magnitude of the velocity vector or $\|\vec{v}\|$ (line 19), is bounded to a maximum velocity V_{max} (lines 15 to 18). The direction of the robot is represented by the angle of components of the velocity vector $\tan^{-1}(v_y/v_x)$ (line 20). Finally the robot moves with the calculated speed and direction (line 21)

Listing 5.1 Compute Motion for FCI.

```

1: for all peers do
2:   determine the distance  $d$  and relative direction  $\theta$  to peer  $R_j$ 
3:   calculate peer  $\vec{A}$  attraction force (d)
4:   calculate peer  $\vec{R}$  repulsion force (d)
5:   Robot-Peer force  $\leftarrow \vec{A} + \vec{R}$ 
6: end for
7:
8: determine the distance  $d$  and relative direction  $\theta$  to nearest obstacle  $O$  within  $SB$ 
9: calculate Robot-Obstacle force (d)
10:
11:  $\vec{F}_S \leftarrow$  Robot-Peer force + Robot-Obstacle force
12:
13:  $\vec{v} \leftarrow \vec{v} + \Delta t \cdot \vec{F}_S$ 
14:
15: if  $\|v\| > V_{max}$  then
16:    $v_x \leftarrow (v_x \cdot V_{max}) / \|v\|$ 
17:    $v_y \leftarrow (v_y \cdot V_{max}) / \|v\|$ 
18: end if
19:  $speed \leftarrow \|v\|$ 
20:  $direction \leftarrow \tan^{-1}(v_y/v_x)$ 
21: move the robot with speed and direction

```

5.3 Control Model

Let us define the social artificial force considering N autonomous mobile agents denoted with R_n , where $n = 1, 2, \dots, N$ and the nearest obstacle denoted with O , situated in a two dimensional plane \mathcal{R}^2 . The social artificial force \vec{F}_S of R_n is defined as

$$\vec{F}_S(R_n) = -\nabla \mathcal{P}_{Obs}(d_{R_n}^O) + \sum_{j=1, j \neq n}^N -\nabla \mathcal{P}_{Peer}(d_{R_n}^{R_j}) \quad (5.3.1)$$

where \mathcal{P}_{Obs} is the robot-obstacle potential function, \mathcal{P}_{Peer} is the robot-peer potential function, $d_{R_n}^O$ is the relative distance of R_n with the nearest obstacle O within SB , $d_{R_n}^{R_j}$ is the relative distance of R_n with other peers R_j within SB

The line along which the “forces” derived from the potential functions act, is defined by a unit vector \hat{U} which by convention always points to the centre of the object under consideration from surrounding objects. So for example, if we were calculating the force on a robot R_i due to a neighbouring robot R_j (Figure 5.1) the direction vector would be defined as $\hat{U} = U_{R_i}^{R_j} / |U_{R_i}^{R_j}| = (X(R_i) - X(R_j)) / |X(R_i) - X(R_j)|$ where $X(R_i)$ and $X(R_j)$ are the positions of robots R_i and R_j respectively. To obtain the resulting force we multiply the unit direction vector by the

magnitude of the artificial force. By convention we deem repulsive potentials to be positive and attractive potentials to be negative. Therefore a positive potential results in a force driving R_i away from R_j whilst a negative potential would give a force pulling R_i towards R_j . Determining the direction of a force from the sign of the potential is somewhat unsatisfactory, normally a force is defined as minus the gradient with respect to distance d of the potential, the sign of the potential is irrelevant. As a result, equation 5.3.1 is simplified as follows:

$$\vec{F}_S(R_n) = f_{Obs}(d_{R_n}^O)\hat{U}_{R_n}^O + \sum_{j=1, j \neq n}^N f_{Peer}(d_{R_n}^{R_j})\hat{U}_{R_n}^{R_j} \quad (5.3.2)$$

where $f_{Obs}(d_{R_n}^O)$ is the magnitude of the robot-obstacle artificial force, $f_{Peer}(d_{R_n}^{R_j})$ is the magnitude of the robot-peer artificial force and \hat{U} represents the unit vector, $\hat{U} = U/\|U\|$.

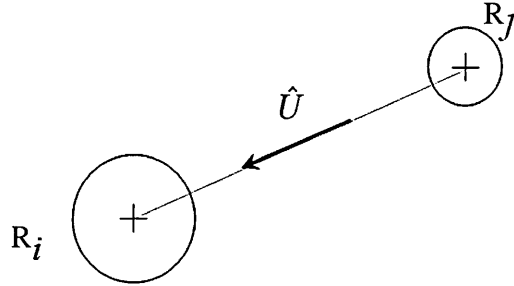


Figure 5.1: Convention for differentiating repulsive and attractive forces.

The repulsive robot-obstacle artificial force which prevents the robots to collide with the nearest obstacle in the environment is defined by

$$f_{Obs}(d_{R_n}^O) = \begin{cases} -f_{max} , & d_{R_n}^O \leq w_o \\ -\frac{1}{(k_o(d_{R_n}^O - w_o))^2} , & d_{R_n}^O > w_o \end{cases} \quad (5.3.3)$$

where k_o , w_o and f_{max} are scaling parameters. A more detailed description of this force and parameters will be given in Appendix A.1.

The robot-peer artificial force that allows each robot to approach and keep the human and other robots within their sensor range is defined by

$$f_{Peer}(d_{R_n}^{R_j}) = \begin{cases} -f_{max}, & d_{R_n}^{R_j} \leq w_r \\ f, & w_a > d_{R_n}^{R_j} > w_r \\ f_{max}, & d_{R_n}^{R_j} \geq w_a \end{cases} \quad (5.3.4)$$

where w_r , w_a and f_{max} are scaling parameters, f is composed by a repulsive term to prevent R_n colliding with the peers within SB and an attractive term to keep the robot at safe distance. Both, repulsive and attraction are inversely proportional with the distance $d_{R_n}^{R_j}$ of the form:

$$f = \frac{1}{(k_a(d_{R_n}^{R_j} - w_a))^2} - \frac{1}{(k_r(d_{R_n}^{R_j} - w_r))^2} \quad (5.3.5)$$

where k_r , k_a , w_r , w_a and f_{max} are scaling parameters (Appendix A.1), and \vec{F}_S is used to compute the individual robot's motion (direction and speed) as stated in Listing 5.1.

The values of the parameters of Robot-Obstacle and Robot-Peer artificial forces employed to control the motion of each robot with the FCI are shown in Table 5.2.

Table 5.2: Values of the parameters for FCI.

Artificial force	Parameter Value
Robot-Obstacle	$k_o = 5.00, w_o = 0.45$
Robot-Peer	$k_r = 5.00, w_r = 0.95$ $k_a = 2.00, w_a = 4.00$

5.4 Simulation trials

5.4.1 Procedure FCI is first tested in simulation using the software and methods explained in Section 4.1.3. The human is placed at the starting position (for all the trials in Simulation and in Real-World the human position will be always the same) and the simulated robots are placed in the environment at the same initial positions as in the real-world trials, allowing for a later comparison.

The simulation starts and the positions of the robots and the human are logged for the whole trial. After a minute the human starts moving at a constant speed of $0.2m/sec$ towards a final position, that has been chosen to be 7 meters from the start. Once at the goal, the human stops

moving but the system is still running until it stabilises (i.e. becomes motionless) allowing continued observation of the system behaviour. The experiment was repeated ten times and in each trial the simulated robots were placed at the same positions (Figures in Appendix B shows the values of the initial positions of the robots in each trial).

5.4.2 Example Simulated Trial In order to better understand the simulation trials here an example is given and explained step by step.

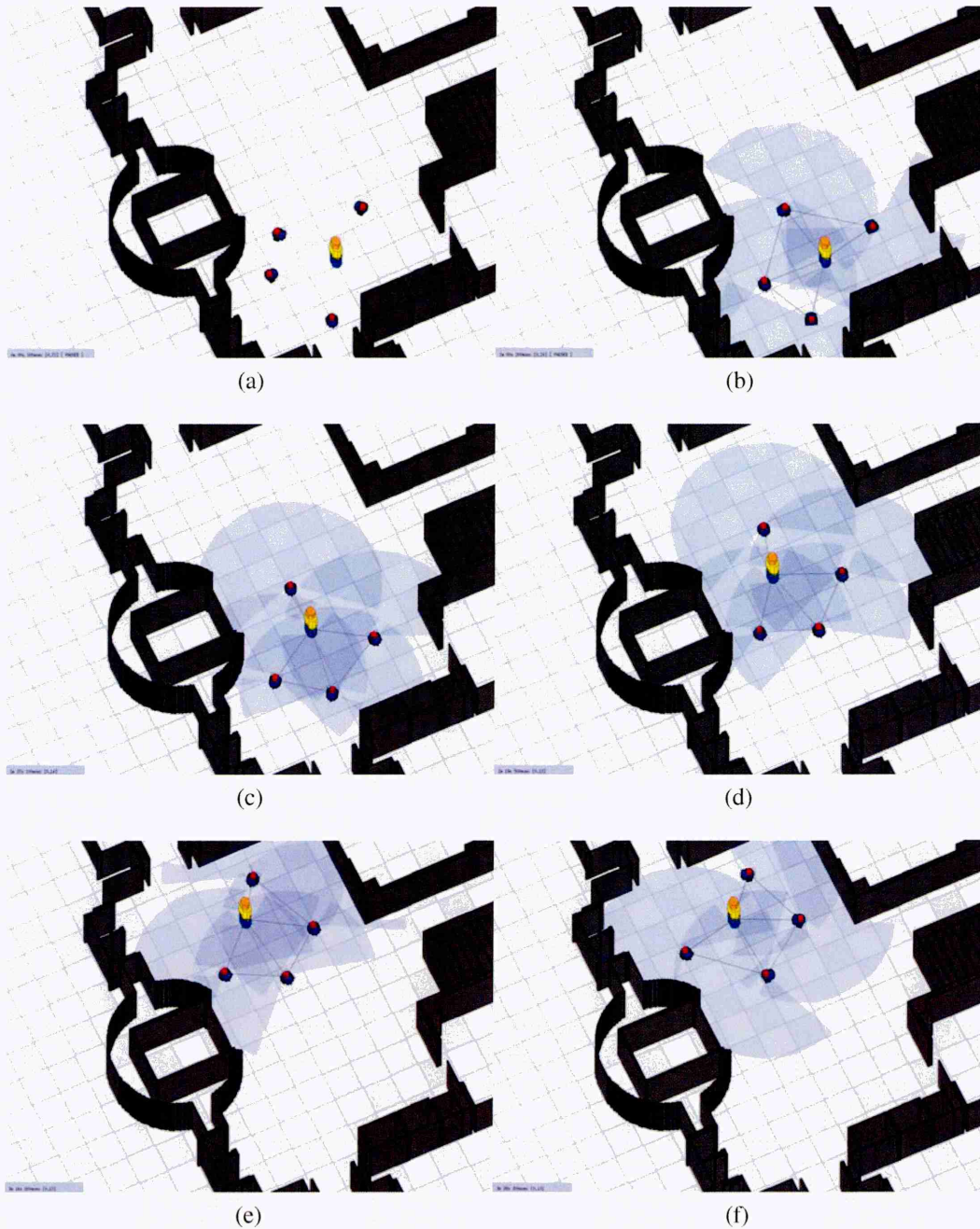


Figure 5.2: Example of the FCI in a simulated trial.

Figure 5.2 shows snapshots from the simulator during a single trial, with the snapshots labeled (a) to (f) in time sequence. This sequence shows that controller performs the required task with some success. As the trial begins (Figure 5.2a) the robots are placed at their initial positions in the environment and the human will be always placed at the same starting location. It is interesting to notice that the robots are placed in a dispersed way but always maintaining a connected graph among the elements of the team (as defined in Section 3.2). The simulation begins and the human is kept still whereas the robots' motion goes under FCI. The robots are allowed to settle for a minute (Figure 5.2b). It is important to notice that the robots get dispersed in the environment according the robot peers and obstacles positions within SB. This first step will be referred as the "formation generation" stage.

After the formation has been generated, the human starts moving towards the top side of the environment in straight line and pulls the group of robots with it (Figure 5.2c). The mobile platforms follow the human's movement through the environment whereas avoiding collision with other robot peers and the surrounding walls/objects (Figure 5.2d). It is interesting to observe how the robots reorganise themselves in an emergent mode to occupy the empty space of the environment. Once the human reaches its final position on the top side of the scene and after traveling for seven meters the human stops moving (Figure 5.2e). The robots are allowed to continue moving until they settle down (Figure 5.2f). From the situation where the human starts moving until it stops will be referred as the "formation maintenance" stage.

5.4.3 Results According to the percentage of time in formation ($\%tif$) parameter shown in Table 5.3 we will present the simulation trials figures corresponding to the trial 5 (Figure 5.3) and trial 9 (Figure 5.4). Trial 9 represents in simulation the trial with lowest $\%tif$ while trial 5 represents the trial with highest $\%tif$. The rest of the simulation trials figures for the FCI can be found in Appendix B. The environment used for the trials in the simulations is a representation of the environment used in the real-world trials in Section 5.5.

A plot of the paths of each robot ($R1 \rightarrow R4$) during the formation generation stage with the still human (*Human*) at the starting position is given (top). The plots of each robot path are labeled with the robot starting position (*SP*), robot finishing position (*FP*) and the robot trajectory (*RT*). Also given is the figure of the formation maintenance stage (bottom) with the plot of the human path labeled as the human trajectory (*HT*).

The *Percentage of Time In Formation* ($\%tif$) and the *System Efficiency* (SE) data is presented in Table 5.3 with their means and standard deviations.

During trial 5 the percentage of time in formation of the team is 100%. Meaning that the robots and the human are the whole time of the formation maintenance stage in formation. On the other

hand, the percentage of time in formation for the trial 9 is 31.50%, which is the lowest performance among the ten trials realised for the FCI in simulation. The reason is basically because two robots do not detect the human ($R2$ and $R3$) and therefore they drop the performance of the system.

At this stage the FCI looked promising. The trials in simulation showed that it works over of range of parameters and starting robot starting positions and situations. The way the group of robots moved with the human is not ideal; it would be preferable for the group of robots to move more cohesively. However, the simplicity of the method was appealing and it seemed directly to prove the hypotheses at the beginning of this chapter. It was determined that FCI would be tested on the real-world system.

For comparison with later trials the average percentage of time in formation over ten trials for FCI in simulation was 84.81% with a standard deviation of 22.29%. The average efficiency over ten trials was 0.89%.

Table 5.3: Summary of results for FCI simulation trials.

	SE	%tif
Trial 1	0.86	72.23
Trial 2	0.96	95.52
Trial 3	1.01	100.00
Trial 4	0.89	89.88
Trial 5	0.85	100.00
Trial 6	0.97	100.00
Trial 7	0.94	100.00
Trial 8	0.85	100.00
Trial 9	0.74	31.50
Trial 10	0.87	61.99
Mean	0.89	84.81
std.dev.	8.12	22.29

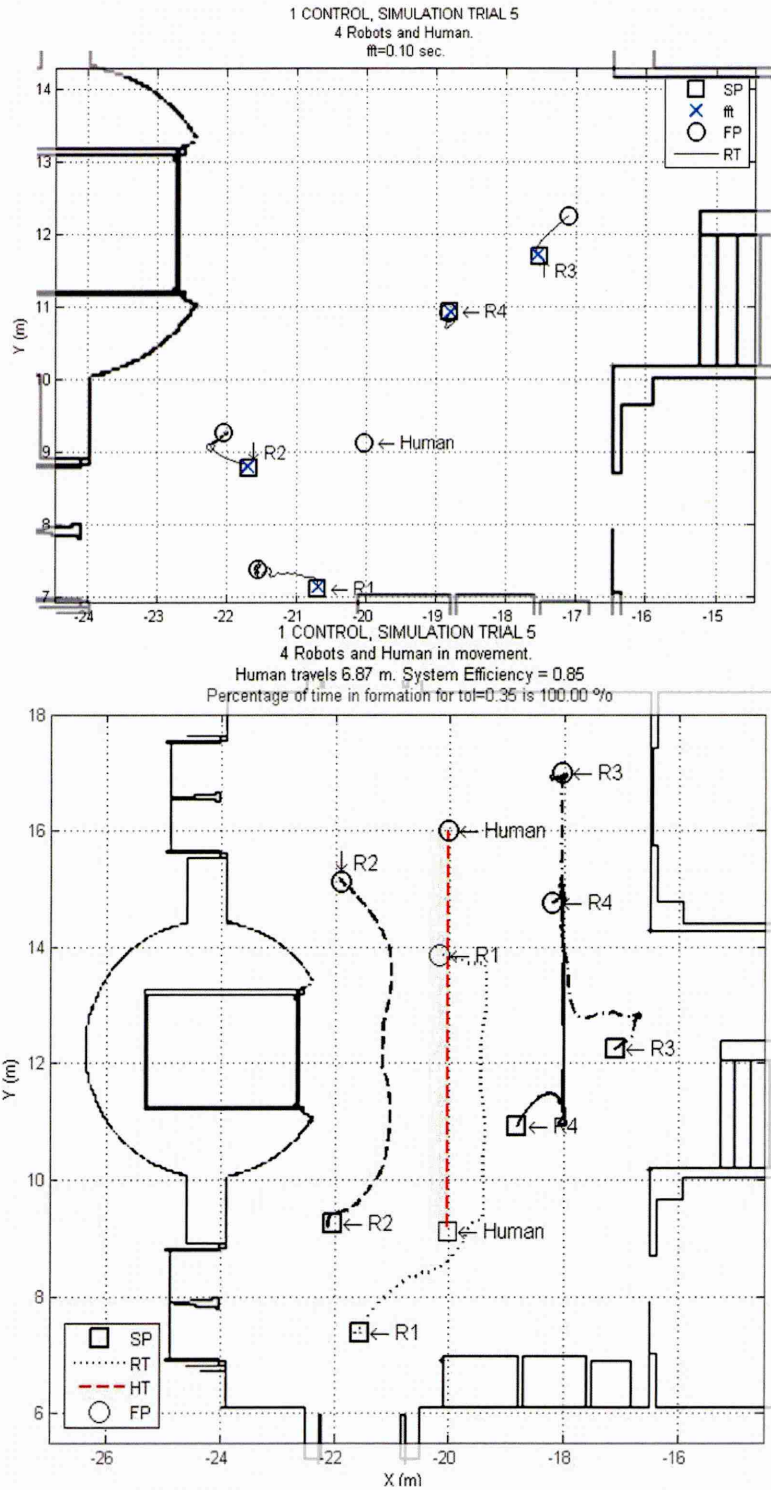


Figure 5.3: Trial 5 of the FCI in simulation (highest %*tif*).

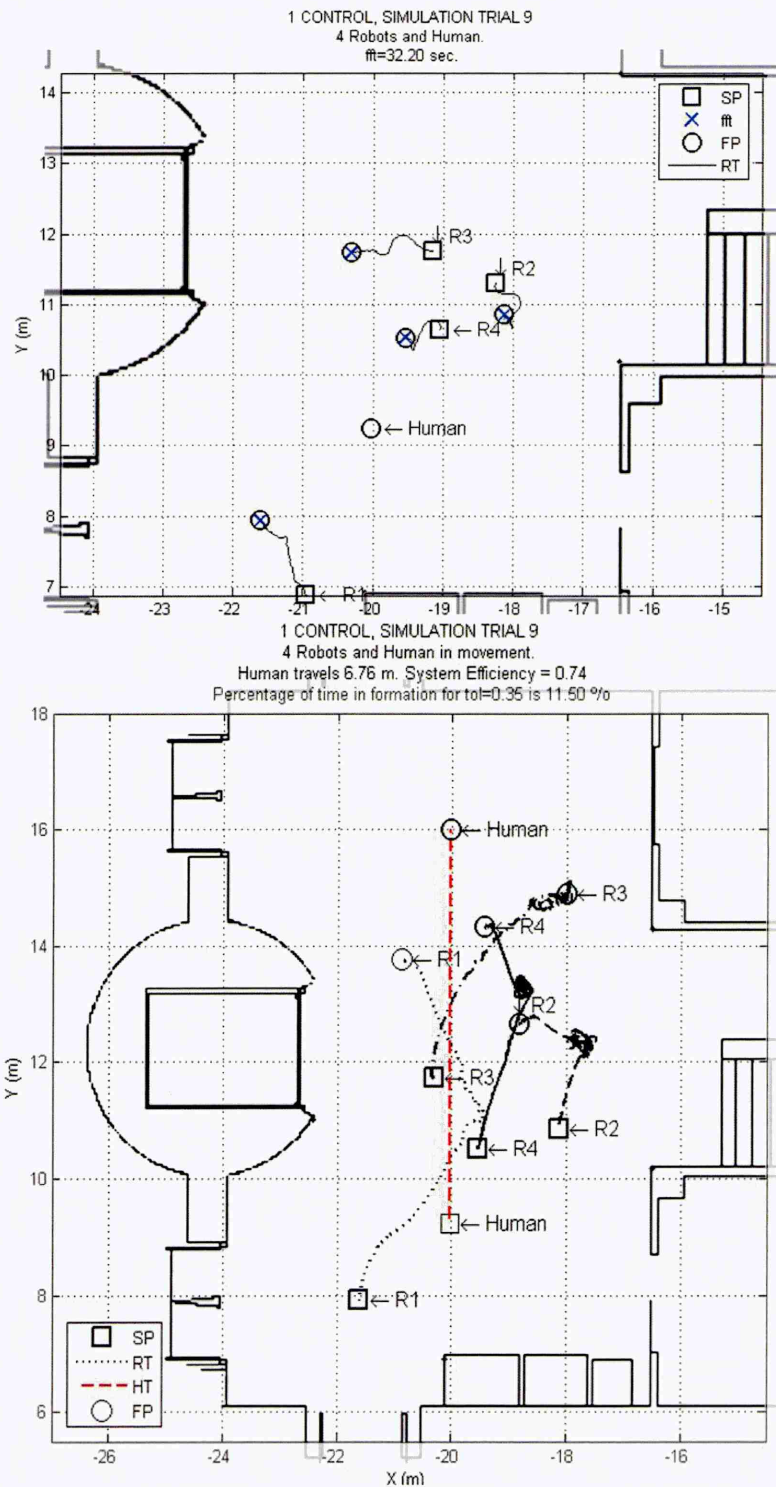


Figure 5.4: Trial 9 of the FCI in simulation (lowest %*tif*).

5.5 Real-world trials

5.5.1 Procedure The trials in the real-world was then repeated using the human multi-robot architecture explained in Section 4.2. We aimed to set the procedure for the real-world trials as closely as possible to the conditions allowed by the simulation trials. The mobile robots were placed randomly in the environment but always distributed in a connected graph. With the human still at the initial location the system starts, the robots start moving under FCI. As in simulation, we let the system to run for a minute for the “formation generation” stage. One minute is time sufficient for the formation to be built up. Afterwards, the human starts to move at constant velocity to a final position that is 7 meters further to the other end of the environment. The robots start to follow the human (“formation maintenance”). When the human arrives at the final position it stops but the systems continues running until the systems stabilises, i.e. the robots stop moving, allowing continued observation of the system’s behaviour

The real-world experiment, from the formation control point of view, is identical to the simulation experiment. From the functional perspective, the main difference is the human-follower dedicated vehicle in the real-world trials. The motion of this dedicated robot is dictated by the human since the follower’s task is to detect, follow and broadcast the human position to each robot in the system. It is agreed, that the robots do not possess any mutual localisation sensors for detecting other robots, the human and obstacles of the environment due to the lack of a robust and efficient technology to solve this problem. However a solution was presented in Section 4.2.1. This consists in designing a distributed software architecture that would bring an alternative to using mutual detection sensors. The usage of central repository agent instead to collect each agent absolute pose and publish the aforementioned list is a transparent and equivalent alternative from the perspective of the robots, the control strategy and the expected grouping behaviour.

As in the simulations, the real-world experiment was repeated ten times (as in simulation) with the ERA-MOBI robotic platforms at different positions, which are matched to the simulation starting positions. The initial location of the human is intended to be always approximately the same for all the real-world trials. The number of real-world trials was conditioned by the considerable time required for each trial, not from the execution time point of view, but from the preparation and set-up perspective. These experiments were conducted at the amenities of the University Jaume I, Castellò, Spain. Figure 5.5 shows some snapshots of the real-world experiments sequence. Figure 5.5a presents the starting positions of the robots and the human. Figure 5.5b represents the “formation generation” stage. Figure 5.5c and Figure 5.5d represent the “formation maintenance” stage.

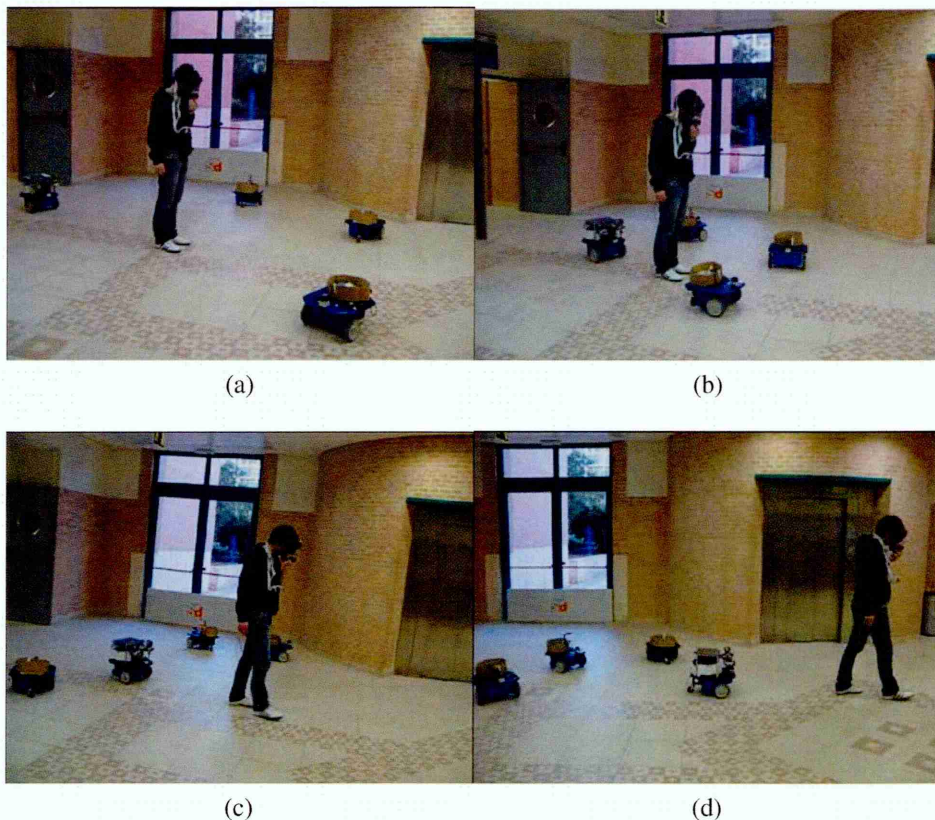


Figure 5.5: Real-world trial.

5.5.2 Results As in simulation, Figure 5.6 and Figure 5.7 represent the real-world trials with highest and lowest $\%t_{if}$ respectively, according to the performance parameters presented in Table 5.4. The rest of the figures corresponding to the real-world trials for the FCI can be found in Appendix B.

As in simulation, plots of the paths of each robot and the human during the formation generation (left) and formation maintenance (right) are given. The path plots of each robot ($R1 \rightarrow R4$) and the human (H) are labeled with the robot start position (**SP**), robot finish position (**FP**), the robot trajectory (**RT**) and the human trajectory (**HT**). The *percentage of time in formation* ($\%t_{if}$) and the *system efficiency* (SE) data is presented in Table 5.4 with their means and standard deviations.

Trial 5 is representative of the moderately successful real-world trials. Figure 5.6 shows that its behaviour is similar to that seen in the simulation trials. The percentage of time in formation for this trial is 60.44%. In the formation generation stage (left) the mobile robots gather around the peers within its sensor boundary. After the human starts moving the mobile robots follow and avoid obstacles (right), where most representative is the noticeable trajectory of robot 2 ($R2$). More significantly is the final positions (FP) of the mobile robots at the end of the trial, where they gather uniformly around the human. Trial 9, represented in Figure 5.7, illustrates a complicated

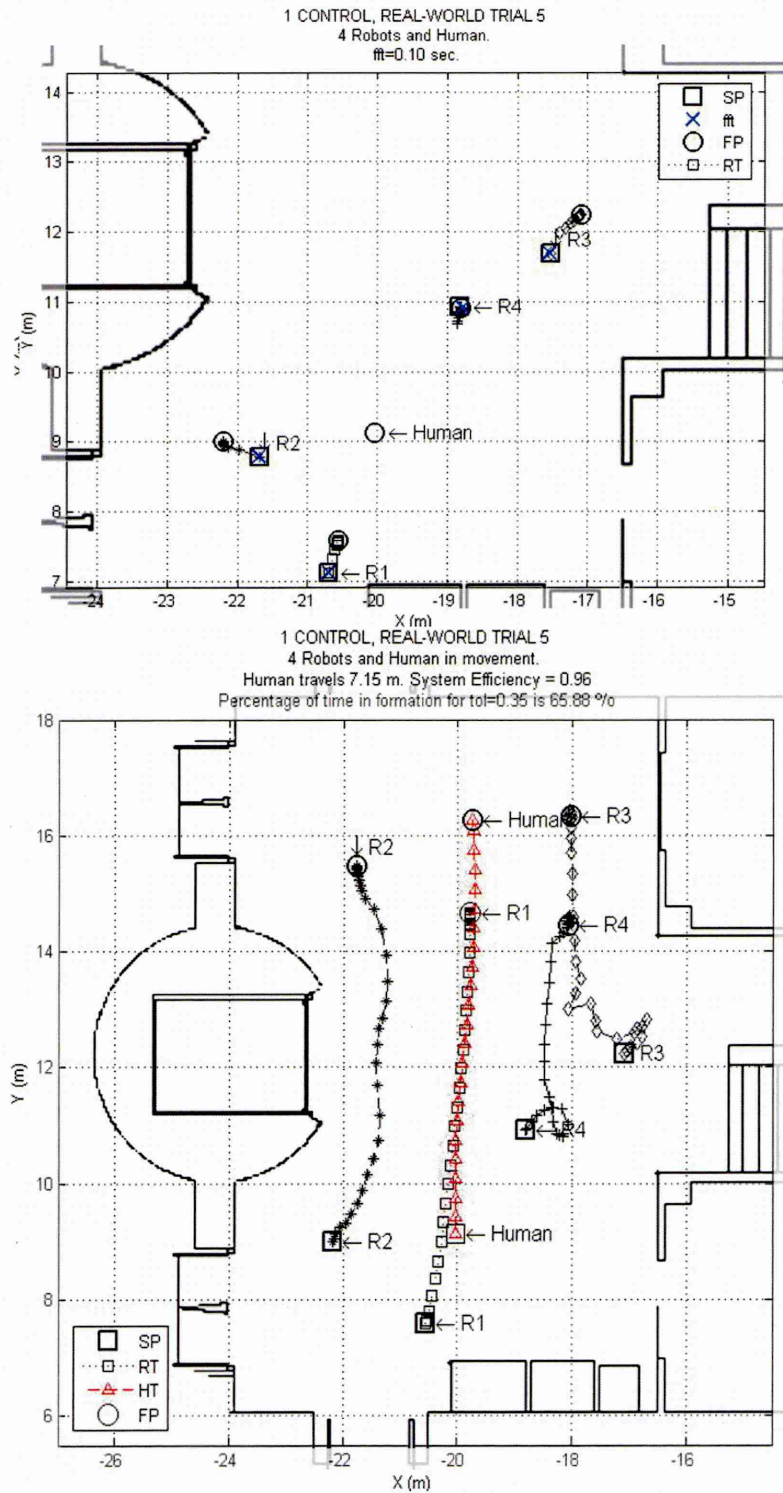


Figure 5.6: Trial 5 of the FCI in the real-world.

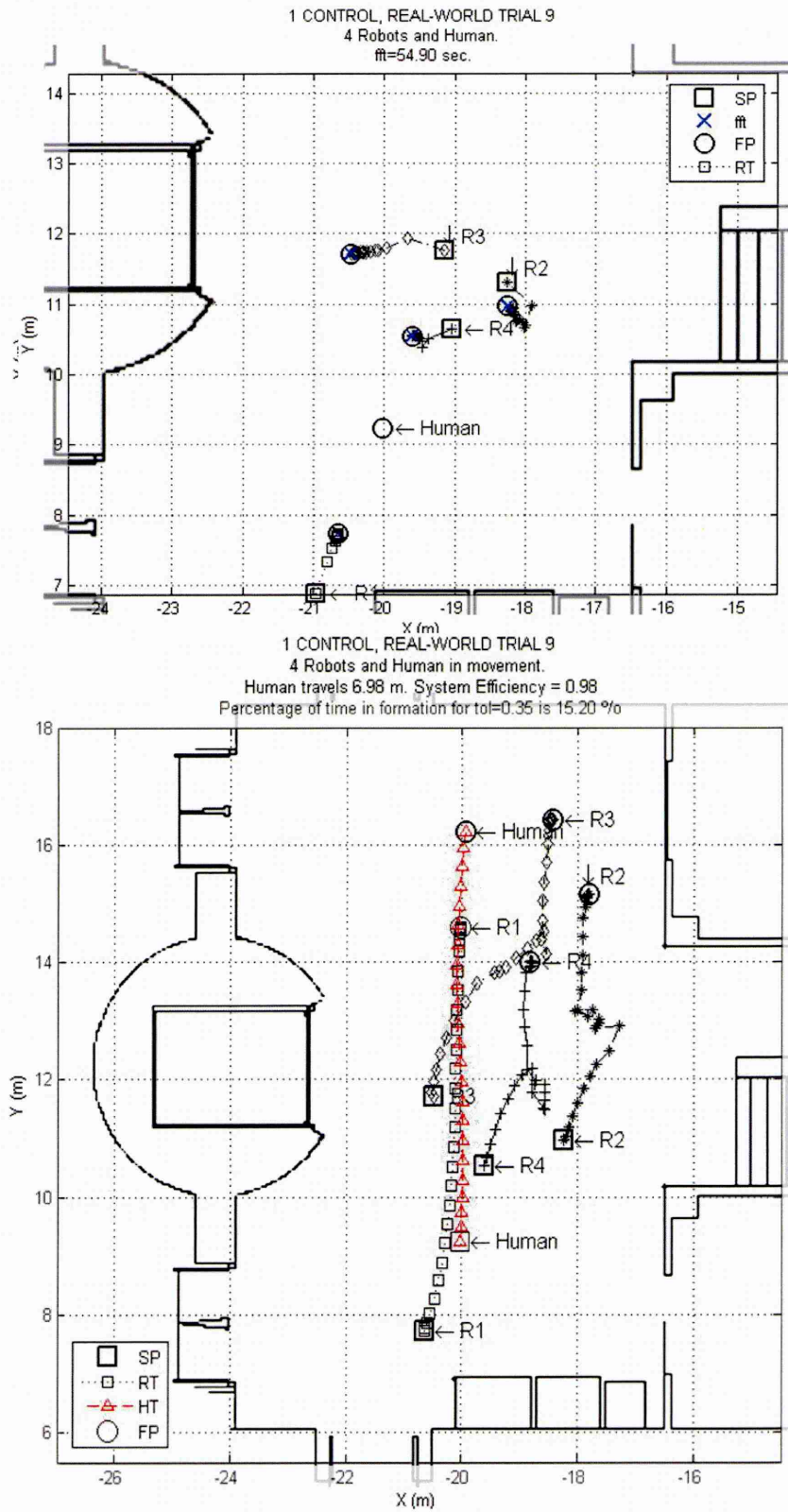


Figure 5.7: Trial 9 of the FCI in the real-world.

Table 5.4: Summary of results of the FCI trials in real-world.

	SE	%tif
Trial 1	0.67	48.18
Trial 2	1.01	60.44
Trial 3	0.39	18.45
Trial 4	0.55	27.77
Trial 5	0.96	65.88
Trial 6	1.10	49.33
Trial 7	0.82	22.94
Trial 8	1.07	34.94
Trial 9	0.98	15.20
Trial 10	0.78	27.20
Mean	0.83	37.73
std.dev.	23.63	17.35

situation, where $R2$ and $R3$ do not have the human within SB . The percentage of time in formation for the this trial is 15.20%. The formation for first time occurs 54.90 seconds after the trial begins (left). During human's movement the group of robots follow with a moderated success. Qualitatively the performance of the FCI in real-world is acceptable, although according to the metrics shown in Table 5.4, the results differ significantly from simulation.

For comparison with later trials the average percentage of time in formation over 10 trials for FCI in the real-world trials was 37.74% with a standard deviation of 17.35%. The average efficiency over ten trials was 0.83%.

5.6 Discussion

Table 5.3 shows that in simulation FCI has 5 out of 10 trials with 100% time in formation ($\%tif$). During the other 5 trials the $\%tif$ varies considerably, as in the trial 9 where this metric drops to 31.5%. However, the $\%tif$ mean of the FCI in simulation is 84.81 with a standard deviation of 22.29. When compared with the metrics of the FCI in real-world experiments this performance metric drops drastically. In real-world the highest $\%tif$ is 65.88, with a mean of 37.33 and a standard deviation of 17.35. The system efficiency (SE) metric of the FCI in simulation has a mean of 0.89 with a standard deviation of 8.12, however in real-world the SE is 0.83 with a standard deviation of 23.63.

It has been very useful to define and employ a set of performance metrics whereby the system can be said to be successful. Without these exemplary metrics would have be very complicated

to consider which trials have been successful or not. One might say that a real-world trial has been successful in the subjective sense that the behaviour is similar to the counterpart simulation trial, and in the objective sense that the group of robots first gather and then accompany the human through the environment. However, let us take for example trial 9 and compare the formation generation and maintenance stages of the simulation and real-world experiments, Figure 5.4 and Figure 5.7, respectively. As it can be seen qualitatively the figures present a similar behaviour and the group of robots manage to accomplish the goal, that is to generate and maintain a flexible formation with a human. Nevertheless, the metrics show that the group of robot do not perform properly and that the robots are most of the time out of formation. Furthermore, these metrics will allow for later comparison with the other method proposed to control the motion of the robots.

5.7 Conclusions

FCI is representative of the moderate success of generating and maintaining a flexible formation of a group of robots with a human in the group. It presents the simplest yet sufficient control framework to achieve human multi-robot system navigation. It has been shown that a flexible formation can be achieved by exploiting the “social relations” among robots, whereby the formation is generated directly from the attraction/repulsion interaction between human and robots, and the repulsion with the obstacles of the environment (hypothesis 1). Moreover, it has been shown that with FCI a group of robots can move according to the human’s movement (hypothesis 2) and that a simulated formation control can be used to design and test a formation controller, which has been transferred to the control of the real robots (hypothesis 3).

Results of several trials are presented and metrics are devised to assess performance. The identical controller for FCI is run on the real robots and tested in a real-world environment. FCI is easy to implement in the real robots and represents a simple yet reliable method. The control strategy allows for a flexible formation capable of dealing with the (static and dynamic) obstacles of the environment and with different amount of robots. However, in the real-world the results are less reliable than in the simulation, but do demonstrate the first decentralised multi-robot control to navigate with a human.

5.8 Further Work

Further informal trials with the simulator have shown that performance can be enhanced by tuning the scaling parameters of the artificial forces employed in FCI. The parameters k_a and k_r can be tuned to control the mutual distance between the peers according to the task the squad is required to perform, allowing for example the group to better deal with obstacles or narrow corridors. The

success of the system is sensitive to changes in these parameters. The large variation likely to be found between different scenarios and over time means that to achieve good performance requires tuning the parameter for each experiment. This could perhaps be achieved with an appropriate adaptive algorithm, but first let us make a consideration of the results obtained with FCI.

The most relevant inconvenient of FCI is that the robots do not distribute uniformly in the environment, that in turn reduces the system performance. Consideration of these results suggested another, simpler formation control algorithm which may solve this problem. This is the subject of the next chapter.

Chapter 6

Formation Control II

The previous chapter showed the design of the Formation Control I in simulation, and its direct transfer to the real world. Though the method succeeded in generating a formation in both simulation and real-world, and maintaining the formation with the human in movement, performance metrics showed that FCI did not work reliably in the real world. This chapter presents an improved control algorithm which is assessed in a set of similar experiments.

The work presented in this chapter has been published as a refereed conference paper in (Saez-Pons et al., 2011a).

This chapter follows the structure of Chapter 5 for easy comparison of figures and tables. The terminology employed here is similar to the previous chapter, however in Table 6.1 we have summarised the terminology that is new in this chapter.

Table 6.1: Terminology.

Parameter	Description
H	Human
Robot-Human force	Force that acts between robot and human
Robot-Robot force	Force that acts between robots
\mathcal{P}_{Hum}	Robot-Human potential function
\mathcal{P}_{Rob}	Robot-Robot potential function
f_{Hum}	Magnitude of the Robot-Human artificial force
f_{Rob}	Magnitude of the Robot-Robot artificial force

6.1 Hypothesis

After observing the results obtained in the previous chapter we conclude that although FCI managed to generate human multi-robot formations, FCI is not suitable to maintain formations when the human is in movement. A general issue of all the trials for FCI is the lack of coherence in the robot team movement. Figure 6.1 shows a general situation of the FCI in action with 6 robots (in blue) and a human (in red). To simplify the illustration there are no obstacles and the sensor boundary has not been drawn. However the arrows between the components of the group indicate which components are neighbouring or within sensor boundary.

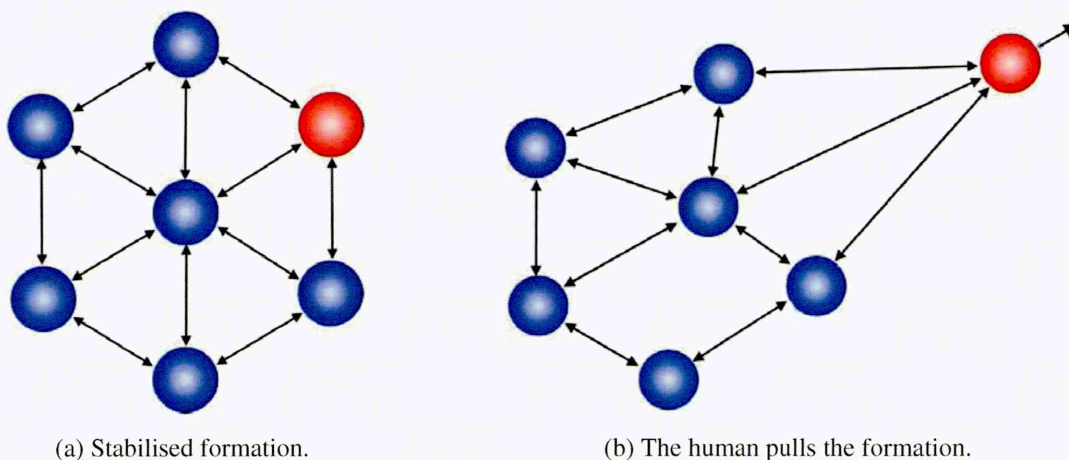


Figure 6.1: Robots acting under FCI.

As it can be seen, FCI can successfully generate a human multi-robot formation (left) and moderately maintain it when the human is in movement (right). However, during the maintenance stage the human pulls the robot team (further referred as the *pulling situation*) and hence the non-coherent movement. In order to solve this problem clearly the human can not simply be another component of the group. Some sort of priority has to be given to the human in order to dictate the motion of the robot team. It is needed somehow to combine simple behaviours to obtain a more complex global behaviour, also known as behaviour-based approach, which in the literature has been shown to be effortlessly implemented in real robots. Our hypothesis is therefore to combine the Social Potential Fields method with the popular behaviour-based approach in order to improve performance metrics in the real-world.

The difficulty when using a behaviour-based approach is to decide when to switch among the simple behaviours in an optimised way. In our case, the decision is clearly imposed by the key component of the robot group: *the human*. The presence or absence of the human within the sensor boundary of each robot will be used as the switching behaviour factor. Therefore, considering the

human as the switching factor two different situations will be possible: the human is within robot sensor boundary (human is present) or it is not (human is absent).

In the case that the human is absent the robots behaviour will be simply the same as in the previous chapter, FCI. In other words, there will be attraction/repulsion with the neighbouring components and repulsion with the obstacles within SB. In the case that the human is present the attraction between the robots will become zero keeping only the repulsion as with the obstacles, whereas there will be attraction/repulsion with the human. This should increase the movement coherence of the group and the uniform dispersion of the robots. This new control strategy, whose algorithm is explained with more detail further down, will be referred as *Formation Control II*.

6.2 Algorithm

Each time step the control algorithm generates a velocity vector \vec{v} for each robot's controller to execute. Each robot's velocity vector is given by the Listing 6.1. If the human is present (line 1) each robot is attracted/repulsed by the human (lines 2-5) and repulsed by the neighbouring robots (lines 6-9). These forces are referred as "Robot-Human force" and "Robot-Robot force" respectively. The sum of these forces results in the "Social Artificial force" (line 10). If the human is absent FCI is applied (line 14).

As with FCI, using time-step Δt and the social artificial force \vec{F}_S , the velocity vector of each robot $\vec{v} = (v_x, v_y)$ is determined (line 17). The speed of the robot $\|\vec{v}\|$ is bounded to a maximum velocity V_{max} (lines 19 to 22) and the direction of the robot $\tan^{-1}(v_y/v_x)$ (line 21) is estimated. Finally the robot moves with the calculated speed and direction (line 25).

Listing 6.1 Compute motion for FCII

```

1: if Human is within  $SB$  then
2:   determine the distance  $d$  and relative direction  $\theta$  to human  $H$ 
3:   calculate human  $\vec{A}$ traction force (d)
4:   calculate human  $\vec{R}$ epulsion force (d)
5:   Robot-Human force  $\leftarrow \vec{A} + \vec{R}$ 
6:   for all other robots within  $SB$  do
7:     determine the distance  $d$  and relative direction  $\theta$  to robot  $R_j$ 
8:     calculate Robot-Robot  $\vec{r}$ epulsion force (d)
9:   end for
10:  determine the distance  $d$  and relative direction  $\theta$  to nearest obstacle  $O$  within  $SB$ 
11:  calculate Robot-Obstacle  $\vec{r}$ epulsion force (d)
12:   $\vec{F}_S \leftarrow$  Robot-Human + Robot-Robot + Robot-Obstacle
13: else
14:  apply FCI
15: end if
16:
17:  $\vec{v} \leftarrow \vec{v} + \Delta t \cdot \vec{F}_S$ 
18:
19: if  $\|v\| > V_{max}$  then
20:    $v_x \leftarrow (v_x \cdot V_{max}) / \|v\|$ 
21:    $v_y \leftarrow (v_y \cdot V_{max}) / \|v\|$ 
22: end if
23:  $speed \leftarrow \|v\|$ 
24:  $direction \leftarrow \tan^{-1}(v_y/v_x)$ 
25: move the robot with speed and direction

```

6.3 Control Model

Contrary to the previous method, FCII needs to make a distinction between the human, the robots and obstacles and apply the corresponding artificial force. Therefore, let us define the social artificial force considering a human denoted with H , N robots denoted with R_n , where $n = 1, 2, \dots, N$ and the nearest obstacle O situated in a two dimensional plane \mathcal{R}^2 . For that reason, we describe the Social Artificial force $\vec{\mathcal{F}}_S$ of R_n as

$$\vec{\mathcal{F}}_S(R_n) = \begin{cases} -\nabla \mathcal{P}_{Hum}(d_{R_n}^H) + \sum_{j=1, j \neq n}^N (-\nabla \mathcal{P}_{Rob}(d_{R_n}^{R_j})) - \nabla \mathcal{P}_{Obs}(d_{R_n}^O), & H \leq SB \\ \text{FCI}, & H > SB \end{cases} \quad (6.3.1)$$

where \mathcal{P}_{Hum} is the robot-human potential function, \mathcal{P}_{Rob} is the robot-robot potential function, \mathcal{P}_{Obs} is the robot-obstacle potential function and $d_{R_n}^O$, $d_{R_n}^H$, $d_{R_n}^{R_j}$ are the relative distances of R_n with the nearest obstacle O .

Following the same notation as with FCI in previous chapter (Figure 5.1) the Social Artificial force can be simplified as:

$$\vec{\mathcal{F}}_S(R_n) = \begin{cases} f_{Hum}(d_{R_n}^H) \hat{U}_{R_n}^H + \sum_{j=1, j \neq n}^N f_{Rob}(d_{R_n}^{R_j}) \hat{U}_{R_n}^{R_j} + f_{Obs}(d_{R_n}^O) \hat{U}_{R_n}^O, & H \leq SB \\ \text{FCI}, & H > SB \end{cases} \quad (6.3.2)$$

where f_{Hum} is the magnitude of the robot-human artificial force, f_{Rob} is the magnitude of the robot-robot artificial force, f_{Obs} is the magnitude of the robot-obstacle artificial force and \hat{U} represents the unit vector.

The robot-obstacle and robot-robot artificial forces have a repulsive form, identical to the repulsion used in FCI, whereas the robot-human artificial force has an identical form as the robot-peer force used in FCI.

The robot-human artificial force, whose functionality is to provide each robot the capability to approach and keep the human within its sensor range, is defined by

$$f_{Hum}(d_{R_n}^H) = \begin{cases} -f_{max}, & d_{R_n}^H \leq w_{hr} \\ f, & w_{ha} > d_{R_n}^H > w_{hr} \\ f_{max}, & d_{R_n}^H \geq w_{ha} \end{cases} \quad (6.3.3)$$

being f composed by a repulsion (left) and attraction (right) term:

$$f = \frac{1}{(k_{ha}(d_{R_n}^H - w_{ha}))^2} - \frac{1}{(k_{hr}(d_{R_n}^H - w_{hr}))^2} \quad (6.3.4)$$

where k_{hr} , w_{hr} , k_{ha} , w_{ha} and f_{max} are scaling parameters. The repulsion term of f prevents R_n from colliding with the human and the attractive term keeps the human within robot sensor boundary. Both, repulsive and attraction part are inversely proportional with the the distance $d_{R_n}^H$. A detailed description of these parameters and a justification of theirs values are given in Appendix A.2. Table 6.2 gives a summary of the parameters employed on the Robot-Human, Robot-Robot and Robot-Obstacle artificial forces for the FCII.

Table 6.2: Values of the parameters for FCII.

Artificial Force	Parameter Value
Robot-Human	$k_{hr} = 5.00, w_{hr} = 0.77$ $k_{ha} = 3.00, w_{ha} = 4.00$
Robot-Robot	$k_r = 4.00, w_r = 0.90$
Robot-Obstacle	$k_o = 5.00, w_o = 0.45$

6.4 Simulation trials

In order to carry out later comparisons, the procedure for the FCII experiments follows the same structure as with the FCI.

6.4.1 Example Simulated Trial This example intends to explain the behaviour of the FCII. Figure 6.2 shows snapshots from the simulator during a single trial for FCII, with the snapshots labeled (a) to (z) in time sequence. Notice that Figure 6.2 represents the same situation as the one seen in Figure 5.2. As the trial begins (a) the robots and the human are placed at the same starting positions as the situation shown in Figure 5.2(a). During the “formation generation” stage, the simulation begins and the human is at rest whereas the robots go under FCII control. The robots are allowed to move for a minute (b). Notice that, dislike with FCI, the robots get uniformly dispersed around the human, which is kept at the center of the formation.

After the formation is generated, starts the “formation maintenance” stage. The human starts moving towards the top side of the environment in straight line and the group of robots move accordingly (c). The mobile platforms follow the human’s movement through the environment

whereas avoiding collision with other robots and the surrounding walls/objects (*d*). Once the human reaches its final position on the top side of the room and after traveling for seven meters it stops moving (*e*). The robots are allowed to continue moving until they stop (*f*). This sequence shows that FCII qualitatively performs the required task with considerable success.

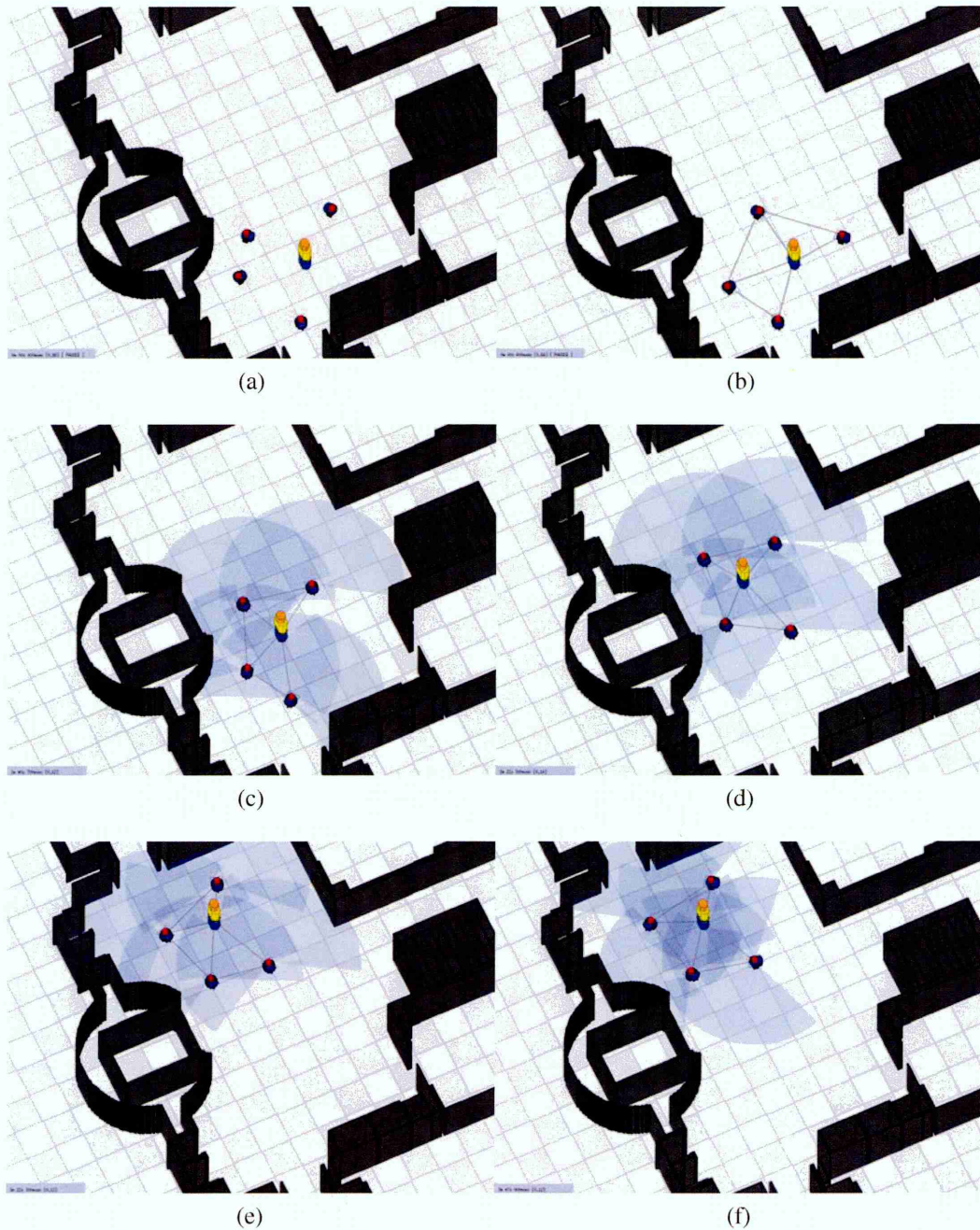


Figure 6.2: Example of the FCII in a simulated trial.

6.4.2 Results According to the percentage of time in formation ($\%tif$) parameter shown in Table 6.3 we will present the simulation trials figures corresponding to the trial 5 (Figure 6.3) and

trial 9 (Figure 6.4). Trial 9 represents the trial with worst $\%tif$ and trial 5 has been chosen as an example of good performance. Notice that trial 5 shows a $\%tif$ as good as trials 1 to 7 and 10. Notice that the situation of Figure 6.3 and Figure 6.4 correspond to Figure 5.3 and Figure 5.4 in FCI, therefore they can be easily compared. The rest of figures for the simulation trials of the FCII can be found in Appendix C.

The top figure gives a plot of the robot's paths during the formation generation with the still human at the starting position. We label the plots of the human path (*Human*) and each robot ($R1 \rightarrow R4$) with robot start position (**SP**), robot finish position (**FP**) and robot trajectory (**RT**). The bottom figure shows the formation maintenance stage with the plot of the human's path labeled as human trajectory (*HT*). Table 6.3 presents the *Percentage of Time In Formation* ($\%tif$) and *System Efficiency* (SE) data with their means and standard deviations.

Table 6.3: Summary of results for FCII simulation trials.

	SE	$\%tif$
Trial 1	0.98	100.00
Trial 2	0.83	100.00
Trial 3	0.96	100.00
Trial 4	0.99	100.00
Trial 5	0.96	100.00
Trial 6	1.04	100.00
Trial 7	0.97	100.00
Trial 8	1.08	93.05
Trial 9	1.09	92.07
Trial 10	0.93	100.00
Mean	0.98	98.51
std.dev.	7.57	3.15

It is important to notice the percentage of time in formation of 92.07 for trial 9. Although it is the lowest of the ten trials in simulation, still represents a very good performance value. Also we shall notice that eight out of ten trials show to be the whole time of the maintenance formation stage in formation, representing good results in simulation for FCII compared with Table 5.3.

At this stage, the performance in simulation for FCII is good. These experiments in simulation shows that FCII works over of range of parameters and different starting robot starting positions and situations. The way the group of robots moved with the human is very close to the expected out; the group of robots moves cohesively and the human is kept qualitatively at the center of the group, due to the new control algorithm FCII. It was determined that FCII would be also tested on the real-world system.

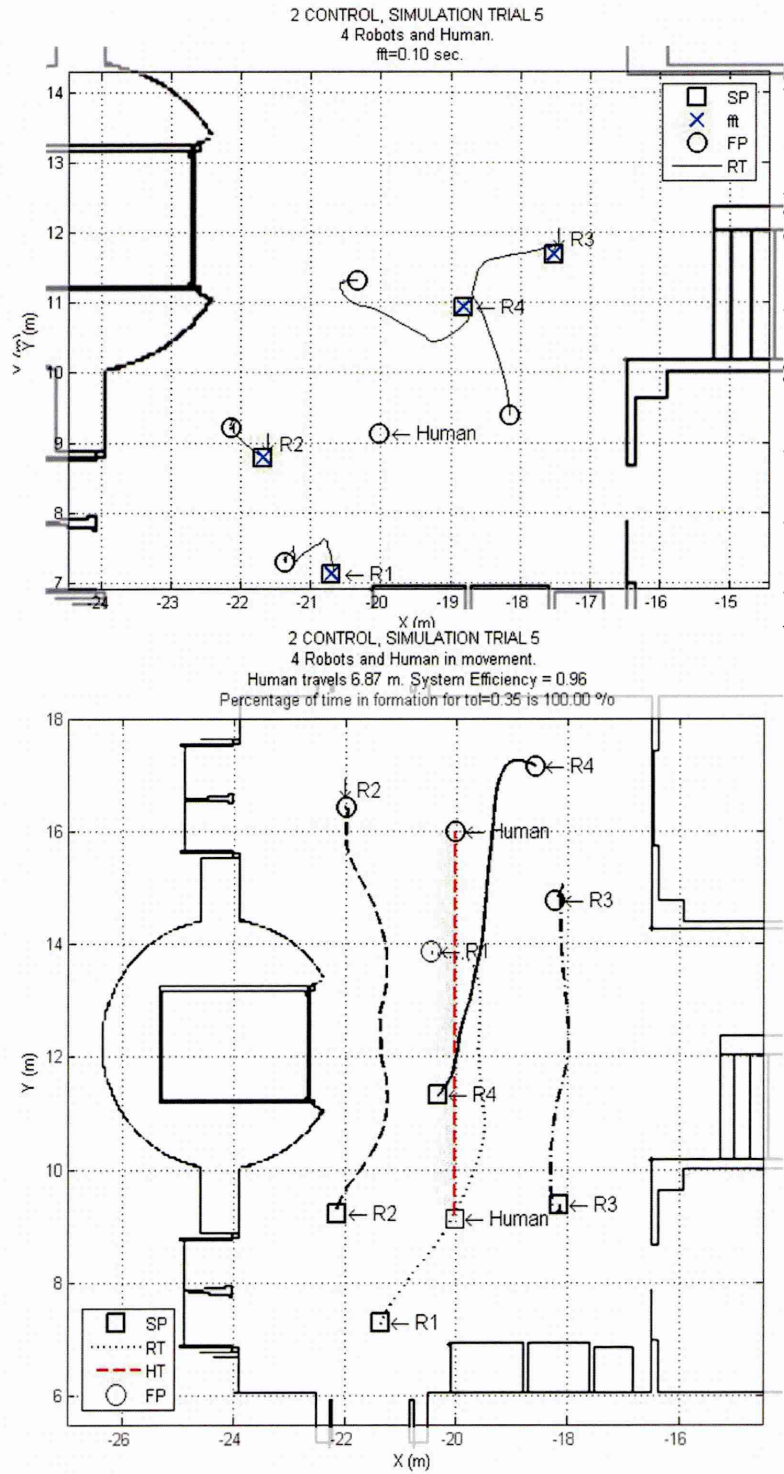


Figure 6.3: Best case. Trial 5 of the FCII in simulation.

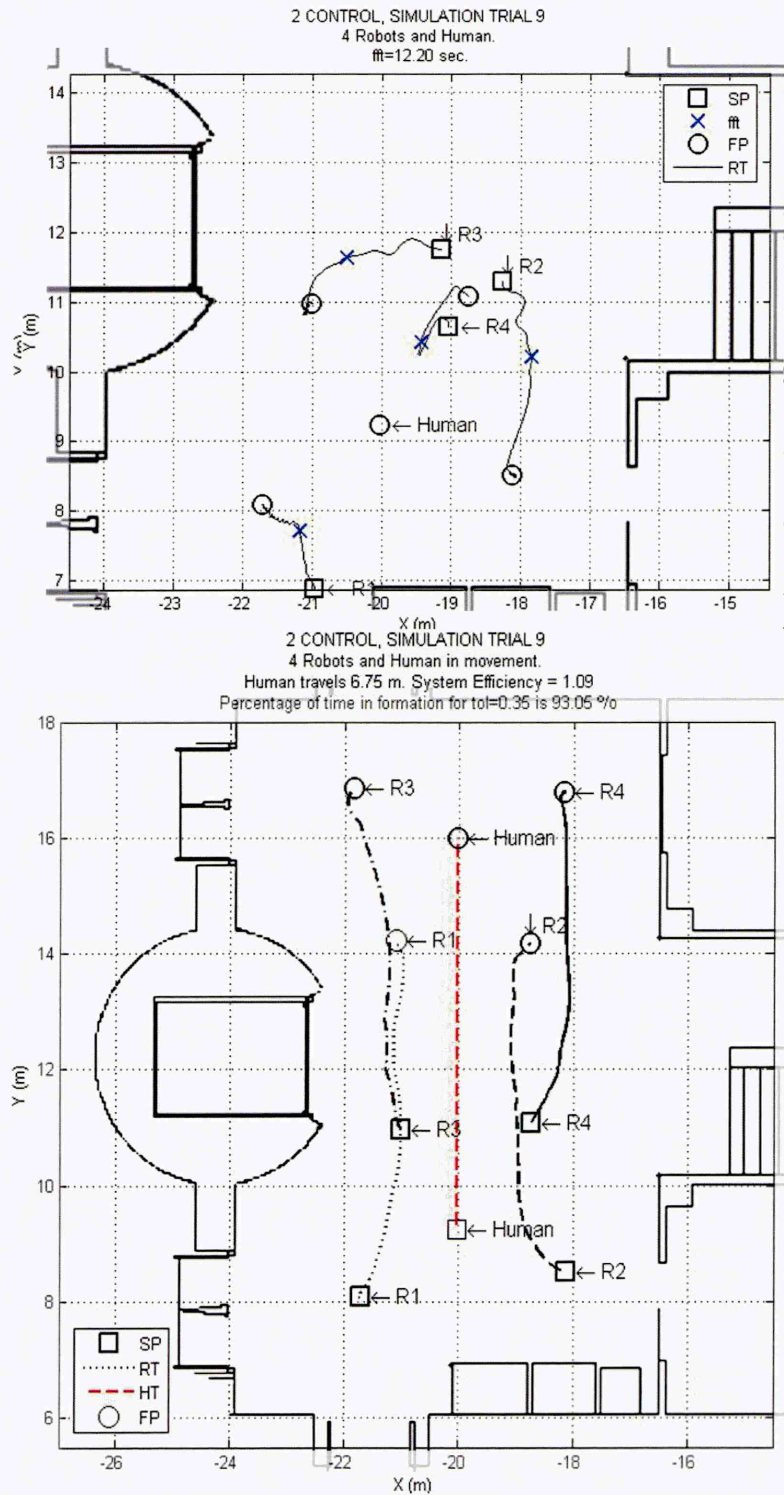


Figure 6.4: Worst case. Trial 9 of the FCII in simulation.

For comparison with later trials the average percentage of time in formation over ten trials for FCII in simulation was 98.51% with a standard deviation of 3.15%. The average efficiency over ten trials was 0.98%.

6.5 Real-world trials

6.5.1 Procedure As with FCI, the real-world trials for FCII were performed in the real world using the same human multi-robot architecture explained in Section 4.2. The mobile robots were placed at the same positions as in the simulation, always maintaining a connected graph. With the human still at its initial location the system starts and the robots start moving under FCII control. Note that in the real-world trials the dedicated robot to detect and track the human does not move according to FCII. During the formation generation stage the systems runs for one minute and the mobile robots start to gather around the human. After a minute the formation maintenance stage takes place, where the human starts to move at constant velocity to a final position that is 7 meters further to the other end of the environment. The robots follow the path whereas keeping the formation. When the human arrives at the final position it stops but the systems continues running until the robots stop moving, allowing continued observation of the systems behaviour.

The real-world experiment, from the formation control point of view, is practically identical to the simulation experiment. As previously mentioned, the main difference is the human-follower dedicated robot in the real-world trials. The usage of the software architecture presented in Section 4.2.1 allow us to seamlessly test the FCII.

As in simulation, the real-world experiment was repeated ten times with the ERA robots at different random positions, and the human always at approximately the same initial location. The number of real-world trials was limited by the considerable time required for each trial.

6.5.2 Results Once again, instead of showing the figures of the ten trials, that can be seen in Appendix C, we will show the trial 4 (Figure 6.6) and trial 5 (Figure 6.5). Trial 4 represents the trials with lowest $\%tif$ while trial 5 is the trial with the highest $\%tif$ metric.

Given for each trial is the *percentage of time in formation* ($\%tif$) and the *system efficiency* (SE). These data are presented in Table 6.4 with their averages and variances.

Trial 5 is representative of the advantage of the FCII in the real-world experiments. The formation generation stage (top) shows the main benefit introduced by FCII. It can be seen that robot 3 ($R3$) does not have the human within its sensor boundary, whereas the other robots ($R1$, $R2$ and $R3$) do. $R1$ is in trial 5 the dedicated follower robot. During formation generation, $R4$ is repulsed from $R3$ under the influence of robot-robot artificial force whereas it is attracted to

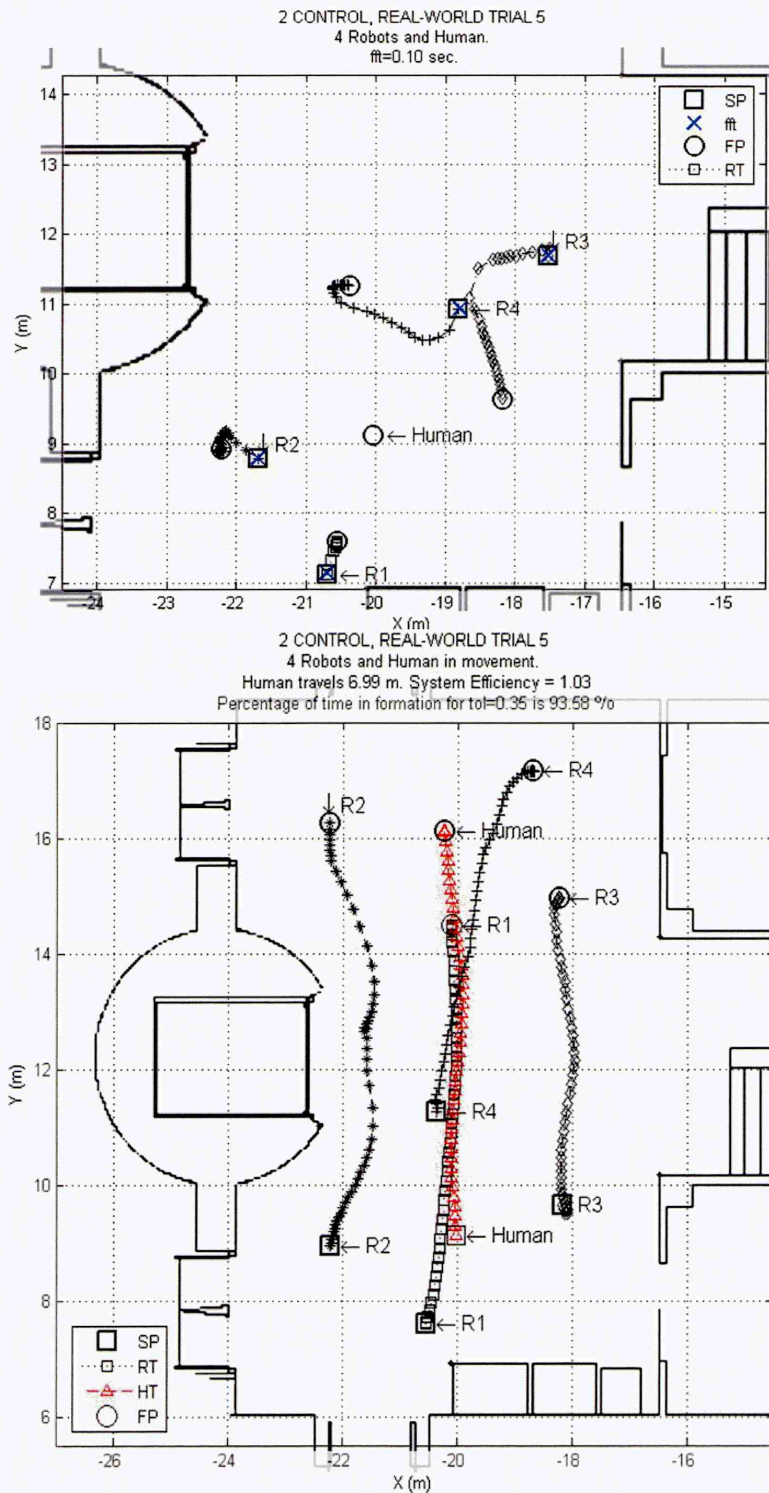


Figure 6.5: Best case. Trial 5 of the FCII in the real-world.

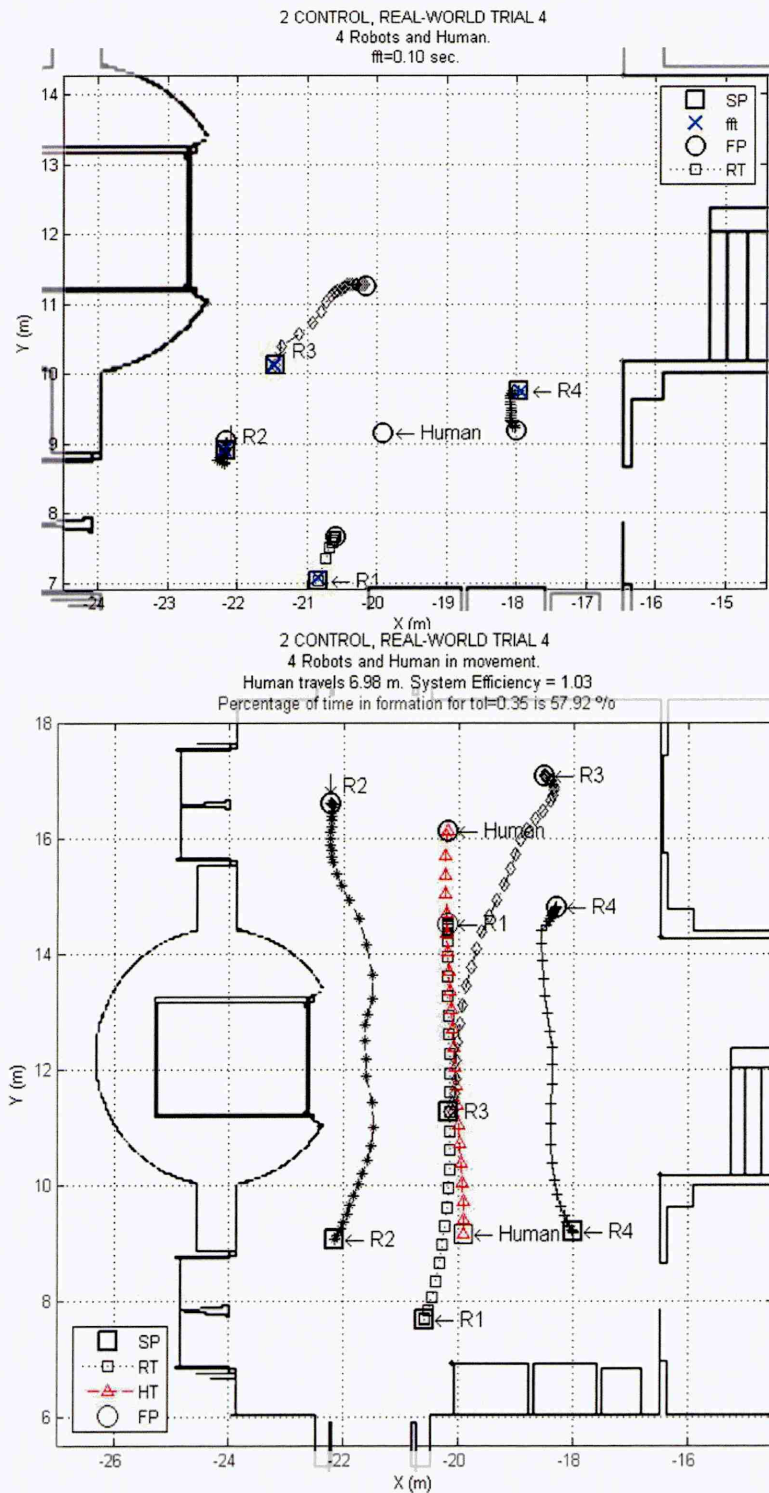


Figure 6.6: Worst case. Trial 4 of the FCII in the real-world.

Table 6.4: Summary of results of the FCII trials in real-world.

	SE	%tif
Trial 1	0.93	60.51
Trial 2	1.06	72.65
Trial 3	0.89	61.09
Trial 4	1.03	57.92
Trial 5	1.03	93.58
Trial 6	1.04	79.14
Trial 7	0.93	73.50
Trial 8	0.99	63.41
Trial 9	1.01	82.38
Trial 10	0.87	79.91
Mean	0.97	72.41
std.dev.	6.94	11.6

the human by the robot-human force influence. As a consequence $R4$ gives space to $R3$, that is attracted to $R4$ by the robot-peer force causing. As a result $R4$ pulls $R3$ towards the human until the human is within its range. At this moment the behaviour changes, $R3$ gets attracted by the human and repulsed by $R4$. As a consequence, all the robots end up surrounding the human with their final positions (FP).

The formation maintenance stage for trial 5 (bottom) shows a percentage of time in formation of 93.58%. The main reason for this satisfactory result is due to the fact that the robots are more uniformly dispersed during the trial. FCII keeps the human most of the time at the center of the formation, whereas the robots spread out (close to uniformly) and avoid colliding with the obstacles and walls.

Although trial 4, according to Table 6.4, presents the lowest of all the percentages in the real-world trials, a %tif of 57.92 is as high as the best %tif metric for the real-world trials of the FCI. For comparison with later trials the average percentage of time information over 10 trials for FCII in the real-world trials is 72.41% with a standard deviation of 11.60%. The average efficiency over 10 trials was 0.97%.

6.6 Discussion

The path plots of all the trials have a similar shape, indicating a much more consistent system performance in this set of trials. This is corroborated by the performance results observed in Table 6.3 which reflects the success of the FCII in simulation. Note that FCII shows that 2 out

of 10 trials have a 100% time in formation in simulation, where the remaining two trials present a *%tif* over 90. The mean *%tif* for FCII in simulation shows a good average of 98.51 with a very low standard deviation of 3.15. When observing the metric performance of the real world trials the results decrease to a mean *%tif* of 72.41 with a standard deviation of 11.6. The lowest performance corresponds to trial 4 with *%tif* of 57.92 and the highest performance happens to be trial 5 with 93.58. The system efficiency (SE) metric for FCII in simulation has a mean of 0.98 with a standard deviation of 7.57, and in real-world the SE is similar with a value of 0.97 and a standard deviation of 6.94.

When considering the results of FCI and FCII, it can be deduced that there exists a performance difference between simulations and real-world experiments. The reasons may vary, therefore I present a priority listing of the possible/probable sources of real-world error.

- *Dynamics of the real-world system.* All parameters in the FCI and FCII controllers for the real-world experiments were identical to those used in the simulations, therefore the difference in behaviour must be due to the dynamics of the real-world system. It is likely that the most significant of these is the time delay in the control loop. The simulation assumes zero delay in the communication system, but in the real robots there is delay when broadcasting and receiving positions of the team components through the software architecture. Furthermore, it has not been considered the uncertainty provided by sensor models in simulation, since they are considered to be ideal, whereas in the real-world these measurements are inaccurate and uncertain. More significantly, the simulation has idealised robot dynamics; the robot's wheel speeds match those requested by the controller, so the robot very closely matches the path generated by the algorithm. The controller on each real robot inevitably has a limited frequency response to incoming wheel speed requests. The real robots are also subject to inertia, friction, etc., none of which are modeled in simulation.
- *Localisation errors.* Another cause of the results' discrepancy between the simulations and real-world trials are the errors due to the localisation system. In simulations these localisation errors are non-existing but in real-world trials the situation is somehow different. Each robot uses the adaptive monte-carlo localization algorithm to maintain a probability distribution over a set of all possible robot poses, and updates this distribution using data from odometry and laser range-finder sensor. Inevitably the odometry and sensor measurement uncertainty influence the accuracy of the localisation algorithm.
- *Human detection and tracking errors.* The system (Section 4.2.3) whose functionality is simply to detect and follow the human's legs and broadcast the information to the group, unlike in simulation, is far from perfect. It might have spurious detections caused by any other robot or object walking between the dedicated follower robot and the human the tracking system might fail. This does not happen always, it depends on the size and speed of the intrusive element. However, when this happened during the real-world trials the human

follower algorithm most of the times recovered and did follow afterwards the human. This problem unfortunately has not been evaluated and measured during our work. Moreover, the follower system uses the laser range finder data, which as before has sensor measurement uncertainty whose errors might influence the dynamics of the real-world system.

- *Human and/or robot models.* Improving the accuracy of the robot and/or human models might allow better off-line parameter choices. Indeed, it was found by experiment with the simulation that the size and the uniform dispersion of the robot formations can be adjusted by careful parameter tuning. However, as the goal of our work is to produce a *general* multi-robot human formation control strategy, it is required to keep the models as simple and general as possible. Robustness, including minimal parameter sensitivity, should be an intrinsic property of the algorithms developed.

6.7 Conclusions

Adapting the first original formation control algorithm in a style of a behaviour-based controller solves the cohesiveness problem and gives an improved performance. FCII is more stable and effective than FCI by means of its uniform dispersion and flexibility, and is therefore a more appropriate solution.

The obtained performance in simulation is competent and in the real-world trials, though as not good as in the simulation, can be considered very good as well. The reasons for that are:

1. due to the priority given to the human using the behaviour-based approach, the mobile robots disperse in a more uniform way during the formation generation stage. The latter means that the robots do spread more in the empty environment which can be observed in both simulations and real-world trials.
2. during the formation maintenance stage in both simulation and real-world experiments the robots move more cohesively with the human. This happens because of the condition introduced by the human's presence, which causes the robots within its area of influence to occupy the empty space, causing the far away robots to come closer to human's position.
3. formation flexibility is kept. The robots are capable of performing properly in a scenario cluttered with dynamic (e.g. moving persons) and static objects (e.g. walls and obstacles) whereas keeping and maintaining the human multi-robot formation.

Chapter 7

Discussion

This chapter further examines the results from the previous experimental chapters and makes some comparisons between simulations and real-world trials and among FCI and FCII methods. The abilities and limitations of the algorithms and experiments are discussed, and some questions and criticisms encountered in the course of the work are addressed.

7.1 Comparison

In the previous chapter we have discussed the performance of both methods FCI and FCII. It was concluded that FCII performed better than FCI according to the shown metrics. Nevertheless, in the following we will statistically compare simulation versus real-world trials in both methods. Furthermore, we will compare as well the performance metrics of the method FCI versus FCII.

7.1.1 Simulated vs real-world results Figure 7.1 and Figure 7.2 show plots of the system efficiency (x axis) and the percentage of time in formation (y axis) of the simulation and real-world trials for FCI and FCII respectively. Recall that a score closer to 1 (drawn on the figures as a gray thick line) on the x axis indicates a better performance whereas on the y axis the higher the score the better the performance. Boxes are drawn around the extremes from each trial to indicate the range of values observed.

The simulation trials for FCI and FCII show a smaller standard deviation than the real-world trials in both axis. Furthermore in both figures the percentage of time in formation for the simulation trials is higher than in real-world. Moreover, the score for the system efficiency in both simulation trials is closer to 1. Therefore, both figures clearly indicate the existing difference between the simulation and the real-world trials for both formation control methods, although this discrepancy is less significant in FCII. This outcome is corroborated in Table 7.1, where it can be seen that simulations for both methods perform better than real-world trials. For more information

Table 7.1: Performance metrics: mean (standard deviation).

		FCI	FCII
Simulation	%tif	84.81(22.29)	98.51(3.15)
	SE	0.89(8.12)	0.98(7.57)
Real-world	%tif	37.73(17.35)	72.41(11.6)
	SE	0.83(23.63)	0.97(6.94)

about the performance metrics see Section 3.3.2 and Section 3.3.3.

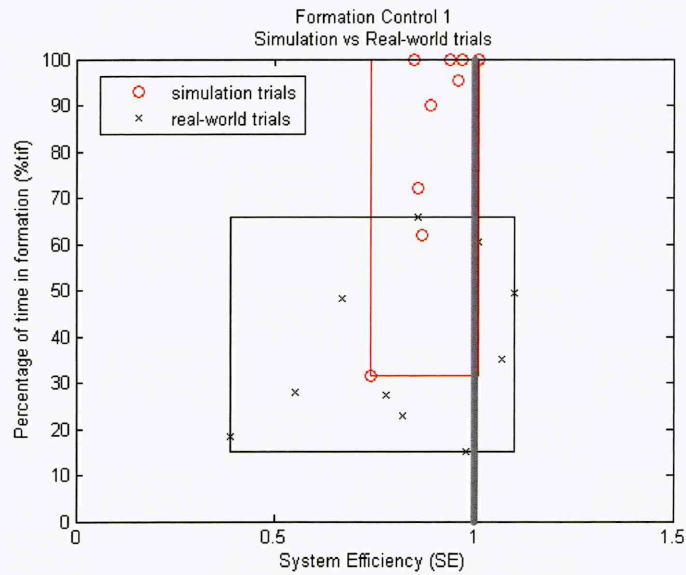


Figure 7.1: Simulation versus Real-world trials performance metrics in FCI.

7.1.2 FCI vs FCII Figure 7.3 and Figure 7.4 show plots of the system efficiency (x axis) and the percentage of time in formation (y axis) of FCI and FCII for the simulation and real-world trials respectively. FCII in both figures shows a smaller standard deviation than FCI in both axis. Furthermore in both figures the percentage of time in formation in the FCII trials is higher than in FCI. Similarly, the score for the system efficiency in both figures for FCII trials is closer to 1 than FCI. The reasons for these differences are summarised in Section 5.6 and Section 6.6.

The performance metrics for FCI and FCII are compared to determine whether the results are significantly different. Table 7.1 shows the mean and the standard deviation of the percentage time in formation and the system efficiency for the simulation and real-world trials in both methods. As with the figures, it shows that the mean and the standard deviation of the %tif in FCII are better

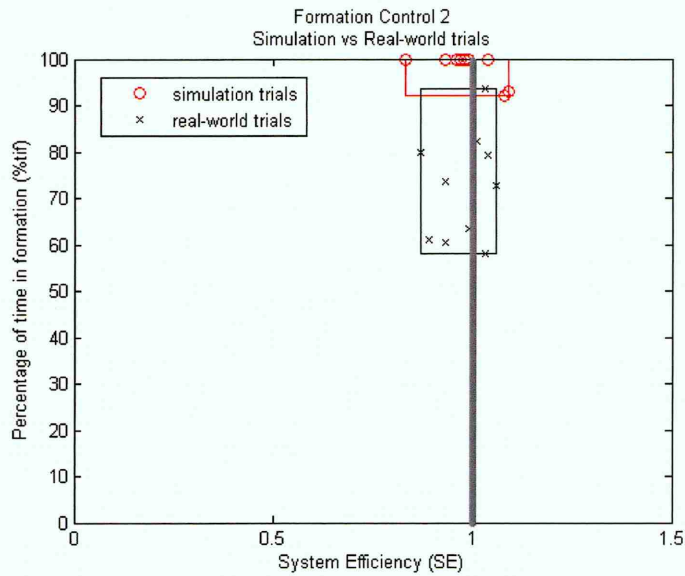


Figure 7.2: Simulation versus Real-world trials performance metrics in FCII.

than in FCI and likewise with the system efficiency.

Therefore, the above results suggest that in both simulation and in the real-world:

1. Results in simulation are better than in the real-world in both FCI and FCII methods.
2. Both methods succeed to gather the robots and the human and maintain a flexible formation.
3. FCII performs better than FCI.

7.2 What if more obstacles are considered?

This section will discuss the strategy employed to select obstacles of the environment. Firstly the reasons for employing the nearest obstacle will be given. Finally possible alternatives and other solutions will be explained and discussed.

FCI and FCII, for the calculation of the social potential function, need to account for the obstacles in the environment. The sort of obstacles that the robot might encounter in the environment vary considerable. Already in Section 4.1.3 a classification of the possible existing obstacles in the environment is given in Figure 4.9. Moreover, the robot is equipped with a single laser range-finder as the sensor to detect not only the environmental obstacles, but also the other robot peers and the human. In both formation control methods, the algorithm for the robots to detect obstacles using the laser range-finder is explained in Section 4.1.3.

In the formation control methods FCI and FCII the obstacle that comes in play is only the nearest obstacle. Each robot uses the relative position of the nearest obstacle to calculate the

7.2 What if more obstacles are considered?

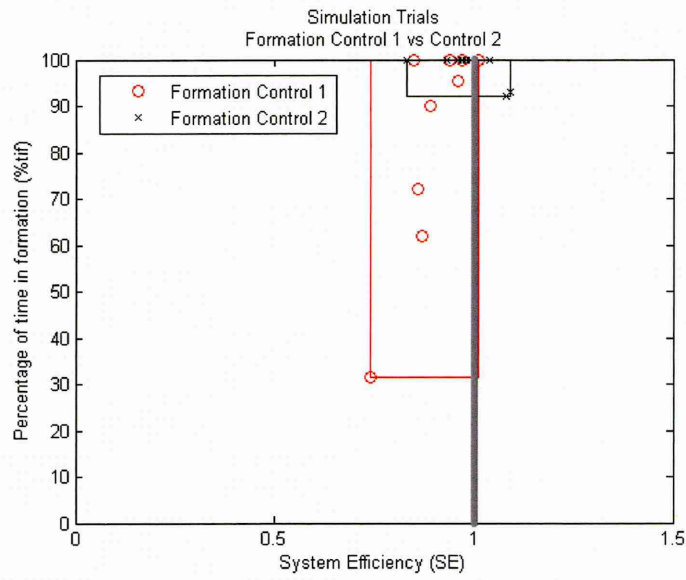


Figure 7.3: The performance metrics of FCI versus FCII for Simulation trials.

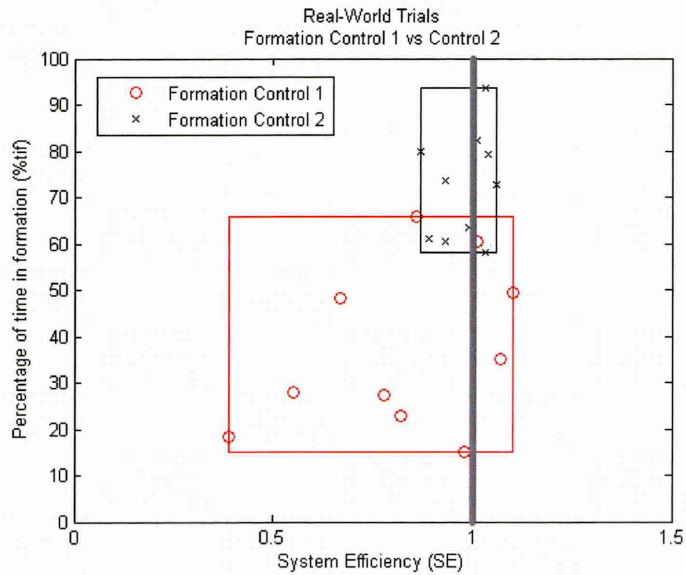


Figure 7.4: The performance metrics of FCI versus FCII for Real-World trials.

7.2 What if more obstacles are considered?

repulsive robot-obstacle potential function, which causes the robot to avoid obstacles. However, during the development of this work, the following question arose, *should more obstacles be used instead of employing only the nearest obstacle?*

The use of more obstacles for the calculation of the social potential function is seamlessly doable. The only requirement for each robot is to receive from the perception layer relative positions of all the obstacles to be included in the calculation. Once these relative positions of the environmental obstacles are available, both FCI and FCII could estimate the social potential function by adding the different components of the robot-obstacle repulsive functions.

At the perception level the problem is somehow more complicated. Figure 7.5 shows the situation in simulation where a human and four robots are in formation (left) and the distance measurements by the sensor range-finder on the circled robot (right). As explain previously in Section 4.2.1, the position of the human is broadcasted by the human follower dedicated robot (also known as PlayerFollowerAgent in the distributed software architecture scheme in Figure 4.13). The robot peers positions is broadcasted by each individual robot through the software architecture and afterwards committed through the pose list by the multi-agent coordinator (MACoord). The nearest object is therefore found segmenting the laser range finder information (Figure 4.11). Once the laser information is segmented, those sectors with occupancy items are disregarded to detect the nearest obstacle.

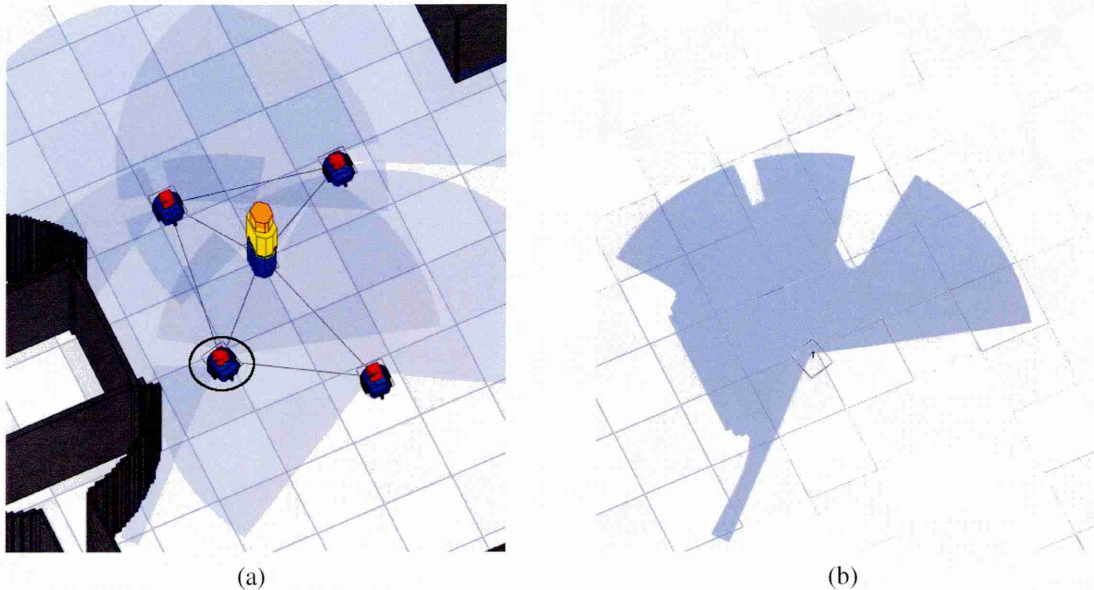


Figure 7.5: Distance measurements with the laser range finder.

7.3 What is the suitable value for the maximal tolerance ε_d ?

This simple method provides a reliable and easy to implement solution to detect and localise the closest obstacle. The detection of more obstacles in the environment would mean to employ a “smarter” perception level. As Figure 7.5b suggests a better scene understanding would become a challenge. A possible solution might be to continue segmenting the laser information only for the areas where obstacles might be present. Naturally, this would increase the computation complexity and reduce the time response. A possible advantage of using more environmental obstacles would be when the robots have to deal with narrow corridors. It is expected that in such situation, the use only of the nearest obstacle might cause the robots to show an oscillation or zig-zag movement between the walls of the corridor. Such situation is not likely to occur due to the types of scenarios considered in this work.

A good indicator of how the robots perform using solely the nearest obstacle can be observed in Figure 5.6. The trajectory of robot 2 (R2) during this real-world trial is smooth and clearly reflects the influence of the obstacles (in this case the wall) on the formation control methods. As it can be observed in the sort of scenarios considered in this work (i.e. wide empty open-space warehouses with eventual static or dynamic obstacles) to take into consideration only the nearest obstacle for the social potential function calculation is sufficient for a satisfactory performance. Nevertheless, the usage of more environmental information might improve in some specific situation how the robots can deal with obstacles, however, due to time restrictions this has not been possible to evaluate during the realization of this work.

Therefore, we can answer to this question that the use of solely the nearest obstacle is sufficient for the sort of scenarios and control methods that we consider. The usage of more obstacles would enhance performance at a cost of computational power at the robots perception layer.

7.3 What is the suitable value for the maximal tolerance ε_d ?

This section discusses the selection of the maximum tolerance (ε_d) value for distance measurements, which is employed by the performance metrics in our work. In order to select a suitable value, a sensibility analysis of ε_d is performed and the percentage of time in formation is observed. Finally, the selected value of ε_d is used for both formation control methods.

First, lets have a look to our definition of flexible formation (Definition 3.2). It states whether a human multi-robot system is in formation or not and it consists of two conditions. The first one states that for a group of robots to be in formation there has to be a connected graph among the components of the group. The second condition states that the components of the group have to be uniformly dispersed or that the inter-agent distance is kept. The former condition is employed to avoid situations where the components of the group might be breaking up or creating a torn

7.3 What is the suitable value for the maximal tolerance ε_d ?

formation (Figure 3.3). The latter condition is specified by the existence of a distance d that is kept among all neighboring components with a maximum tolerance ε_d

$$d - \varepsilon_d < |dist(R, R_j)| < d + \varepsilon_d$$

Selection of the maximum tolerance value influences directly the formation performance. In the literature selection of this parameter has been always chosen empirically according to the sought performance (Lemay et al., 2004; Balch and Arkin, 1998). For example, in (Fredslund and Mataric, 2002) the dispersion of robots was set fairly loosely, allowing the average inter robot distance to differ up to 20% from the desired distance d . Selecting a value sufficiently small means that the condition of uniform dispersion is too restrictive and therefore the group has a strict rigid formation. A rigid formation would mean that the group is not capable of adapting to dynamic environments, which is one of the main goals of the control methods. On the other hand, if the value of the maximum distance is high, this condition does not take effect and the components of the group are in a very loose formation. This situation is not desirable either, since it means that the group does not move as a team and probably they are not capable of accompany the human as it moves. Therefore, to evaluate and select a suitable maximum tolerance value some tests have been performed.

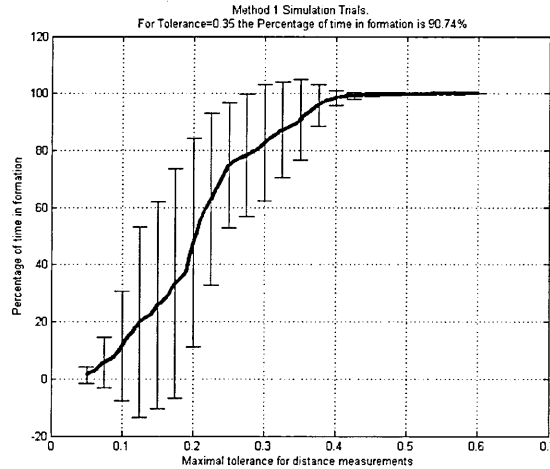


Figure 7.6: Maximal tolerance for Simulation trials in FCI.

For both FCI and FCII, the percentage of time in formation has been measured through a sensitivity analysis of ε_d for the ten trials both in simulation and in real-world trials. Figure 7.6 shows the sensibility analysis of ε_d for the simulation trials of FCI whereas Figure 7.7 is the sensibility analysis of ε_d of the real-world trials. Both figures show the mean and the variation of the percentage of time in formations (y-axis) when ε_d varies (x-axis). The same sensitivity

7.3 What is the suitable value for the maximal tolerance ε_d ?

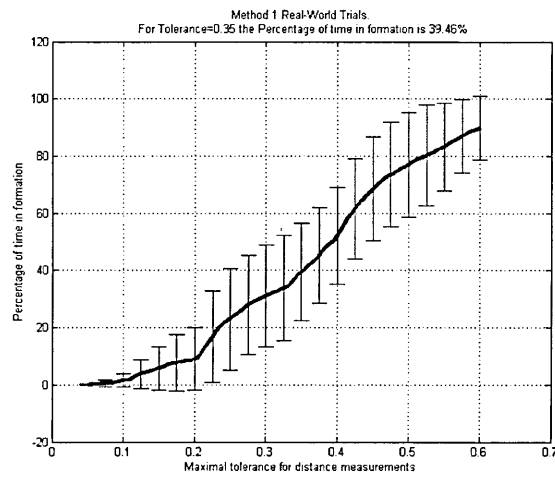


Figure 7.7: Maximal tolerance for Real-world trials in FCI.

analysis of ε_d has been done for FCII. The results are shown in Figure 7.8 and Figure 7.9 for the ten trials of the simulation and real-world trials, respectively.

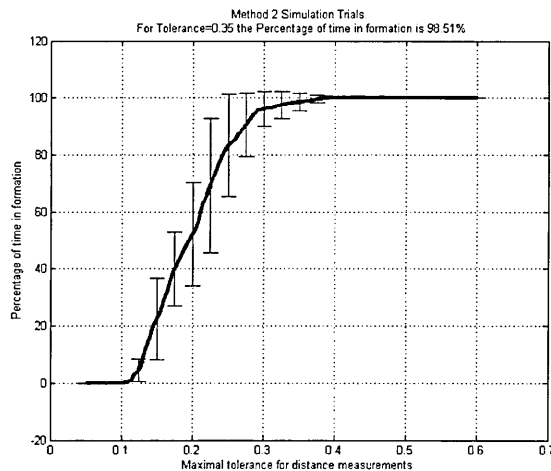


Figure 7.8: Maximal tolerance for Simulation trials in FCII.

The optimal trade-off between rigidity and flexibility can be achieved by selecting the value of ε_d to 0.35. With $\varepsilon_d = 0.35$ the percentage of time in formation for the simulation trials is 90.74% for FCI and 98.51% for FCII. In the case of the real-world trials, the percentage of time in formation for FCI is 40% and for FCII is 72.41%.

As a result, we can conclude that the empirically chosen value of ε_d is not restrained and represents a balanced choice between a flexible and rigid formation. The controls methods are allowed to disperse uniformly and create flexible formation to adapt to dynamic environments.

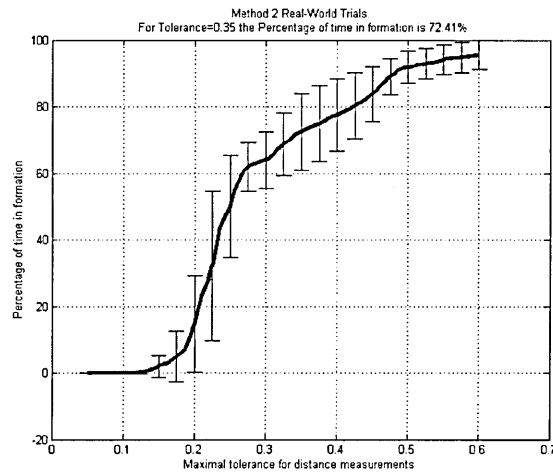


Figure 7.9: Maximal tolerance for Real-world trials in FCII.

According to the previous figures we can derive that FCII is less sensitive to tolerance value, and therefore we can state that FCII is better than FCI as it is more “stable”.

7.4 Considerations about HMRS behaviour

As we have stated previously, we do not predefine neither the shape of human multi-robot formation, nor robots positions in the formation. Nevertheless, application of the described potential functions generates certain formation patterns. If a human does not move the robots will converge to those patterns and if a human is moving the patterns will be undergoing certain deformations. In what follows we describe some typical stability situations as well as possible pattern deformations. We test our considerations in simulation by implementing behaviour patterns with the help of the computing software NetLogo. The pattern forms are dependent on the sensor boundary of the robots and the number of robots.

7.4.1 What is the influence of the sensor boundary size? In the following simulations, in order to observe the influence of the sensing boundary (SB) size, we vary the SB from zero to infinity. Firstly, the field of view of each robot is going to be 360 degrees, resulting in a circular SB; which in real life means that each robot is equipped with at least one omnidirectional sensor. Our real-world robots are equipped with a laser range finder with a field of view of 240 degrees. However, in the forthcoming simulations to observe the effect of the SB on the behaviour patterns, the SB size of the individual robots may shrink or expand depending on the situation.

As we said above each robot possesses a SB, the radius R_{SB} of which can vary from zero (“blind robot”) to infinity (“eagle-eye robot”). Infinity actually means that its radius takes a sufficiently large value R_{∞} that allows a robot to observe the whole surroundings where it operates. For example, a SB with radius of 4 units can be considered infinite if the maximum diagonal of the environment is smaller than 4 units. However the infinite SB does not mean that a robot should react to any agent or object within the SB. A realistic assumption is that a robot reacts to other robots or obstacles only if they are situated at a certain distance within their SB, so that the reaction distance d_{react} satisfies $d_{react} \leq R_{SB}$. Suppose, in the SB of the robot r_i there are two obstacles O_1 and O_2 , one hidden behind the other. In computer simulations a robot can “sense” both obstacles, and a repulsion force can be computed by taking into consideration both of them, whereas in practice a robot will observe only one obstacle, the closest one, and therefore it is sufficient to apply a repulsive force only to the first obstacle. Another reason for introducing the reaction distance is to produce more stable and realistic navigation patterns, such as avoiding unnecessary oscillations (Koren and Borenstein, 1991). An example of such behaviour is navigation of a robot along an obstacle or a wall.

In the following we assume that the human does not move and analyze what typical behavior patterns (formations) can be generated in such a situation. Suppose first we have several robots r_1, \dots, r_n , one human H and no obstacles. The robots are situated somewhere in the environment.

Robots with infinite SB

First we analyze the (simplest) case of some robots with infinite SB. At present we assume that their reaction distances coincide with the radii of SB. We consider holonomic (they can move in any direction) robots, so they can be viewed as points in the plane. Their positions are indicated with $\mathbf{X}_{r_i}, i = 1, \dots, n$, where n is the number of robots. The internal forces that each pair of robots exerts on each other are equal by magnitude but opposite by direction. The center of gravity CG of the group of robots, which position is computed as $\mathbf{X}_{CG} = \sum_{i=1}^n \mathbf{X}_{r_i}/n$, represents an invariant point with respect to internal forces, which follows from the Newton third law.

Situation 1.1. If the robots are the only agents, their CG will not be moved whilst internal forces will bring the group of robots to the equilibrium (Figure 7.10). In the following pictures the CG of the robots’ group is depicted with the cross.

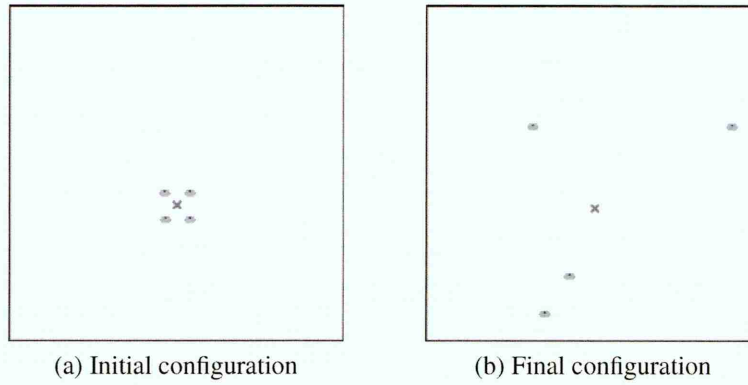


Figure 7.10: Behaviour pattern of a group of robots without a human and obstacles.

Situation 1.2. In the presence of other agents (i.e. human and obstacle), the forces that act between the human and the robots are external for the CG and this will be moved till the position where the sum of these external forces are equal to zero (Figure 7.11 and Figure 7.12).

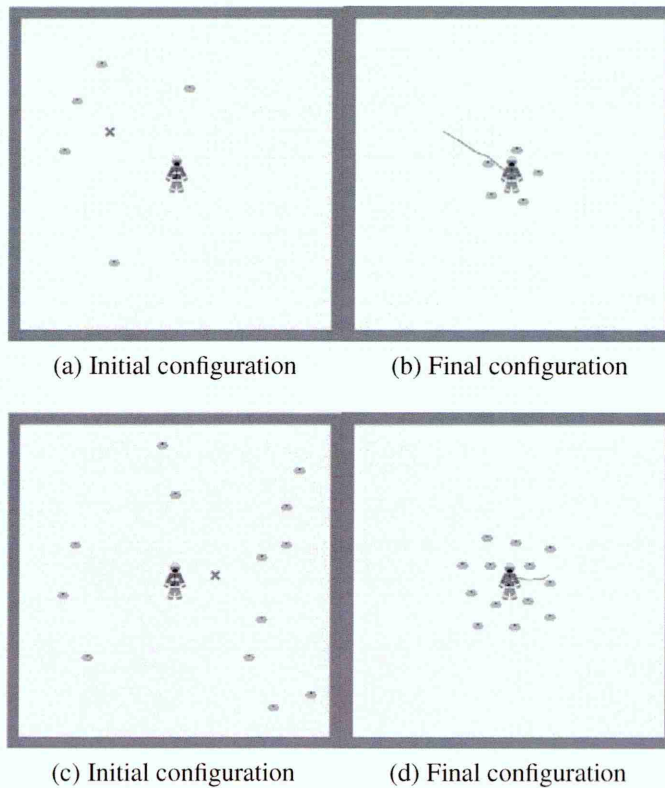


Figure 7.11: Behaviour pattern of the human multi-robot system.

In the absence of obstacles this point will be in the location of the human. After the center of gravity reaches this position, the situation will be similar to the Situation 1.1 and the robots will

7.4 Considerations about HMRS behaviour

end in the equilibrium position. The shape achieved by robots will depend on the number of robots (Figure 7.11), which differs from the work (Gazi and Passino, 2004), where a predefined shape for a given number of robots is considered. In the presence of obstacles the center of gravity will be shifted, and at its position the vector sum of forces exerted on the robots by the obstacles and the attraction forces to the human will be equal to zero (Figure 7.12).

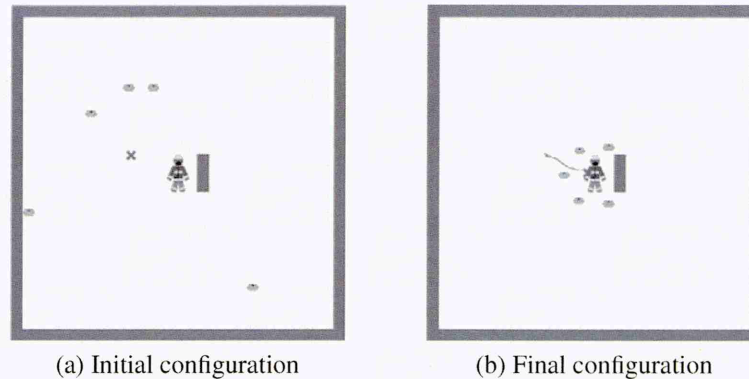


Figure 7.12: Behaviour pattern in the presence of an obstacle.

Robots with limited sensor boundary

In simulation, the case with limited SB of robots is somehow more realistic, since robots are equipped with sensors with a certain range.

Situation 2.1. Robots do not ‘see’ the human, but sense each other. We will get a local minimum where a group will execute a clustering behaviors pattern (Figure 7.13). The robots’ behaviour is similar to the behaviour depicted in Situation 1.1.

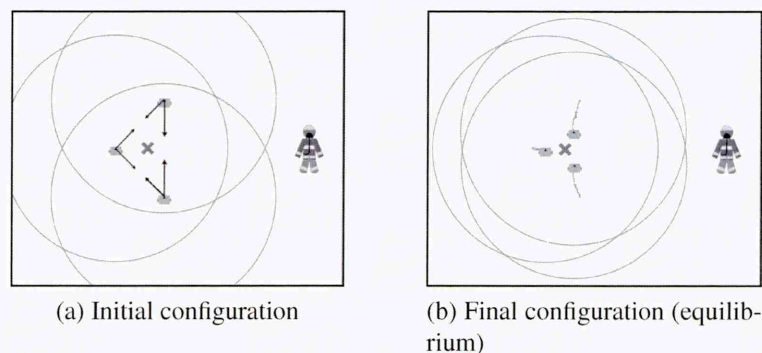


Figure 7.13: Clustering of robots with limited sensor boundary.

If all robots sense the human in their SB, then the robots will gather around the human, the same as in Situation 1.2.

Situation 2.2 This situation occurs when some of n robots (denoted with $r_j^H, j = 1, \dots, l$) sense the human, whereas each of the other robots (denoted with $r_k^r, k = n - l$) senses at least one robot from the first group.

In other words, that there is a connected graph among the components of the group. In this case the robots of the first group will exert only repulsion forces on each other, whereas their center of gravity CG^H will move in the direction of the human by the attraction force exerted by the human. The robots of the second group will exert on each other either repulsion or attraction forces, depending on the mutual distances, whereas their center of gravity CG^r will be subjected to the sum of attraction forces exerted by the robots of the first group. However this force is not monotonically changing, and it may become equal to zero if the robots of the first group is out of the SB of the robots of the second group. In this case the robots of the second group will not reach the human and will organise themselves in a cluster as in Situation 2.1. Therefore we have the following Proposition.

Proposition 2.2. The robots with limited SB will gather around the human, as at any time step the attraction force acting on the CG^r does not vanish.

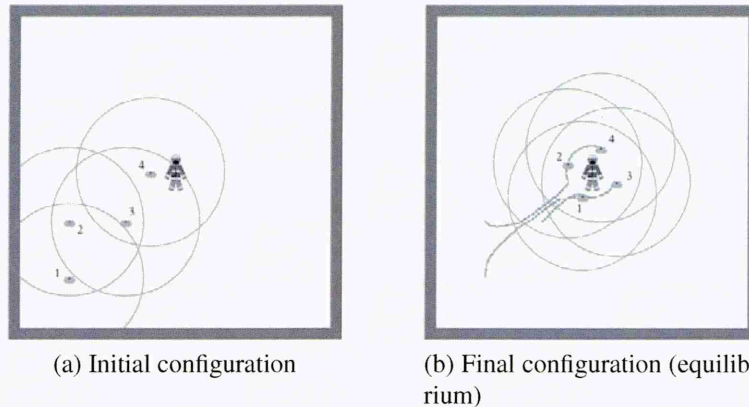


Figure 7.14: A connected group with limited sensor boundary.

Proposition 2.2. states that there should exist a chain of robots so that at each time step the group will be a connected graph. The vertices of this graph will be the robots, whereas edges occur only if the robots that represent the end-vertices are within the SB of each other. A similar type of graphs, called *connectivity graphs*, were considered in (Muhammad and Egerstedt, 2003). The described situation is depicted in Figure 7.14. Robot 1 senses robot 2, which in turn senses robot 3. Robot 3 senses robot 4 which senses the human. Since there is a connected graph, the robots achieve an equilibrium situation around the human.

7.4 Considerations about HMRS behaviour

When Proposition 2.2 holds then some complex situations can be solved. This is the case in Figure 7.15, where the robots escape the trap of the C -concavity and gather around the human without knowing the positions of all other robots.

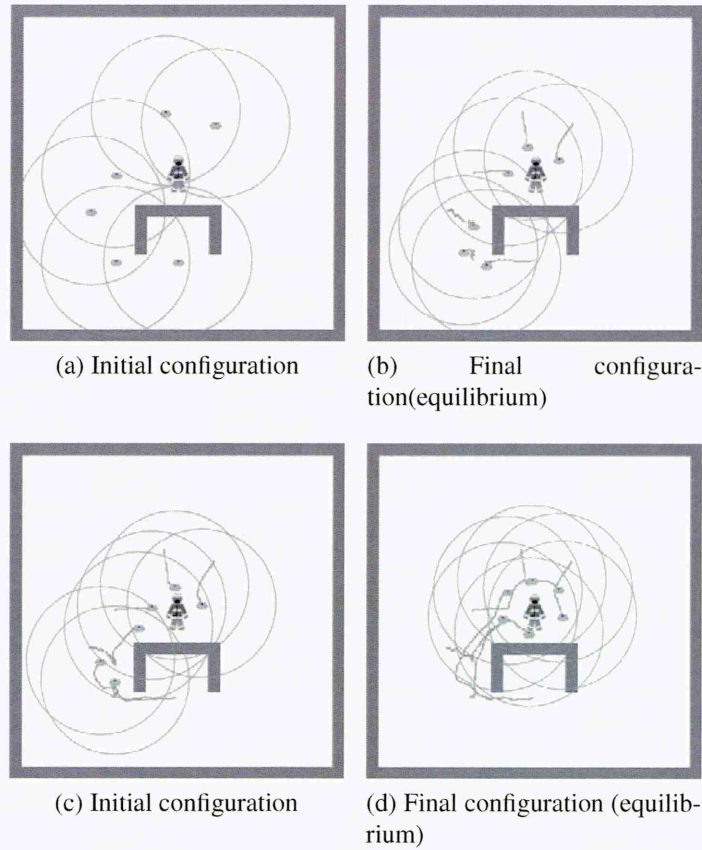


Figure 7.15: Robots ‘escape’ the trap of the C -concave obstacle.

The selection of the optimal sensor boundary or range obviously depends on the application and the environment. For example, if the robots are to navigate in narrow corridors it would be sufficient with small sensor boundary since the robots would not be capable of sensing far and priority should be given to near by obstacle. On the contrary, if the environment consists of open spaces a bigger sensor range would be preferable, since the robots would be able to disperse uniformly in the environment and react to the other components of the group. Nevertheless, the sensor boundary is directly limited by the sensor technology employed. In my case, the laser range finders boundary is $5.6m$ and therefore is technologically impossible to sense any further.

Chapter 8

Conclusions

This thesis seeks to establish the constraints under which coordination control is possible for systems composed of a human and multiple mobile robots. In particular the constraints imposed by real-time action, robustness and human safety. This work, reports on the findings of, to the best of the author's knowledge, the first real-world human / multi-robot system that achieves a complex navigation task.

A main contribution of this thesis is that, as opposed to the most of the related works, a multi-robot system has been created and tested not only in simulation but also in the real-world. I have implemented a software architecture which allows the inclusion of the human in the experiments. Although a suitable simulation tool is employed the transfer between simulation and hardware is not straight forward. Due to the lack of a robust and efficient technology to solve the mutual detection problem an equivalent solution has been presented. This consists in designing a distributed software architecture that would bring an alternative to using mutual detection sensors. The usage of central repository agent instead to collect each agent absolute pose and publish the aforementioned list is a transparent and totally equivalent alternative from the point of view of the robots, the control strategy and the expected grouping behaviour. The software architecture allows to seamlessly change the number of robots, employ different control methods and assign different roles to the robots.

In order to state whether a human multi-robot system is in formation or not I have introduced the flexible formation definition; a HMRS is in formation if two conditions hold: the components of the group are uniformly dispersed with some tolerance and there exists a connected graph. As a consequence, the group of robots can adapt to different environmental constraints and the configuration of the robots is not predefined.

Since one of the main goal of the work is to determine the most suitable formation control method I have selected some general experimental performance metrics. This selection is based

on the generality and applicability of the metrics, which are the percentage of time in formation and the system efficiency. These metrics are employed to compare and analyse the performance of the tested methods.

The Formation Control I is based on a simple social potential field method. FCI can generate a formation in both simulation and real-world, and the formation is maintained with the human in movement. Results of several trials and metrics are presented to assess performance. The identical controller is run on the real robots and tested in a real-world environment. Performance metrics showed that in the real-world this method is less reliable than in simulation, but do demonstrate a multi-robot control to navigate with a human. Consideration of these results leads to an improved strategy based on combining the social potential fields with the behavior based approach, the Formation Control II. Moreover, in FCII the presence or absence of the human is used the key event to decide when to switch among behaviours, fact that increases the movement coherence of the group and the uniform dispersion of the robots.

Performance metrics clearly indicate the existing difference between the simulation and the real-world trials for both formation control methods, although this discrepancy is less significant in FCII. In both simulation and in the real-world FCI and FCII succeed to gather the robots and the human and maintain a flexible formation, however it can be stated that FCII performs better than FCI. FCII solves the cohesiveness problem and gives an improved performance. FCII is more stable and effective than FCI by means of its uniform dispersion and flexibility, and is therefore a more appropriate solution.

The work demonstrates, to the best of the author's knowledge, the first real-world human multi-robot system to achieve a useful navigation task. It is concluded that in a future application a human navigating with a group of robots could be applied in multiple applications. An example is the work within the Guardians framework where a group of autonomous mobile robots is designed to assist fire fighter in searching a large warehouse as the central application. Another example would be the situation where a human could broadly benefit in an industrial environment, whereas the robots would have to navigate with the human and transport large objects.

As for future work I would like to point out two possible directions. One has to do with the correctness of the algorithms; model the dynamics of the multi-robot systems as a nonlinear system, equilibrium points of the dynamic equations and their stability, equilibrium formations and mathematical definition and analysis of the stability of equilibrium formations and finally system convergence. It is important to notice that this would be a challenging job and almost a new thesis, but important for the algorithm to be correct with respect to the specifications. Another general improvement of the system would be to boost the human detection and tracking system. During the final stages of this thesis the popular kinect sensor from Microsoft came out and it would be a

significant contribution to substitute the actual human following system by a dedicated sensor to obtain human pose detection.

Appendix A

Parameters selection

In this appendix I will justify the selection of the parameters used in the potential functions explained in Chapters 5 and Chapter 6. The selection of the parameters of the artificial forces for FCI and FCII is based upon the dimensions of the physical robots, the environmental requirements and the human model, described in Chapter 4.

A.1 FCI

As defined by the Equation 5.3.3 the robot-obstacle artificial force has an inverse power form

$$f_{Obs}(d_{R_n}^O) = \begin{cases} -f_{max} , & d_{R_n}^O \leq w_o \\ -\frac{1}{(k_o(d_{R_n}^O - w_o))^2} , & d_{R_n}^O > w_o \end{cases}$$

where w_o shifts the function along $d_{R_n}^O$ axis and k_o allows the function to be compressed ($k_o > 1$) or stretched ($k_o < 1$) horizontally. The horizontal shift w_o is referred to as the so called contact distance – the distance at which the edges of the robot and the obstacle would come into physical contact. The contact distance is set as

$$w_o = \text{radius}(R_n) + \text{safety margin}, \quad (\text{A.1.1})$$

where the radius of the ERA-MOBI robot is 25cm (see Table 4.1) and the safety margin has to prevent the robot to collide with the obstacle depending on its velocity, therefore is set as

$$\text{safety margin} = \Delta t \times (\text{maximum speed}(R_n)), \quad (\text{A.1.2})$$

For a time step of 0.1s and a maximum speed of 2m/sec the horizontal shift is set to $w_o = 0.45$.

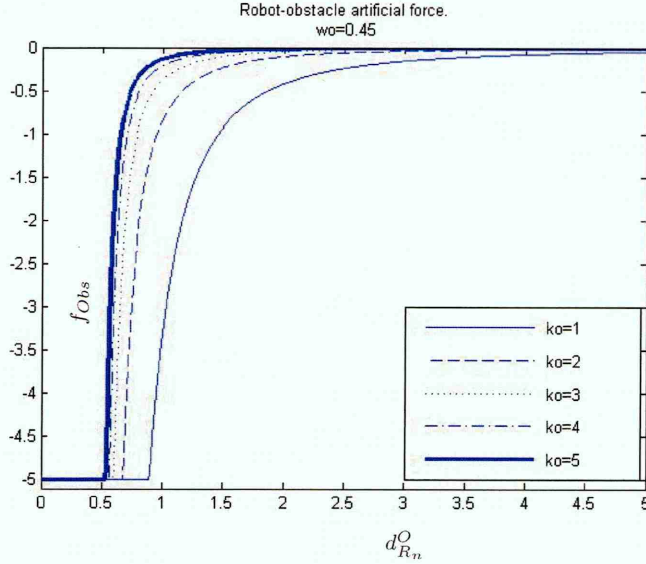


Figure A.1: Robot-obstacle artificial force.

Once the value of the parameter w_o has been set, it is all about choosing a suitable value for k_o . Figure A.1 shows effect of varying the parameter k_o in the robot-obstacle artificial force with $w_o = 0.45$. As it can be seen this parameters determines at which distance the repulsive force starts pushing the robot away from the obstacle. The influence of the obstacles should not start acting until the robot is within some reasonable distance. If the value of $d_{R_n}^O$ is chosen to be one meter and a half, it means the parameter k_o can be set at 5.

Secondly, the parameters of the robot-peer artificial force from the Equation 5.3.5 need to be selected. This force, composed by two terms, the repulsion and the attraction, respectively, has the form

$$f = \frac{1}{(k_a(d_{R_n}^{R_j} - w_a))^2} - \frac{1}{(k_r(d_{R_n}^{R_j} - w_r))^2}$$

where w_r shifts the function along $d_{R_n}^{R_j}$ (distance between the robot R_n and the peer R_j) axis, and the parameter k_r allows the function to be compressed ($k_r > 1$) or stretched ($k_r < 1$) horizontally.

In this case the horizontal shift w_r refers to the distance at which the edges of the robot would come into physical contact with the edge of the peer within the sensor boundary. This contact distance is set as

$$w_r = \text{radius}(R_n) + \text{radius}(R_j) + \text{safety margin}, \quad (\text{A.1.3})$$

where the safety distance, which has to prevent collision between the robot and the peers, is defined as

$$\text{safety margin} = \Delta t \cdot (\text{maximum speed}(R_n) + \text{maximum speed}(R_j)), \quad (\text{A.1.4})$$

In FCI, the human and the robots are considered to be the same sort of agents, the peers. Therefore, to account for worst situation, the characteristics of R_j will have a maximum speed of 2m/sec and radius of 0.3 meters, which corresponds to the ERA-MOBI's maximum speed and to the radius of the humans size. For a time step of 0.1 seconds the contact distance is set to $w_r = 0.95$.

The maximum distance at which the robots can detect the human is limited by the range of the laser range finder and is set to $w_a = 4$ meters according to Table 4.2.

The parameters k_r and k_a can be used to tune the mutual distance between peers according to the task the squad is required to perform. For example by compressing the repulsive component of the artificial force, say by setting $k_r = 5$, the preferred separation is reduced, making it easier for the squad to, for example, negotiate narrow doorways and corridors.

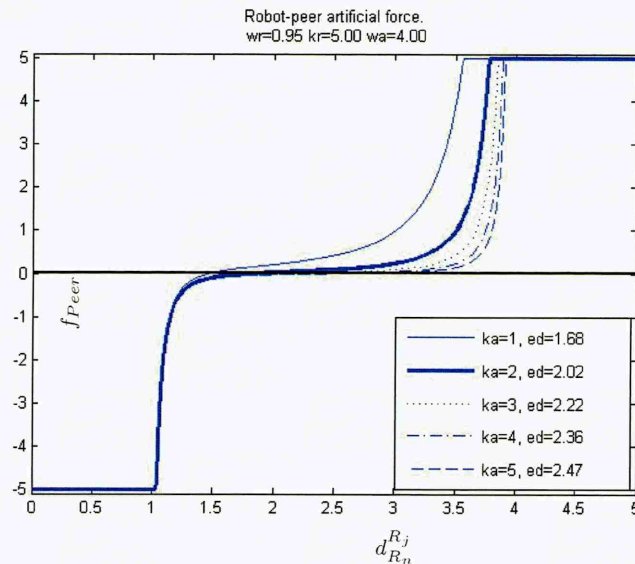


Figure A.2: Robot-peer artificial force.

Figure A.2 shows the combined repulsive and attractive artificial force (Equation 5.3.4) between a robot and a peer with the repulsive parameter $k_r = 5$ and varying the attractive parameter k_a . This parameter has the effect of changing the equilibrium separation (the minimum of the combined artificial force) between robot and peers. A desirable equilibrium distance would be approximately 2m , allowing the robots not to get too close to the peers but keeping it within sensor range. If we choose the parameter $k_a = 2$ the resulting equilibrium distance is 1.94 meters.

All parameters employed for the FCI are summarized in Table 5.2.

A.2 FCII

The robot-robot artificial force is denoted by following equation:

$$f_{Rob}(d_{R_n}^{R_j}) = \begin{cases} -f_{max} , & d_{R_n}^{R_j} \leq w_r \\ -\frac{1}{(k_r(d_{R_n}^{R_j} - w_r))^2} , & d_{R_n}^{R_j} > w_r \end{cases} \quad (\text{A.2.1})$$

where w_r shifts the function along $d_{R_n}^{R_j}$ axis and k_r allows the function to be compressed ($k_r > 1$) or stretched ($k_r < 1$) horizontally. The horizontal shift w_r is mentioned as the contact distance – the distance at which the edges of the robot R_n and the robot R_j would come into physical contact. In this case the contact distance is set as

$$w_r = \text{radius}(R_n) + \text{radius}(R_j) + \text{safety margin}, \quad (\text{A.2.2})$$

where the safety distance is calculated according to:

$$\text{safety distance} = \Delta t \cdot (\text{maximum speed}(R_n) + \text{maximum speed}(R_j)), \quad (\text{A.2.3})$$

where Δt is the simulation time step. Therefore, for a time step of 0.1 seconds the contact distance is set to $w_r = 0.90$.

For the choice of a suitable value for k_r lets look at Figure A.3, that shows the effect of varying the parameter k_r in the robot-robot artificial force with $w_r = 0.90$. Setting a distance of $d_{R_n}^{R_j} = 2$ meters, the parameter results in $k_r = 5$.

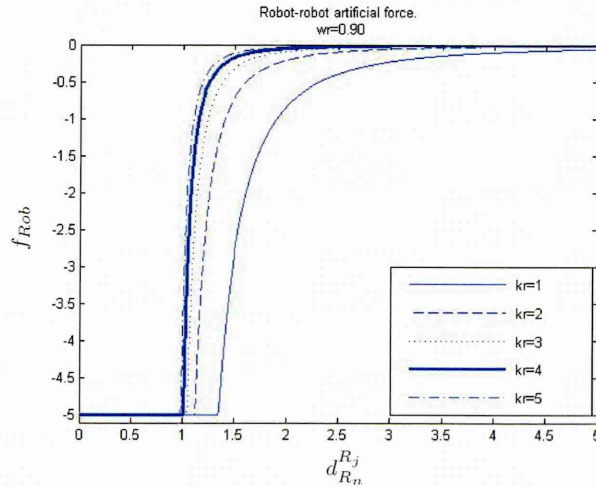


Figure A.3: Robot-robot artificial force.

The robot-human artificial force has been previously presented in Equation 6.3.3. This force is identical to the robot-peer artificial force in FCI, but differs in that it is applied only to the human when within sensor boundary, whereas in FCI is applied to all peers (human and robots). Again, w_{hr} shifts the function along $d_{R_n}^H$ axis, and k_{hr} allows the function to be compressed ($k_{hr} > 1$) or stretched ($k_{hr} < 1$) horizontally. In this conditions, w_r refers to the distance at which the edges of the robot and the human would come into physical contact and is set as

$$w_r = \text{radius}(R_n) + \text{radius}(H) + \text{safety margin}, \quad (\text{A.2.4})$$

where the safety margin is defined as

$$\text{safety margin} = \Delta t \cdot (\text{maximum speed}(R_n) + \text{maximum speed}(H)), \quad (\text{A.2.5})$$

where Δt is the simulation time step. Taking into account the parameters from Table 4.3, for a time step of 0.1 seconds the contact distance is set to $w_{hr} = 0.77$. The parameter w_{ha} is set from the maximum distance at which the robots can detect the human, limited by the range of the laser range finder, which according to Table 4.2, is 4 meters.

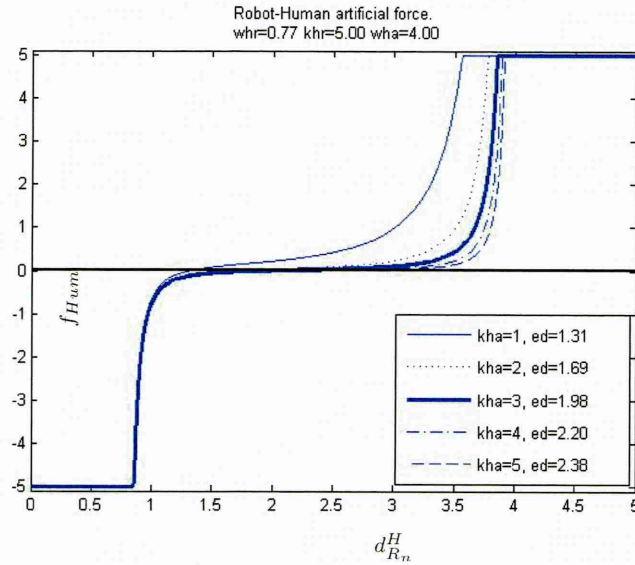


Figure A.4: Robot-human artificial force.

In order to select the values of k 's, Figure A.4 shows the combined repulsive and attractive force between a robot and a human. The repulsive parameter is set to $k_{mr} = 5$ and the attractive parameter k_{ma} is analyzed. The Figure shows that for different values of k_{ma} the equilibrium separation (the minimum of the attraction and repulsion) between the robot and the human changes. For safety reasons, it is suggested an equilibrium distance of approximately 2 meters (equivalent to around the half of the Hokuyo sensor range). This distance will allow the robots not to get too

close to the human but to keep him within sensor boundary. If $k_{ma} = 3$ is selected, the resulting equilibrium distance is 1.98 meters.

All parameters employed for the FCII are summarized in the following Table

Artificial Force	Parameter Value
Robot-Human	$k_{hr} = 5.00, w_{hr} = 0.77$ $k_{ha} = 3.00, w_{ha} = 4.00$
Robot-Robot	$k_r = 4.00, w_r = 0.90$
Robot-Obstacle	$k_o = 5.00, w_o = 0.45$

Appendix B

Figure trials for FCI

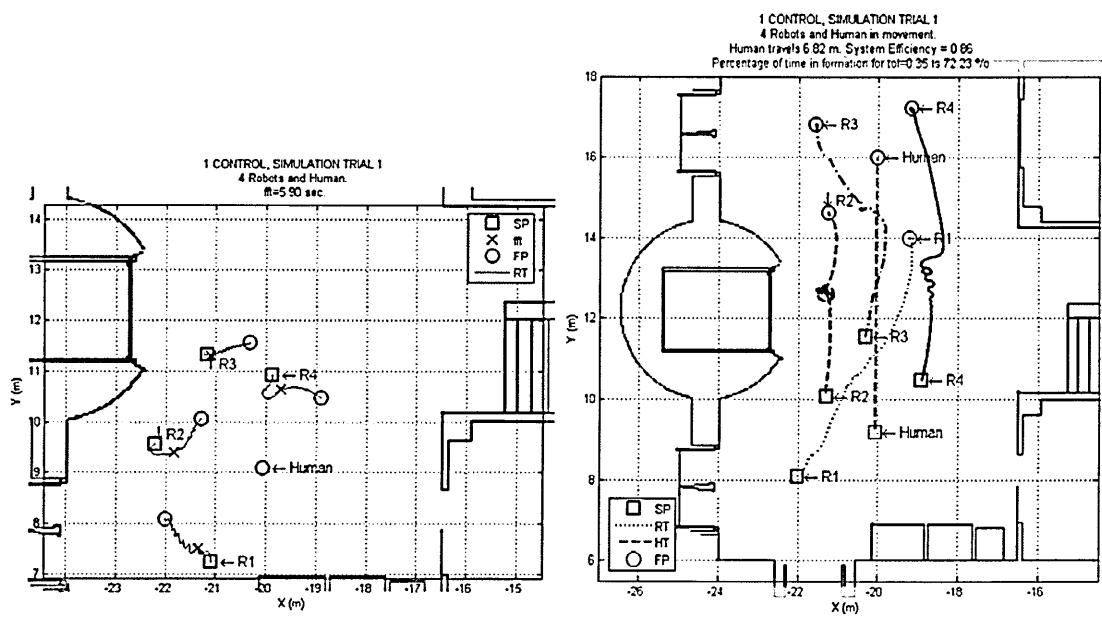


Figure B.1: Trial 1 of the FCI in simulation.

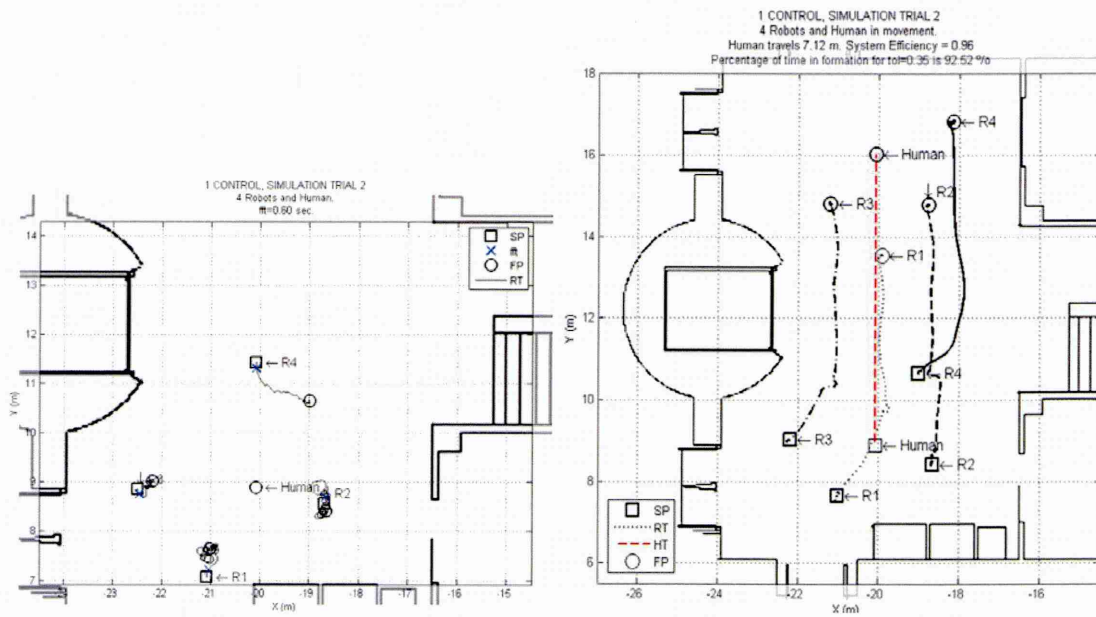


Figure B.2: Trial 2 of the FCI in simulation.

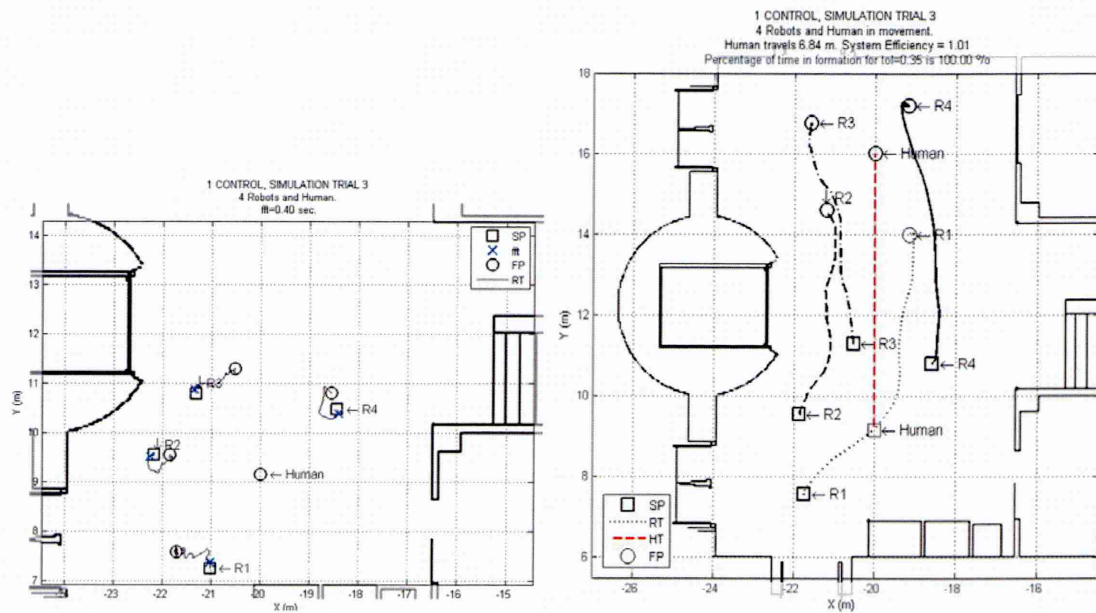


Figure B.3: Trial 3 of the FCI in simulation.

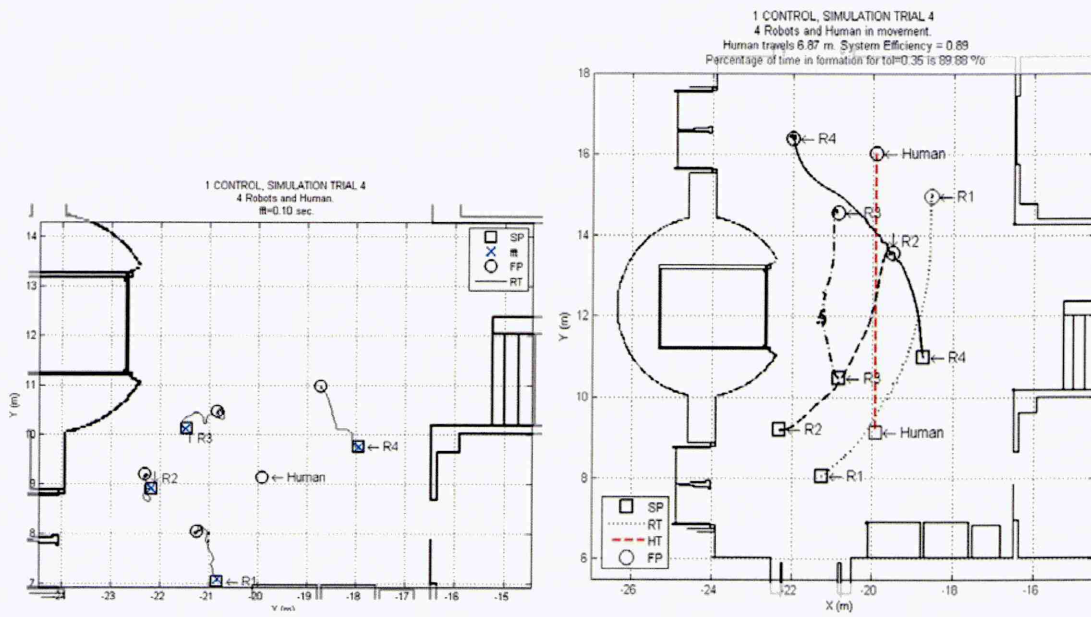


Figure B.4: Trial 4 of the FCI in simulation.

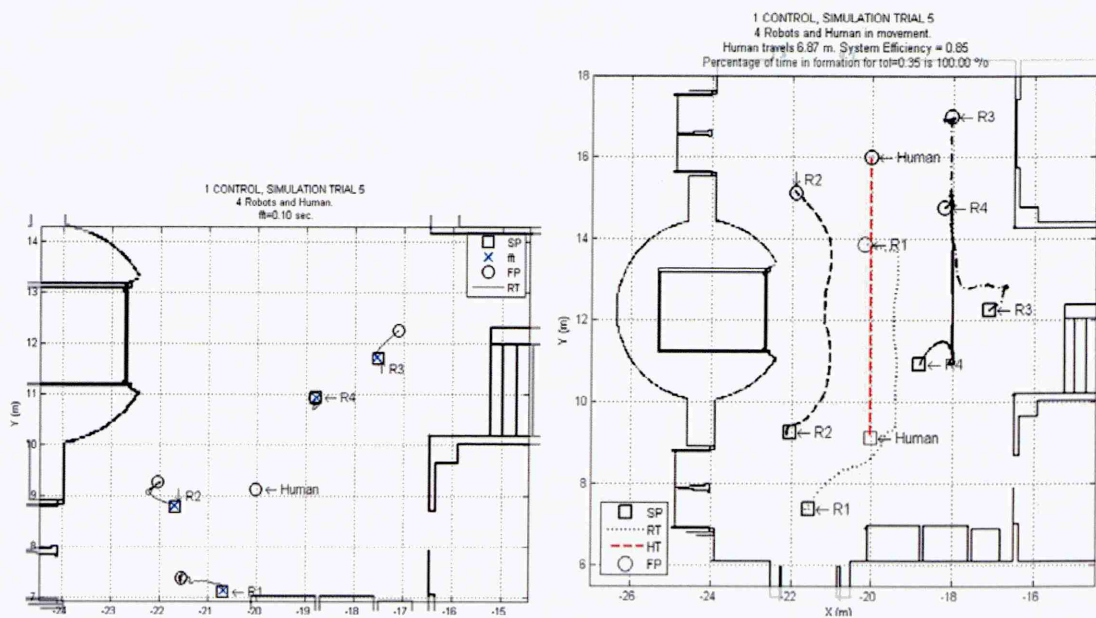


Figure B.5: Trial 5 of the FCI in simulation.

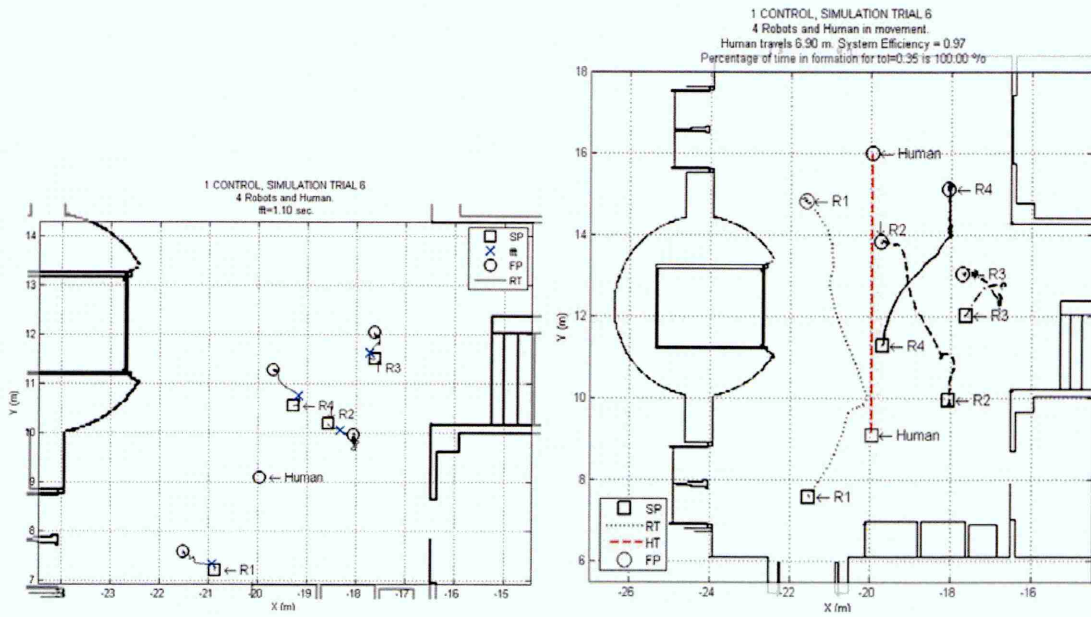


Figure B.6: Trial 6 of the FCI in simulation.

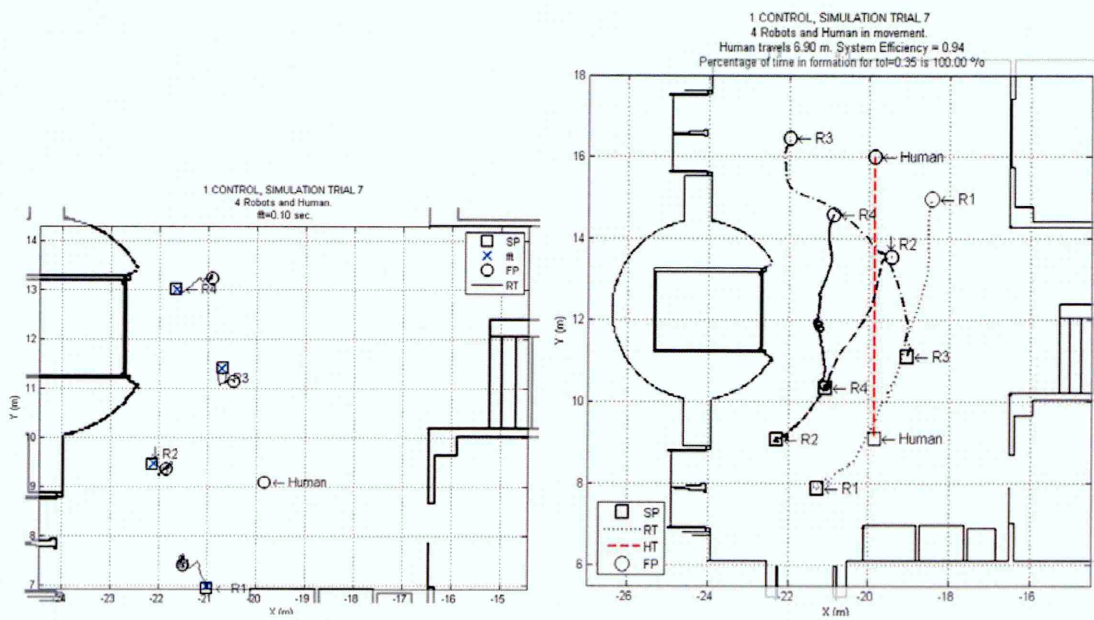


Figure B.7: Trial 7 of the FCI in simulation.

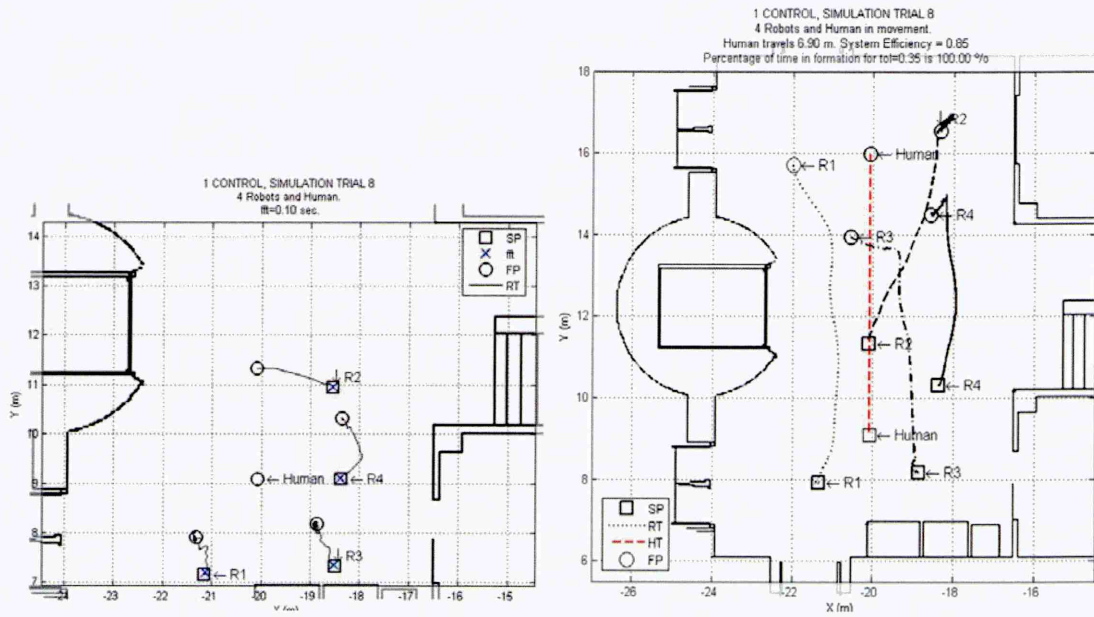


Figure B.8: Trial 8 of the FCI in simulation.

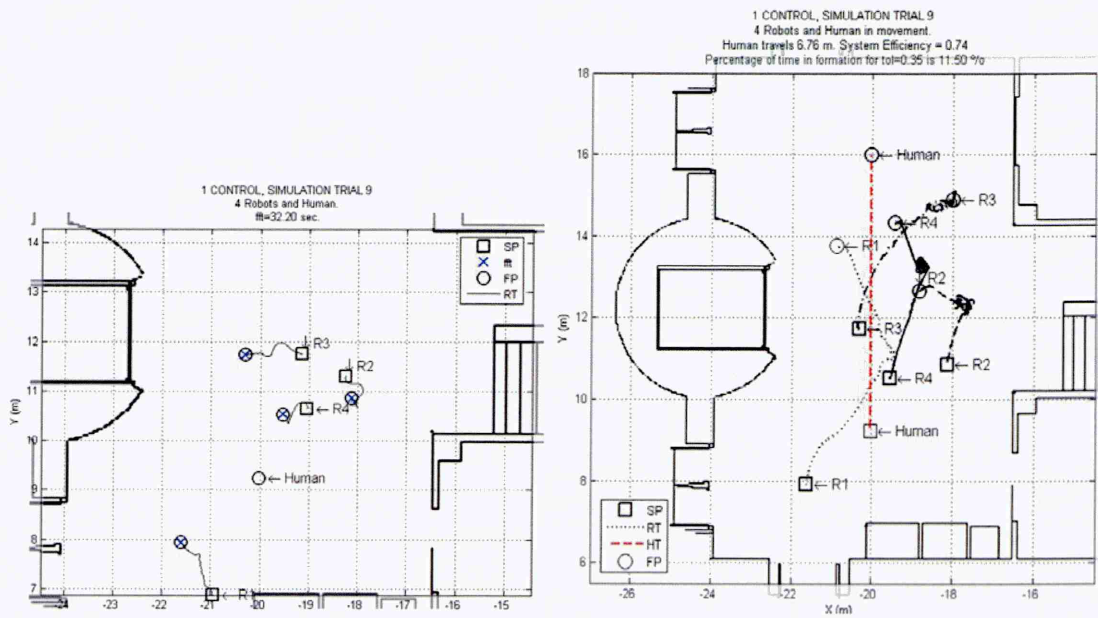


Figure B.9: Trial 9 of the FCI in simulation.

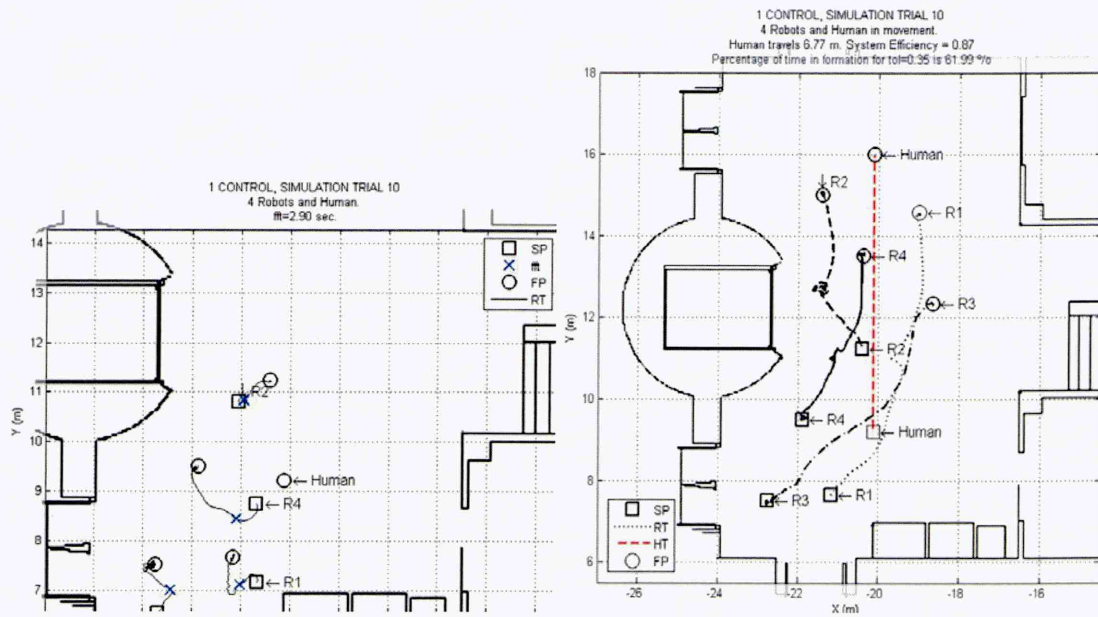


Figure B.10: Trial 10 of the FCI in simulation.

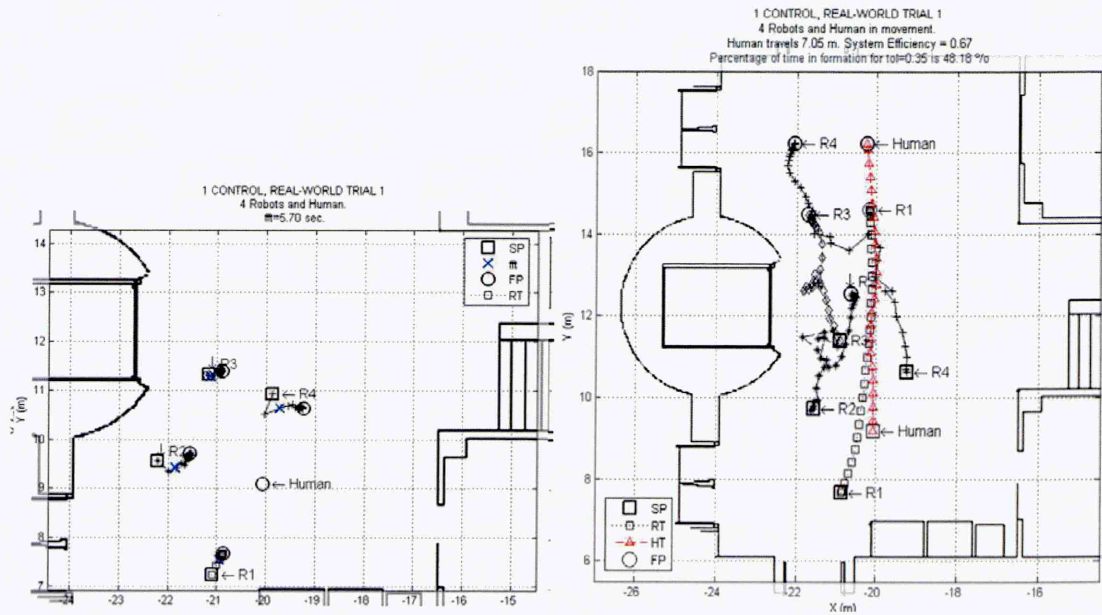


Figure B.11: Trial 1 of the FCI in real-world.

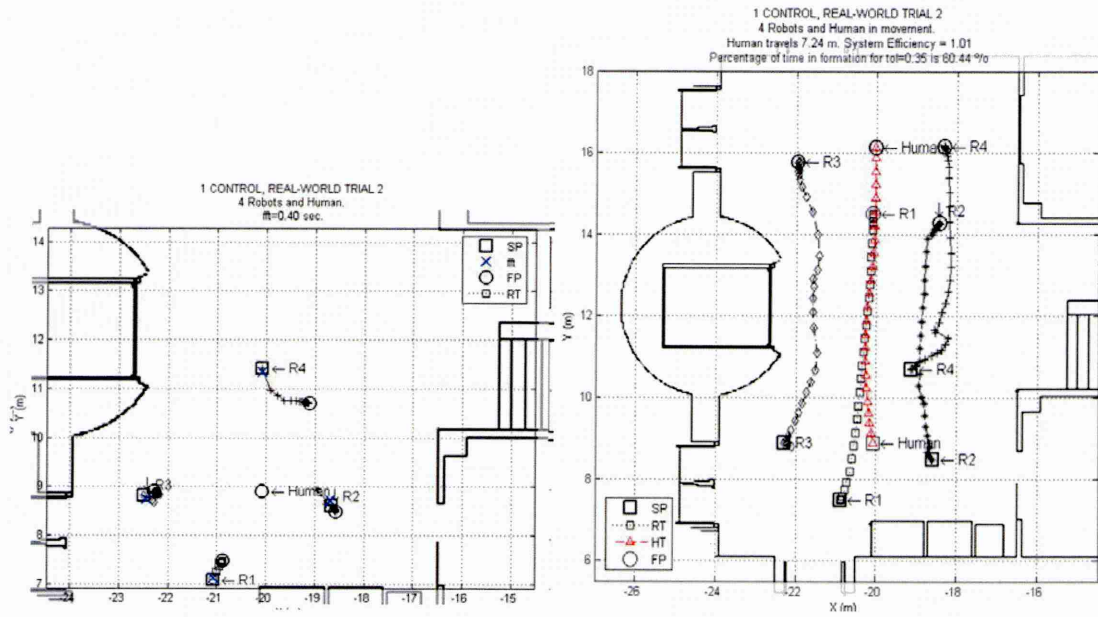


Figure B.12: Trial 2 of the FCI in real-world.

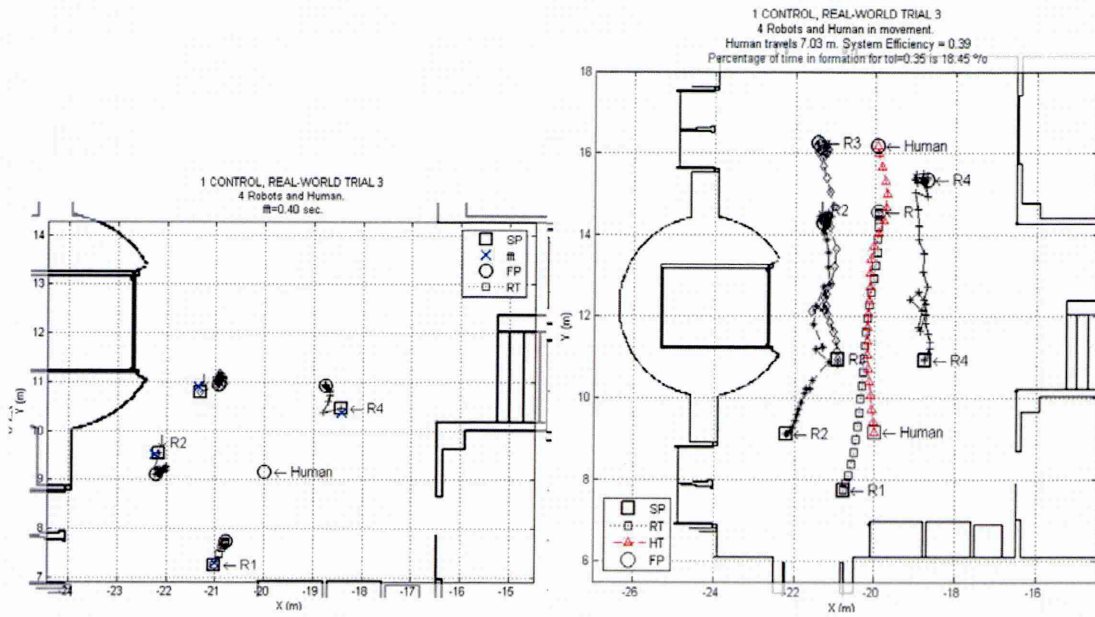


Figure B.13: Trial 3 of the FCI in real-world.

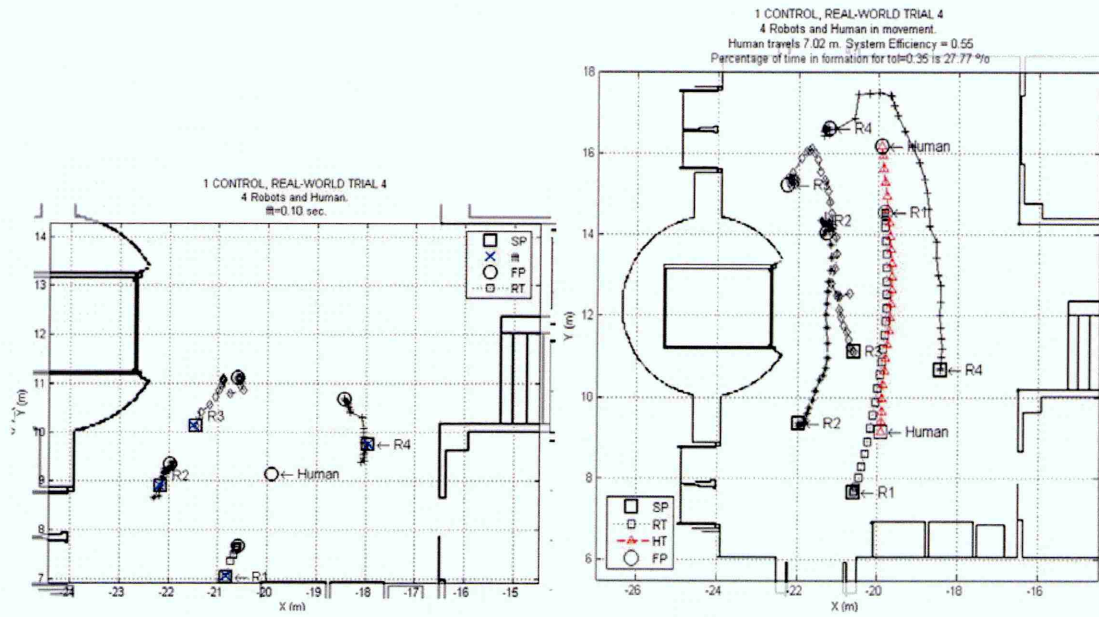


Figure B.14: Trial 4 of the FCI in real-world.

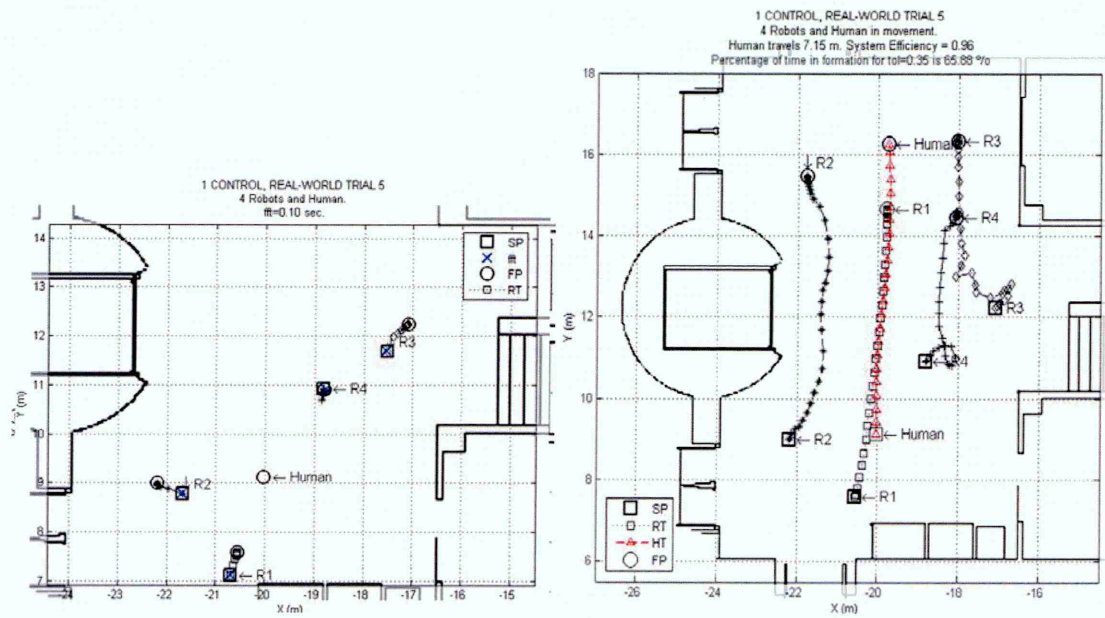


Figure B.15: Trial 5 of the FCI in real-world.

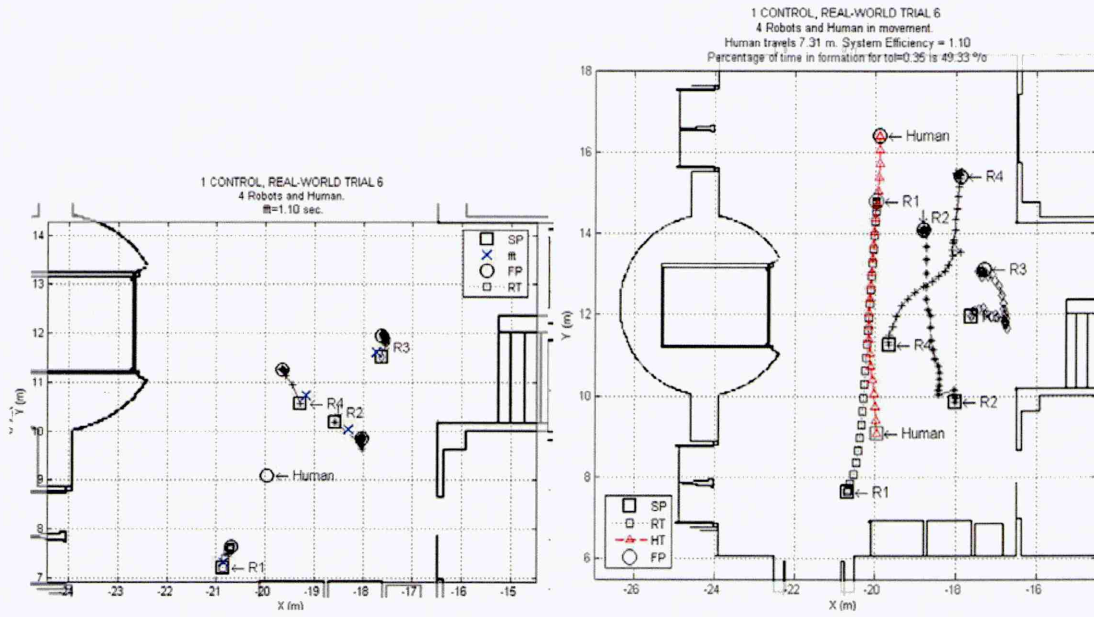


Figure B.16: Trial 6 of the FCI in real-world.

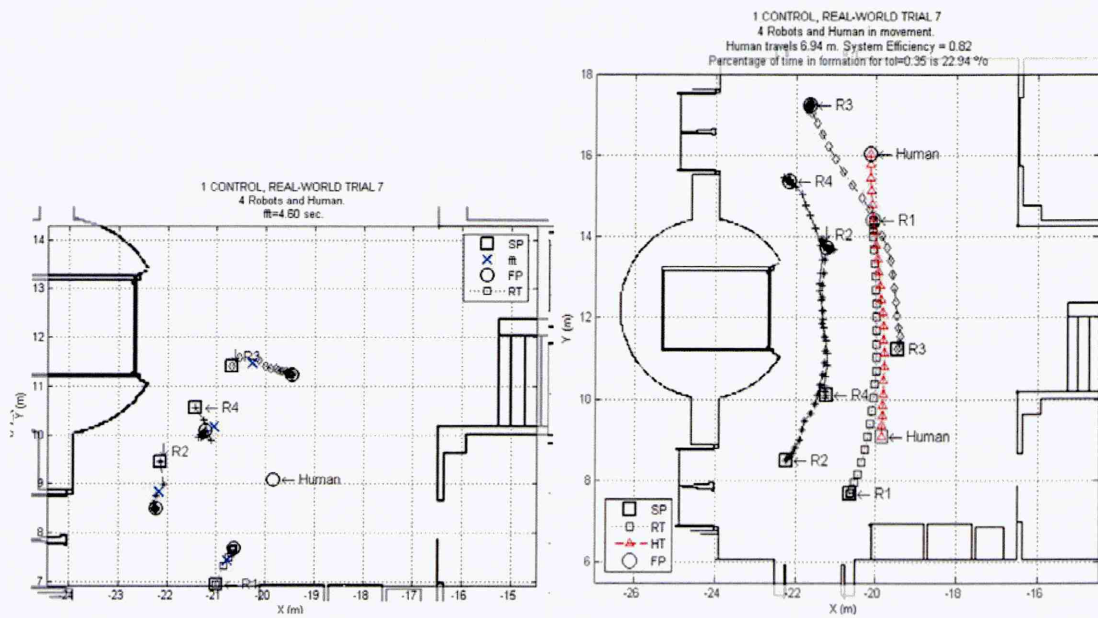


Figure B.17: Trial 7 of the FCI in real-world.

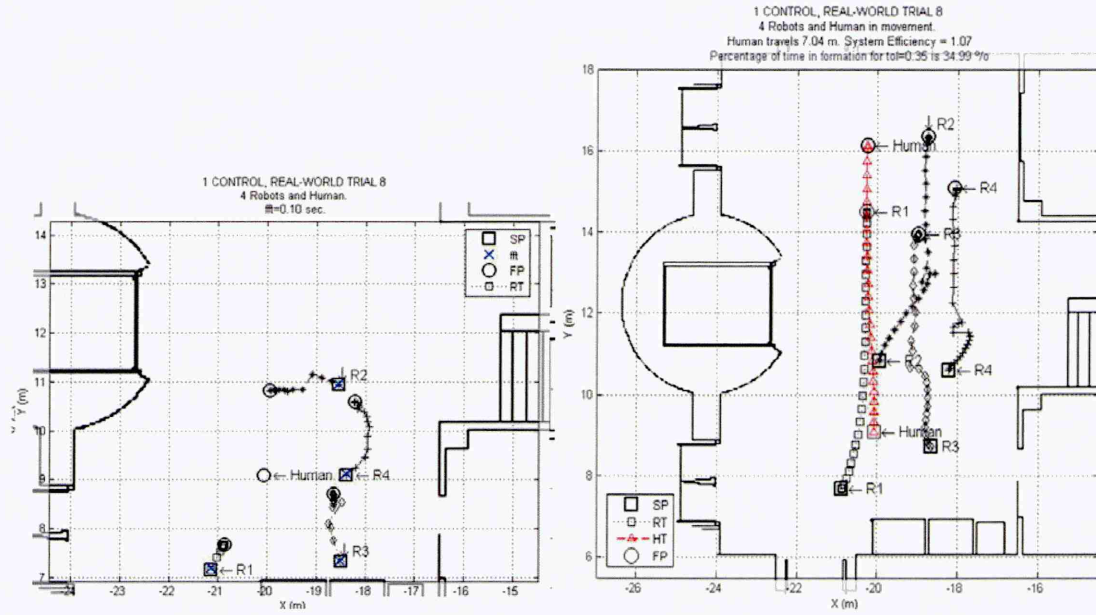


Figure B.18: Trial 8 of the FCI in real-world.

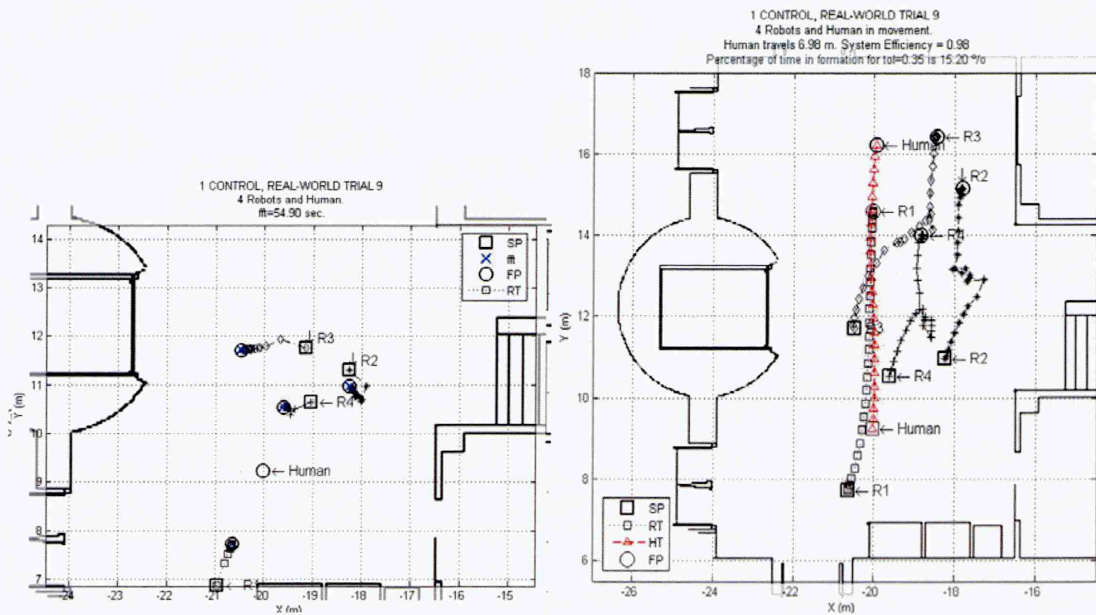


Figure B.19: Trial 9 of the FCI in real-world.

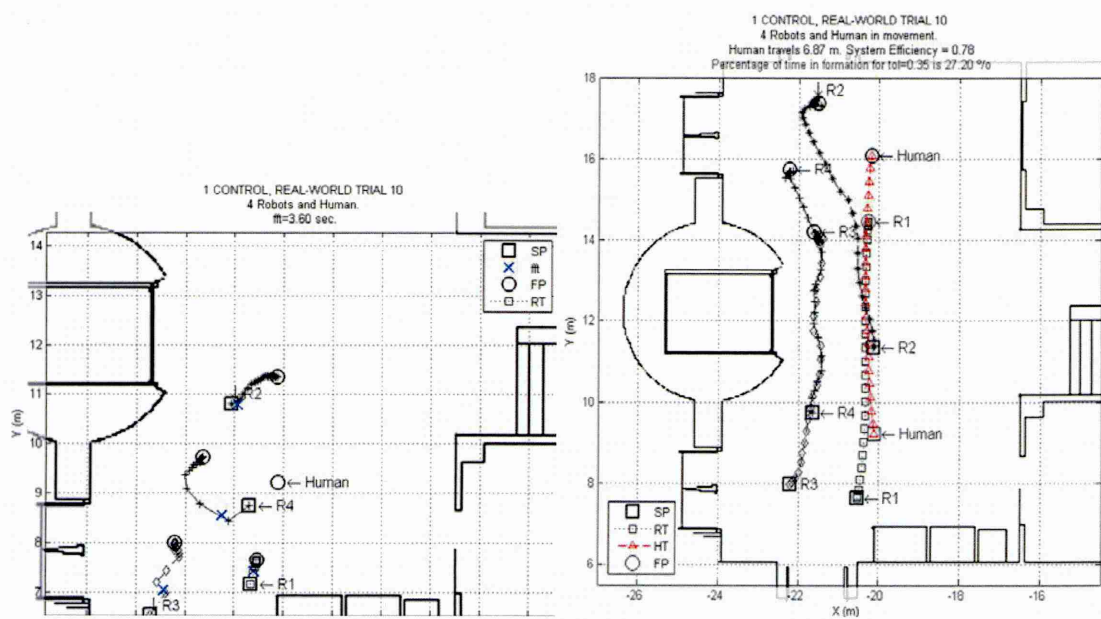


Figure B.20: Trial 10 of the FCI in real-world.

Appendix C

Figure trials for FCII

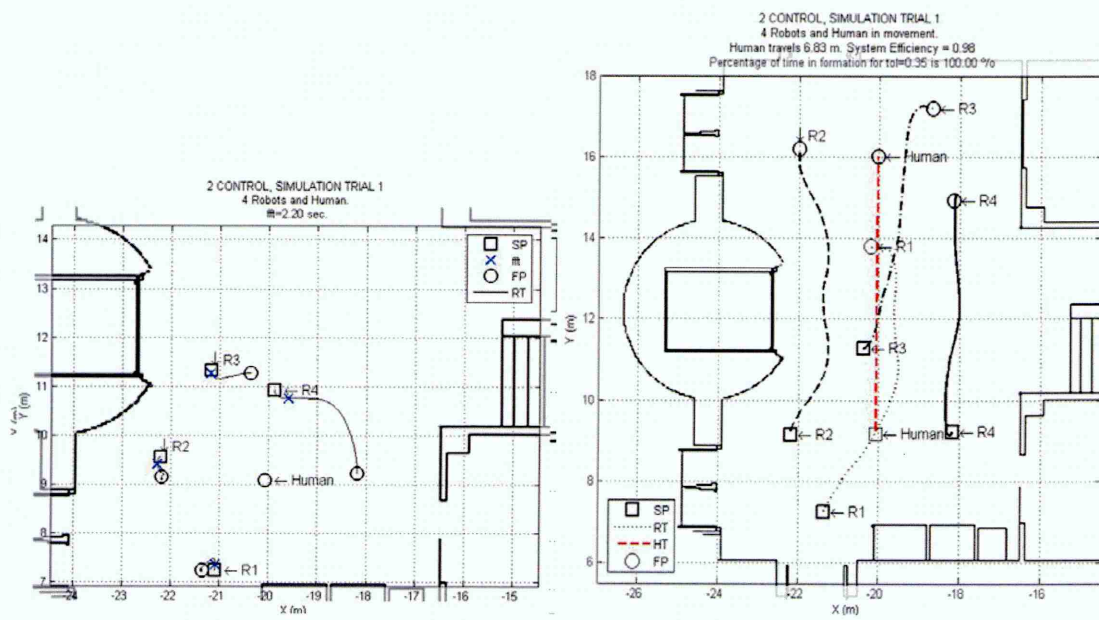


Figure C.1: Trial 1 of the FCII in simulation.

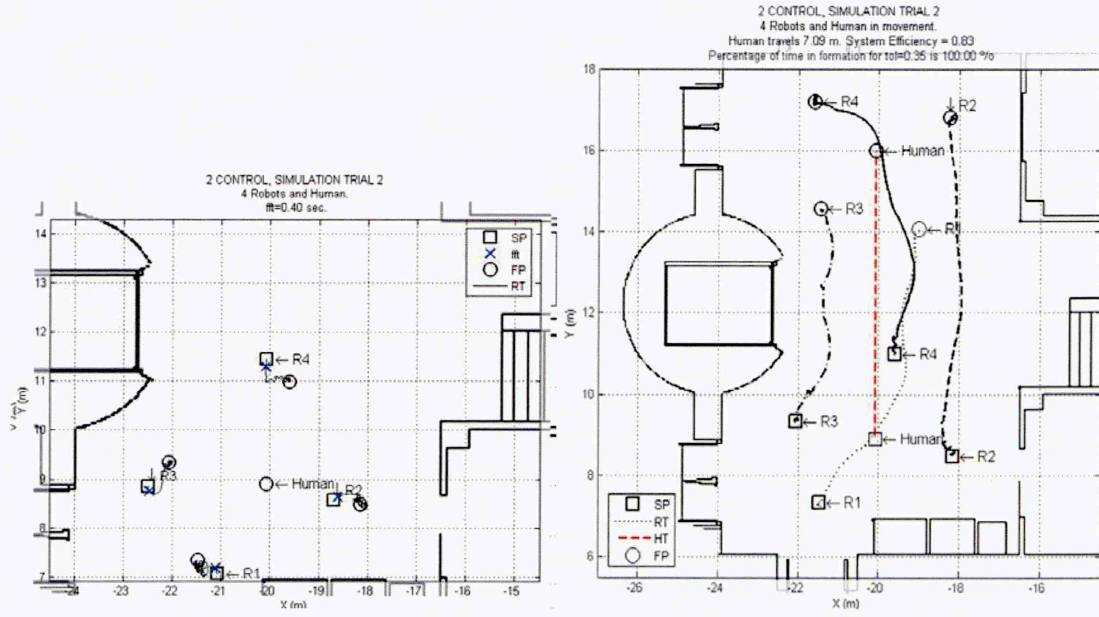


Figure C.2: Trial 2 of the FCII in simulation.

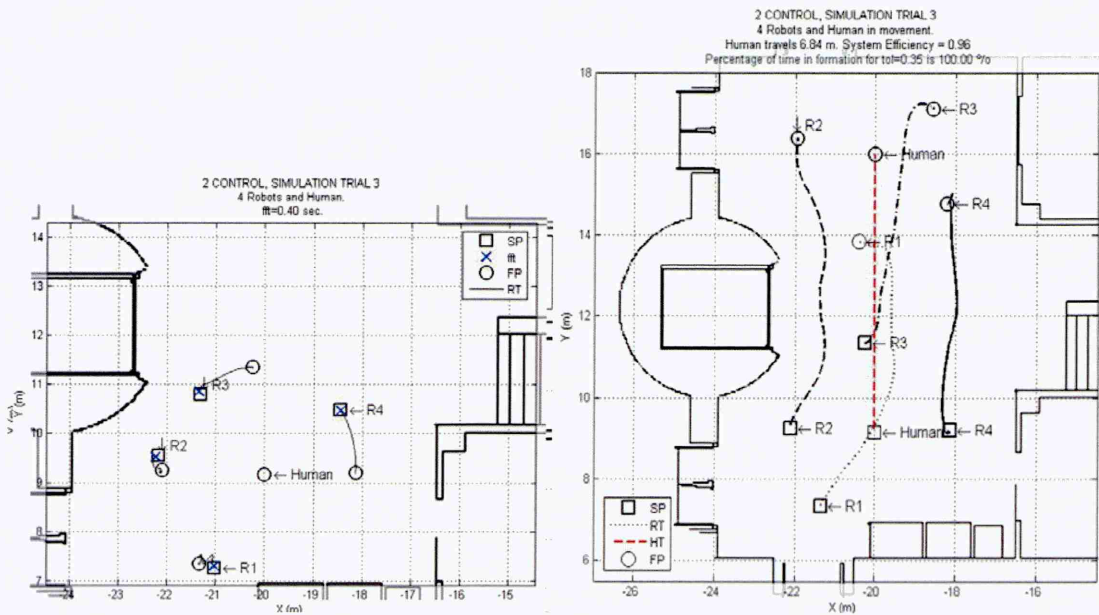


Figure C.3: Trial 3 of the FCII in simulation.

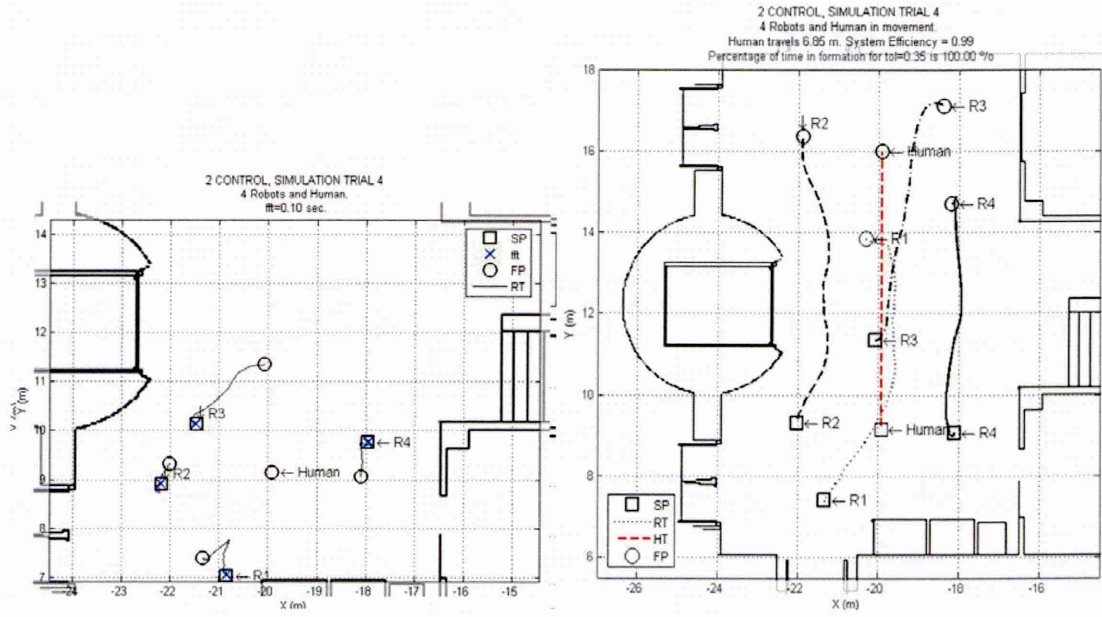


Figure C.4: Trial 4 of the FCII in simulation.

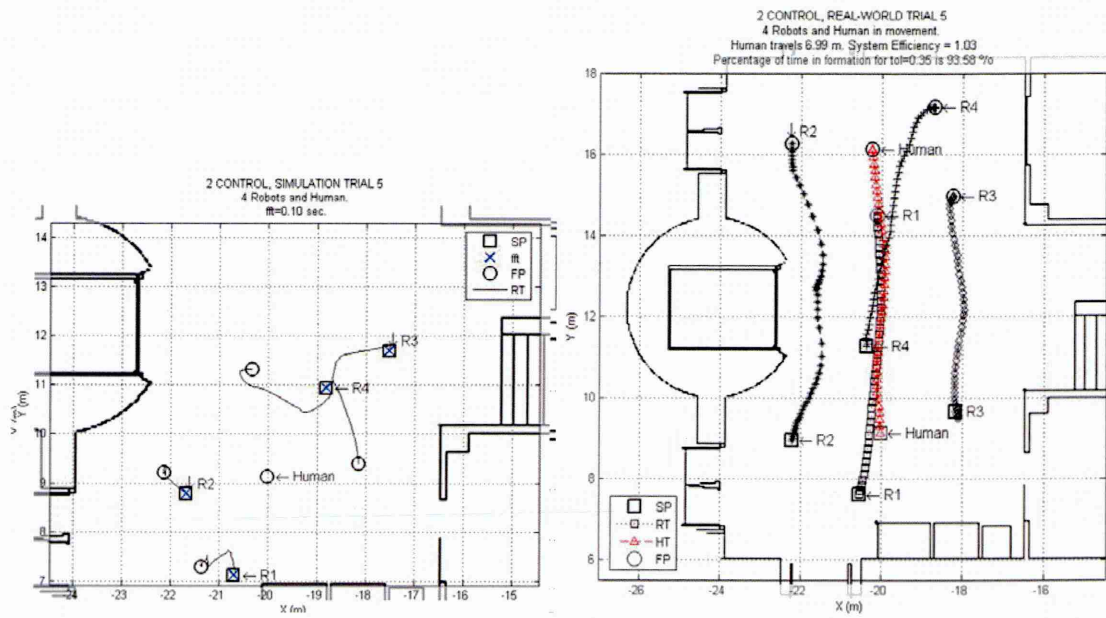


Figure C.5: Trial 5 of the FCII in simulation.

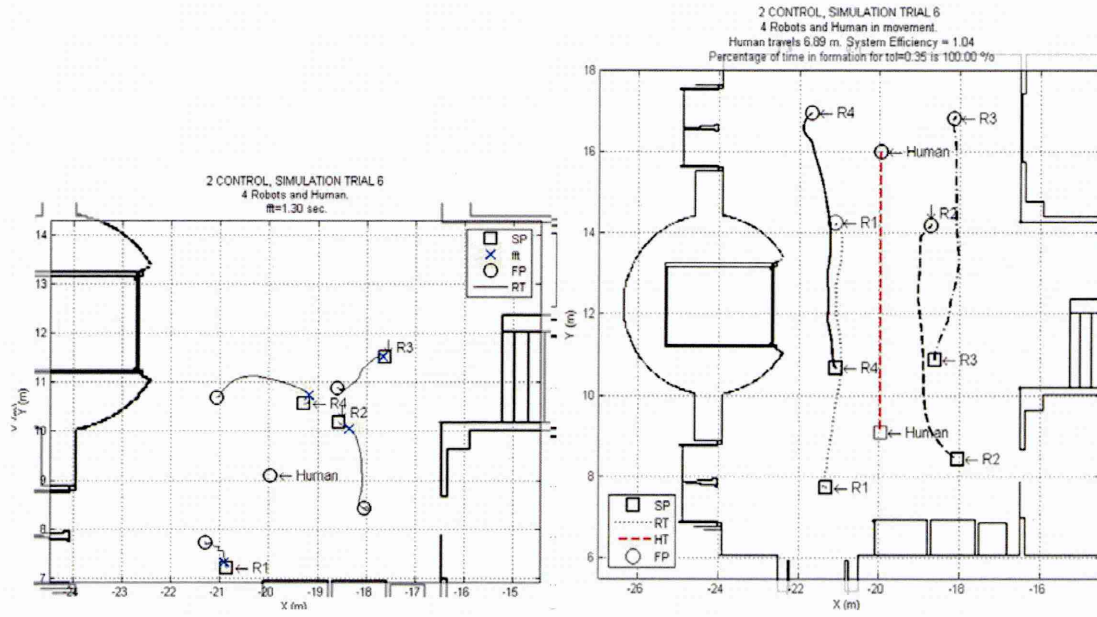


Figure C.6: Trial 6 of the FCII in simulation.

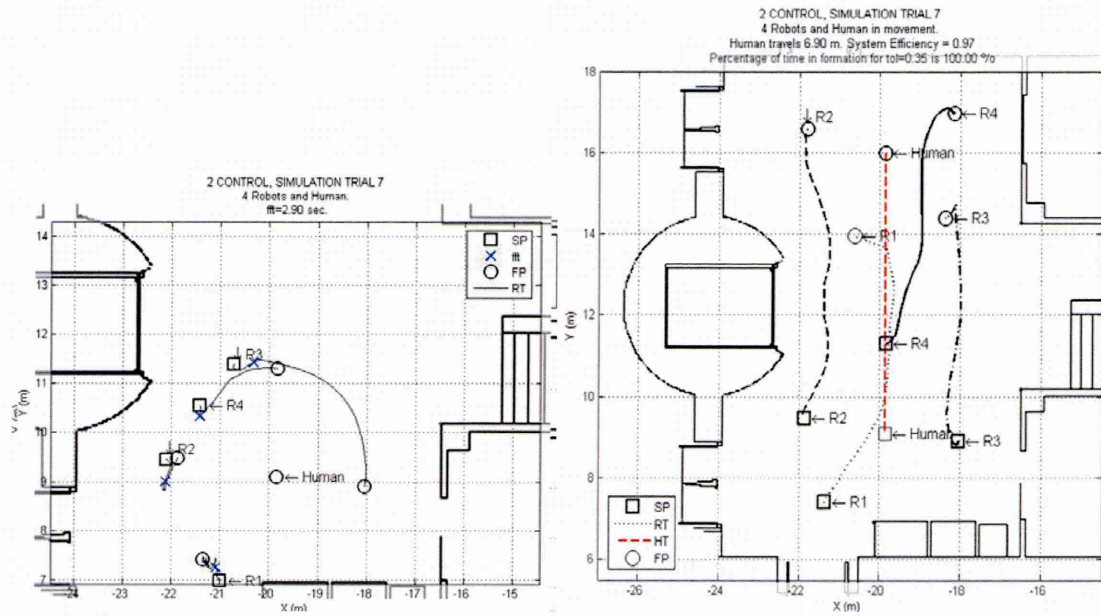


Figure C.7: Trial 7 of the FCII in simulation.

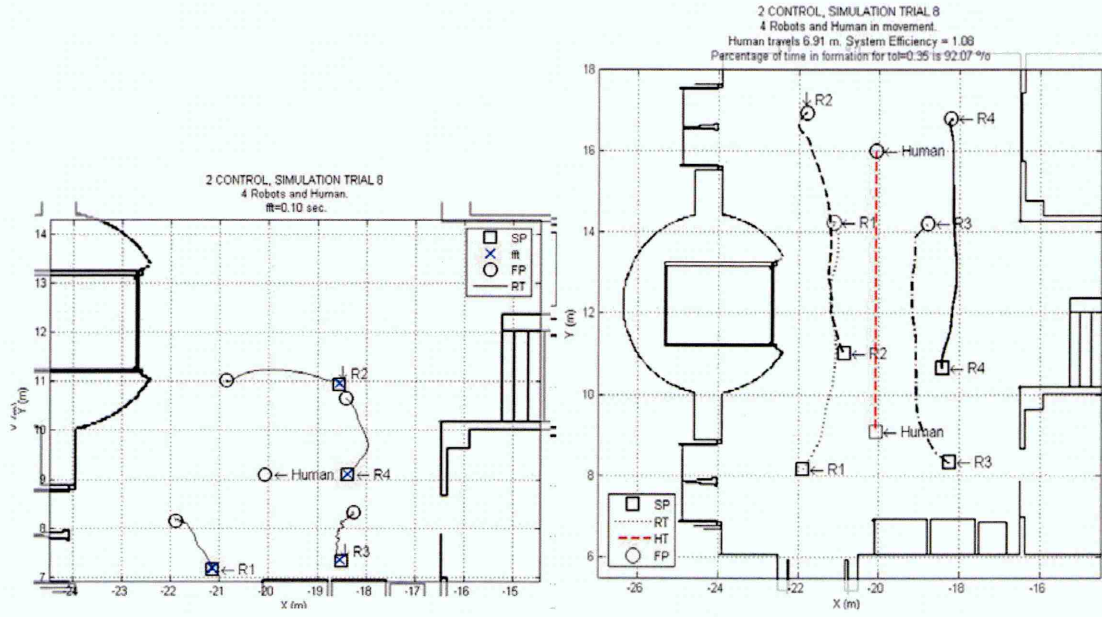


Figure C.8: Trial 8 of the FCII in simulation.

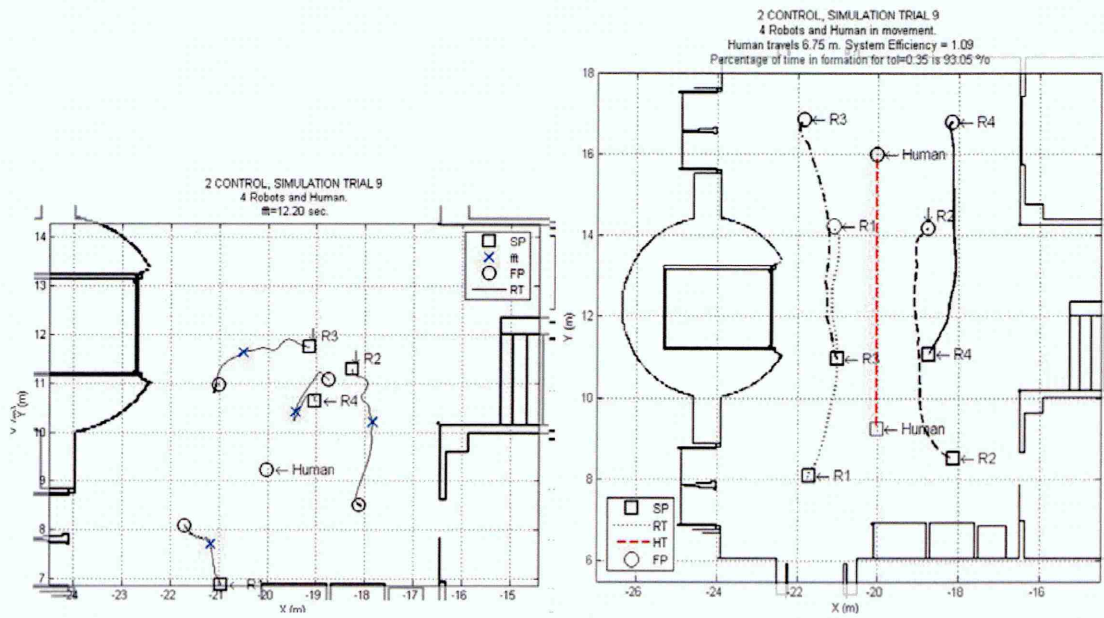


Figure C.9: Trial 9 of the FCII in simulation.

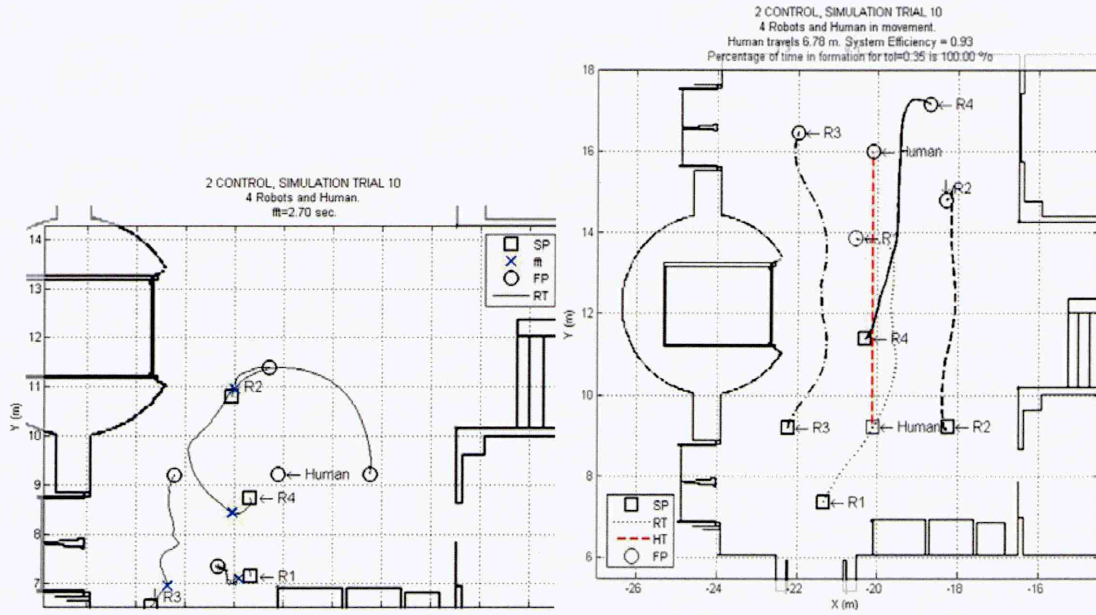


Figure C.10: Trial 10 of the FCII in simulation.

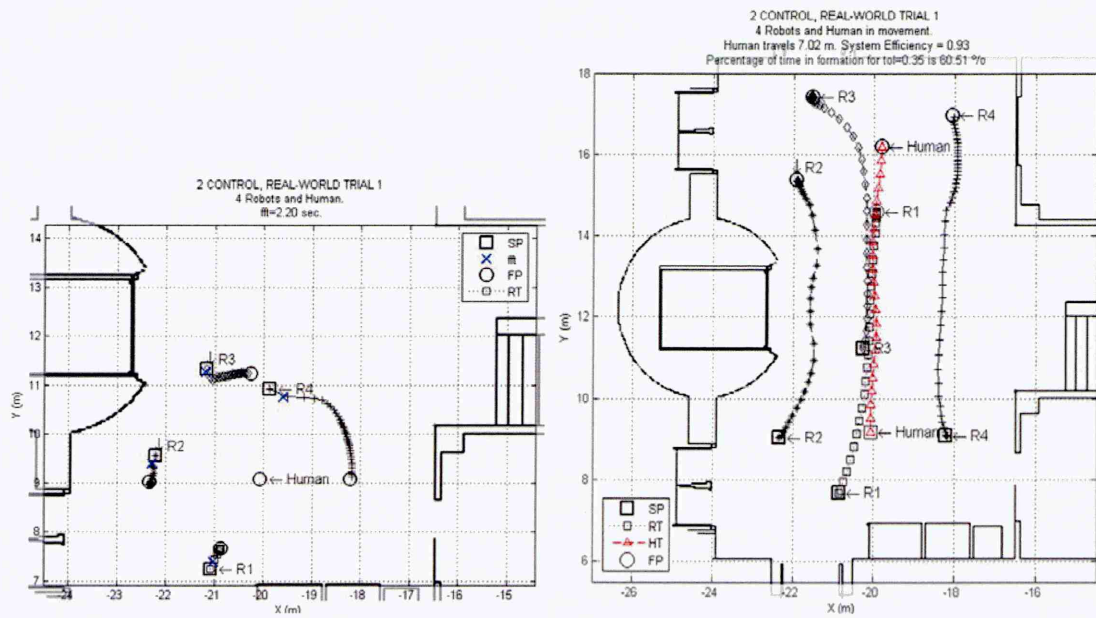


Figure C.11: Trial 1 of the FCII in real-world.

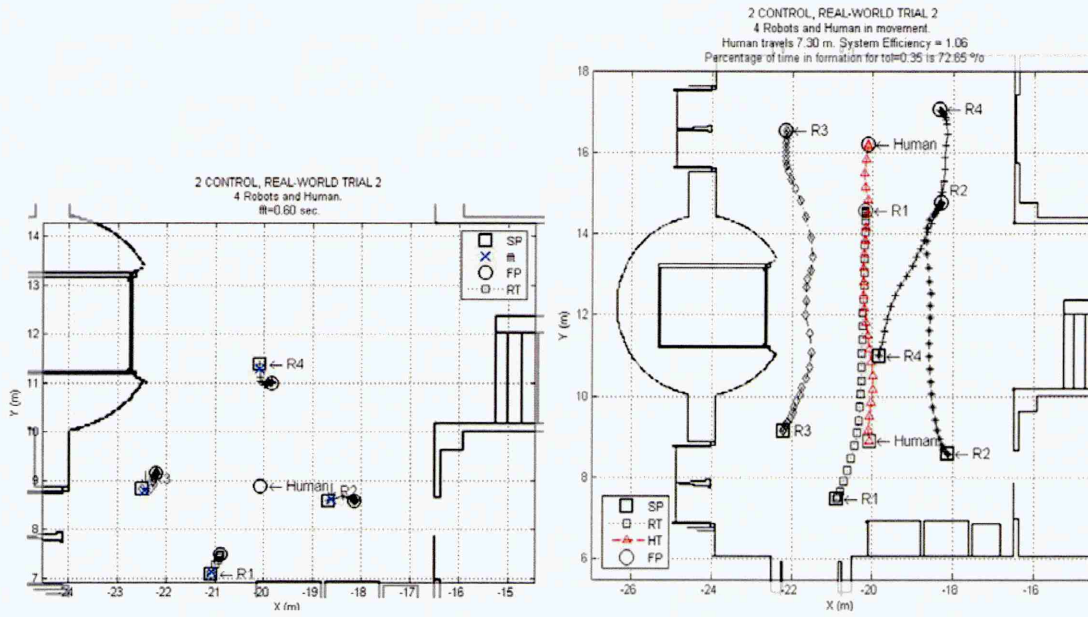


Figure C.12: Trial 2 of the FCII in real-world.

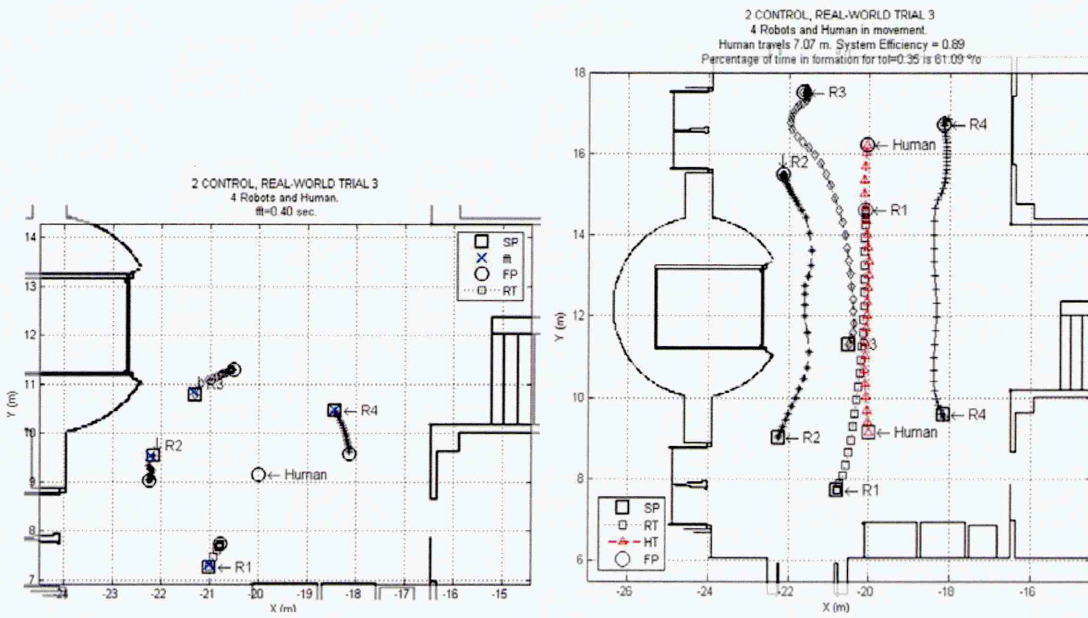


Figure C.13: Trial 3 of the FCII in real-world.

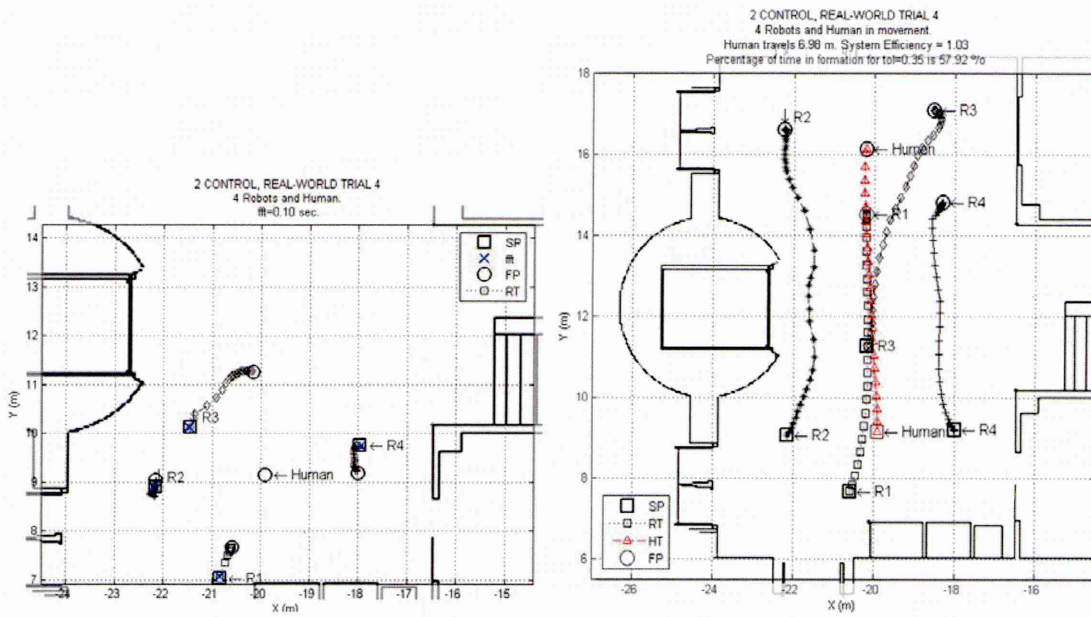


Figure C.14: Trial 4 of the FCII in real-world.

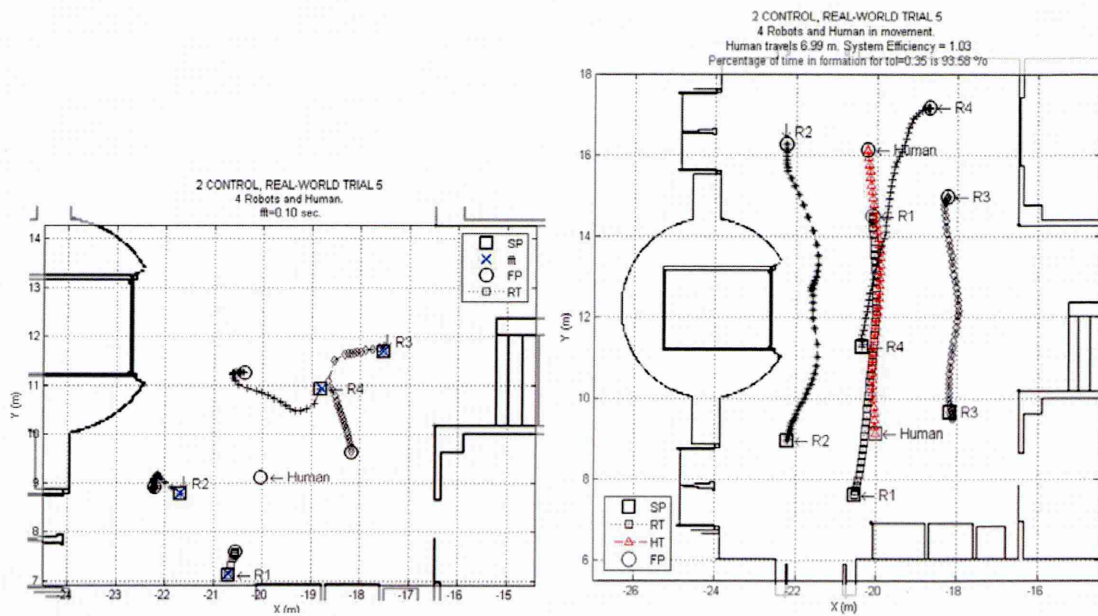


Figure C.15: Trial 5 of the FCII in real-world.

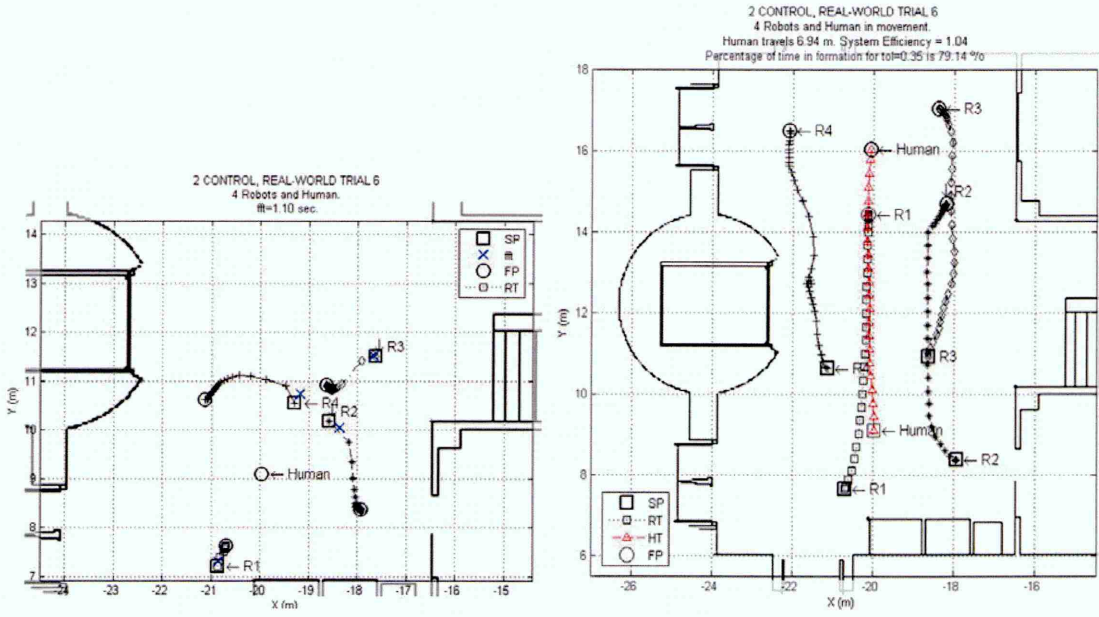


Figure C.16: Trial 6 of the FCII in real-world.

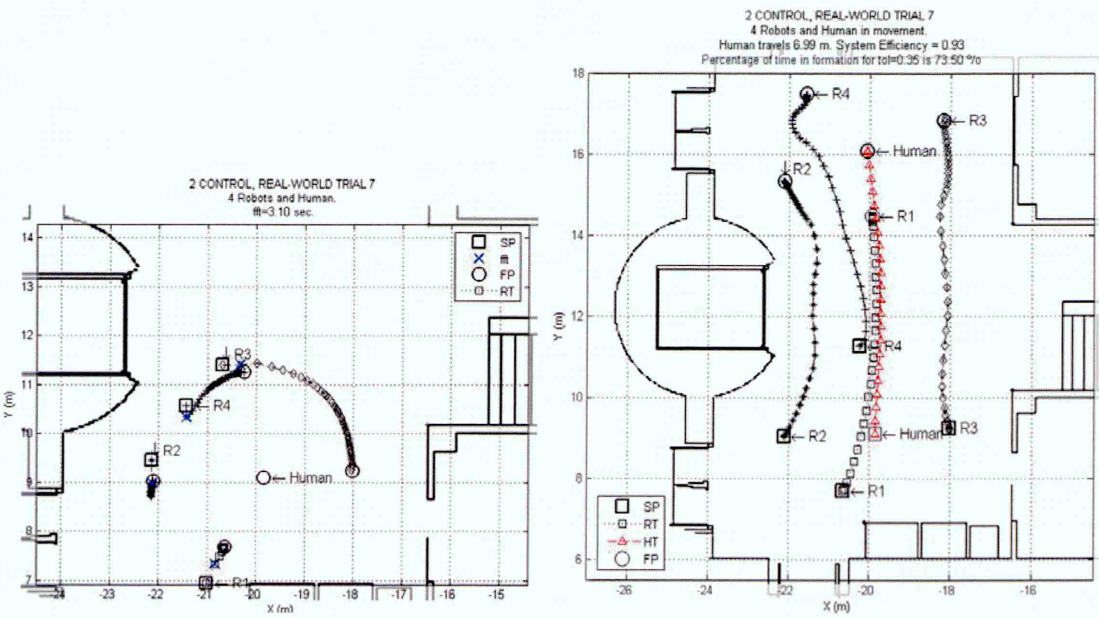


Figure C.17: Trial 7 of the FCII in real-world.

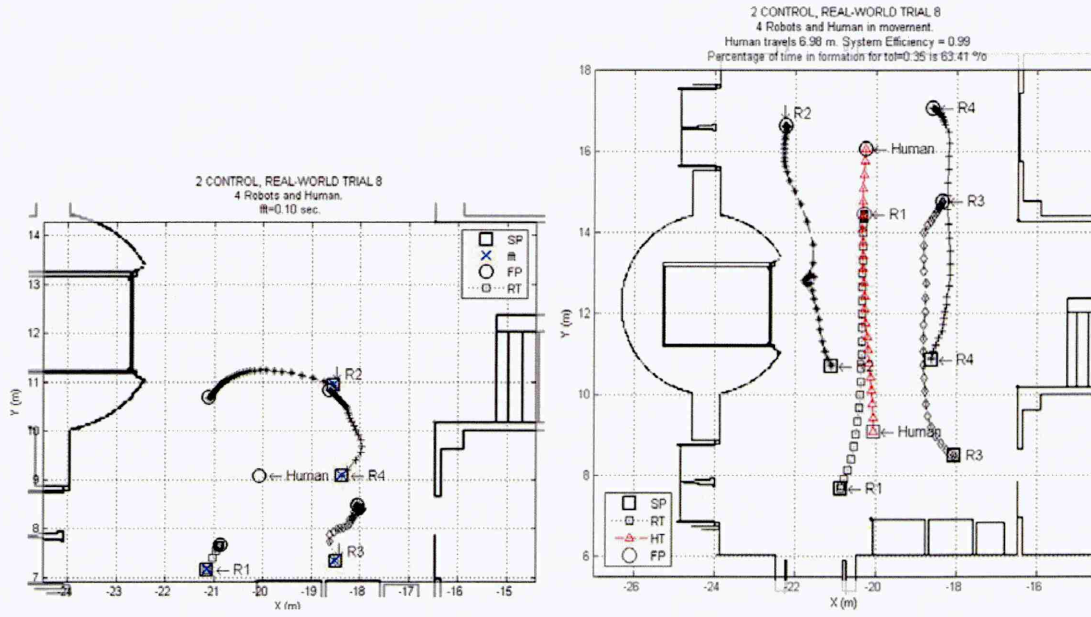


Figure C.18: Trial 8 of the FCII in real-world.

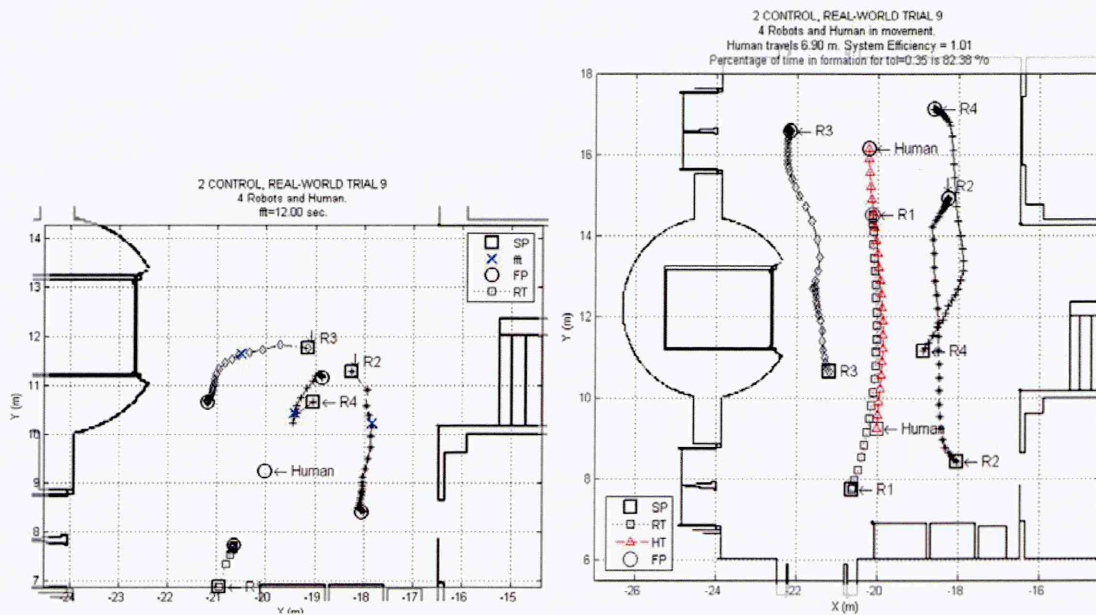


Figure C.19: Trial 9 of the FCII in real-world.

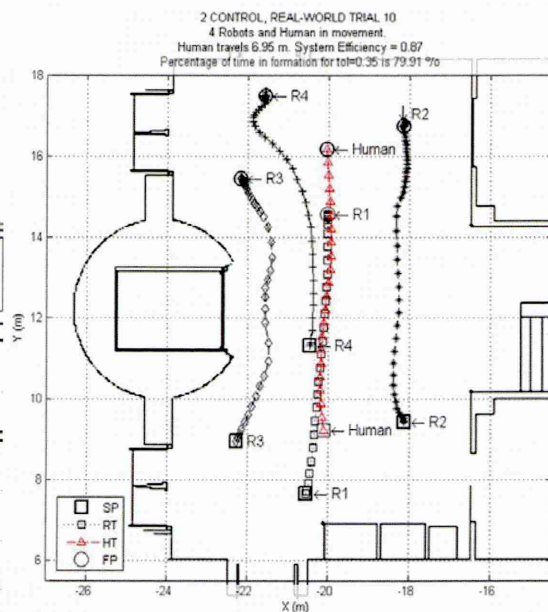
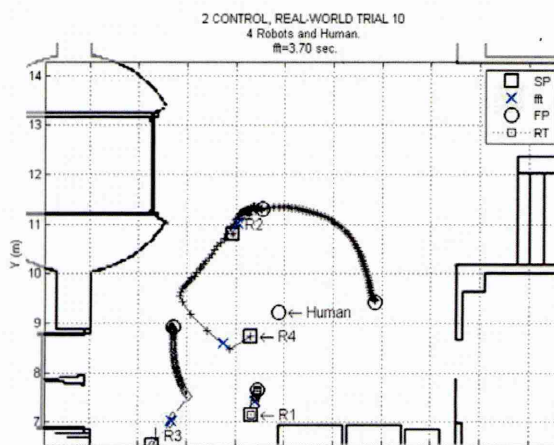


Figure C.20: Trial 10 of the FCII in real-world.

References

- L. Alboul, J. Saez-Pons, and J. Penders. Mixed human-robot team navigation in the guardians project. In *Safety, Security and Rescue Robotics, 2008. SSRR 2008. IEEE Int. Workshop on*, pages 95–101, 2008.
- Lyuba Alboul, Joan Saez-Pons, Jacques Penders, and Leo Nomdedeu. Challenges of the multi-robot team in the guardians project. In *ICIRA '09: Proceedings of the 2nd Int. Conf. on Intelligent Robotics and Applications*, pages 112–125, Berlin, Heidelberg, 2009. Springer-Verlag.
- Lyuba Alboul, Hussein Abdul-Rahman, Paul Haynes, Jacques Penders, and Julien Tharin. Guardians multirobot team as a self-organising system. In *EURON/IARP Int. Workshop on Robotics for Risky Interventions and Surveillance of the Environment (RISE10)*, 2010a.
- Lyuba Alboul, Jacques Penders, and Joan Saez-Pons. Using robots in hazardous environments: Landmine detection, de-mining and other applications. In *Part 5. Multi robotic systems: navigation and cooperation*, 2010b.
- Rajeev Alur, R. Alur, A. Das, J. Esposito, R. Fierro, G. Grudic, Y. Hur, V. Kumar, I. Lee, G. Pappas, J. Ostrowski, B. Southall, J. Spletzer, and C. J. Taylor. A framework and architecture for multirobot coordination. In *Experimental Robotics VII, LNCIS 271*, pages 289–299, 2000.
- G. Antonelli, F. Arrichiello, and S. Chiaverini. The null-space-based behavioural control for autonomous robotic systems. *Intelligent Service Robotics*, 1(1):27–39, 2008.
- R. Arkin. Motor schema based navigation for a mobile robot: An approach to programming by behaviour. In *Robotics and Automation. Proceedings. 1987 IEEE Int. Conf. on*, volume 4, pages 264–271, 1987.
- H. Axelsson, M. Egerstedt, and Y. Wardi. Optimal switching surfaces in behaviour-based robotics. *Decision and Control, 2006 45th IEEE Conf. on*, page 1959, 2006.
- T. Balch and R. C. Arkin. behaviour-based formation control for multirobot teams. *Robotics and Automation, IEEE Trans. on*, 14(6):926–939, 1998.

- T. Balch and M. Hybinette. Social potentials for scalable multi-robot formations. *Robotics and Automation, 2000. Proceedings. ICRA '00. IEEE Int. Conf. on*, 1:73–80, 2000.
- T. D. Barfoot and C. M. Clark. Motion planning for formations of mobile robots. *Robotics and Autonomous Systems*, 46(2):65–78, 2/29 2004.
- D.P. Barnes and J.O. Gray. Behaviour synthesis for co-operant mobile robot control. In *Control 1991. Control '91., Int. Conf. on*, pages 1135–1140 vol.2, Mar 1991.
- R.W. Beard, J. Lawton, and F.Y. Hadaegh. A coordination architecture for spacecraft formation control. *Control Systems Technology, IEEE Trans. on*, 9(6):777–790, nov 2001.
- R.W. Beard, T.W. McLain, D.B. Nelson, D. Kingston, and D. Johanson. Decentralized cooperative aerial surveillance using fixed-wing miniature uavs. *Proceedings of the IEEE*, 94(7):1306–1324, July 2006.
- Y. Ben-Asher, S. Feldman, P. Gurfil, and M. Feldman. Distributed Decision and Control for Cooperative UAVs Using; emphasis; Ad Hoc;/emphasis; Communication. *Control Systems Technology, IEEE Trans. on*, 16(3):511–516, 2008. ISSN 1063-6536.
- E. Bicho and S. Monteiro. Formation control for multiple mobile robots: a non-linear attractor dynamics approach. In *Intelligent Robots and Systems, 2003. (IROS 2003). Proceedings. 2003 IEEE/RSJ Int. Conf. on*, volume 2, pages 2016–2022, 27-31 2003.
- J. Borenstein and Y. Koren. Real-time obstacle avoidance for fast mobile robots in cluttered environments. In *Robotics and Automation, 1990. Proceedings., 1990 IEEE Int. Conf. on*, volume 1, pages 572–577, 13-18 1990.
- R. Brooks. A robust layered control system for a mobile robot. *Robotics and Automation, IEEE Journal of*, 2; 2(1):14–23, 1986.
- D. Bruemmer, D. Dudenhoeffer, and M. McKay. A robotic swarm for spill finding and perimeter formation. In *Spectrum*, August 2002.
- Wolfram Burgard, Mark Moors, Cyrill Stachniss, and Frank Schneider. Coordinated multi-robot exploration. *IEEE Trans. on Robotics*, 21:376–386, 2005.
- Y. U. Cao, A. S. Fukunaga, A. B. Kahng, and F. Meng. Cooperative mobile robotics: antecedents and directions, 1995.
- Y. Uny Cao, Alex S. Fukunaga, and A. B. Kahng. Cooperative mobile robotics: Antecedents and directions. *Autonomous Robots*, 4:226–234, 1997.

- S. Carpin and L.E. Parker. Cooperative leader following in a distributed multi-robot system. In *Robotics and Automation, 2002. Proceedings. ICRA '02. IEEE Int. Conf. on*, volume 3, pages 2994–3001, 2002.
- A. Cezayirli and F. Kerestecioglu. Navigation of autonomous mobile robots in connected groups. *Communications, Control and Signal Processing, 2008. ISCCSP 2008. 3rd Int. Symposium on*, pages 162–167, 2008.
- L. Chaimowicz, B. Grocholsky, J.F. Keller, Vijay Kumar, and C.J. Taylor. Experiments in multi-robot air-ground coordination. In *Robotics and Automation, 2004. Proceedings. ICRA '04. 2004 IEEE Int. Conf. on*, volume 4, pages 4053–4058, 26-May 1, 2004.
- Qin Chen and J.Y.S. Luh. Coordination and control of a group of small mobile robots. In *Robotics and Automation, 1994. Proceedings., 1994 IEEE Int. Conf. on*, volume 3, pages 2315–2320, 8-13 1994.
- Xin Chen and Yangmin Li. Smooth formation navigation of multiple mobile robots for avoiding moving obstacles. *Int. Journal of Control, Automation, and Systems*, 4(4):466–473, August 2006. *Int. Journal of Control, Automation, and Systems*, vol. 4, no. 4, pp. 466-479, August 2006.
- A. Das, J. Spletzer, V. Kumar, and C. Taylor. Ad hoc networks for localization and control. In *Decision and Control, 2002, Proceedings of the 41st IEEE Conf. on*, volume 3, pages 2978–2983, 10-13 2002a.
- A.K. Das, R. Fierro, V. Kumar, J.P. Ostrowski, J. Spletzer, and C.J. Taylor. A vision-based formation control framework. *Robotics and Automation, IEEE Trans. on*, 18(5):813–825, oct 2002b. ISSN 1042-296X. doi: 10.1109/TRA.2002.803463.
- J. P. Desai, J. Ostrowski, and V. Kumar. Controlling formations of multiple mobile robots. *Robotics and Automation, 1998. Proceedings. 1998 IEEE Int. Conf. on*, 4:2864–2869, 1998.
- J. P. Desai, J. P. Ostrowski, and V. Kumar. Modeling and control of formations of nonholonomic mobile robots. *Robotics and Automation, IEEE Trans. on*, 17(6):905–908, 2001.
- G. Dudek, M. R. M. Jenkin, E. Milios, and D. Wilkes. A taxonomy for multi-agent robotics. *Autonomous Robots*, 3(4):375–397, 1996.
- A. Farinelli, L. Iocchi, and D. Nardi. Multirobot systems: a classification focused on coordination. *Systems, Man, and Cybernetics, Part B: Cybernetics, IEEE Trans. on*, 34(5):2015–2028, 2004.
- R. Fierro, A. K. Das, V. Kumar, and J. P. Ostrowski. Hybrid control of formations of robots. *Robotics and Automation, 2001. Proceedings 2001 ICRA. IEEE Int. Conf. on*, 1:157–162, 2001.

- E. Fiorelli, N. E. Leonard, P. Bhatta, D. Paley, R. Bachmayer, and D. M. Fratantoni. Multi-
auv control and adaptive sampling in monterey bay. *Autonomous Underwater Vehicles, 2004
IEEE/OES*, pages 134–147, 2004.
- Dieter Fox. Kld-sampling: Adaptive particle filters. In *In Advances in Neural Information Pro-
cessing Systems 14*, pages 713–720. MIT Press, 2001.
- Antonio Franchi, Giuseppe Oriolo, and Paolo Stegagno. Mutual localization in a multi-robot
system with anonymous relative position measures. In *IROS'09: Proceedings of the 2009
IEEE/RSJ Int. Conf. on Intelligent robots and systems*, pages 3974–3980, Piscataway, NJ, USA,
2009. IEEE Press.
- J. Fredslund and M. J. Mataric. A general algorithm for robot formations using local sensing and
minimal communication. *Robotics and Automation, IEEE Trans. on*, 18(5):837–846, 2002.
- Douglas W. Gage. Sensor abstractions to support many-robot systems. In *Proceedings of SPIE
Mobile Robots VII*, pages 235–246, 1992.
- V. Gazi and K. M. Passino. A class of attractions/repulsion functions for stable swarm aggrega-
tions. *Int. J. Control*, 77(18):1567–1579, 2004.
- S.S. Ge and C.-H. Fua. Queues and artificial potential trenches for multirobot formations.
Robotics, IEEE Trans. on, 21(4):646–656, aug. 2005. ISSN 1552-3098. doi: 10.1109/TRO.
2005.847617.
- B.P. Gerkey and M.J. Mataric. Sold!: auction methods for multirobot coordination. *Robotics and
Automation, IEEE Trans. on*, 18(5):758–768, 2002.
- Brian Gerkey, Richard T. Vaughan, and Andrew Howard. The player/stage project: Tools for
multi-robot and distributed sensor systems. In *Proceedings of the 11th Int. Conf. on Advanced
Robotics (ICAR'03)*, pages 317–323, 2003.
- Brian P. Gerkey and M. J. Mataric. A formal framework for the study of task allocation in multi-
robot systems. *Intl. J. of Robotics Research*, July 2003.
- Vincenzo Gervasi and Giuseppe Prencipe. Coordination without communication: the case of the
flocking problem. *Discrete Applied Mathematics*, 144(3):324–344, 12/15 2004.
- P. Gurfil and E. Kivelevitch. Flock properties effect on task assignment and formation flying of
cooperating unmanned aerial vehicles. *Proceedings of the Institution of Mechanical Engineers,
Part G: Journal of Aerospace Engineering*, 221(3):401–416, 01/01 2007.

- M. Yamashita H. Ando, I. Suzuki. Formation and agreement problems for synchronous mobile robots with limited visibility. In *IEEE Symp. of Intelligent Control*, pages 453–460, 1995.
- H. Hashimoto, S. Aso, S. Yokota, A. Sasaki, Y. Ohyama, and H. Kobayashi. Cooperative movement of human and swarm robot maintaining stability of swarm. *Robot and Human Interactive Communication, 2008. RO-MAN 2008. IEEE Int. Symposium on*, pages 249–254, 2008.
- O. Holland and C. Melhuish. Stigmergy, self-organization, and sorting in collective robotics. *Artificial Life*, 5:173–202, April 1999.
- Andrew Howard, Maja J. Mataric, and Gaurav S. Sukhatme. Mobile sensor network deployment using potential fields: A distributed, scalable solution to the area coverage problem. In *Distrib. Auton. Robot Syst.*, pages 299–308, 2002.
- Andrew Howard, Lynne E. Parker, and Gaurav S. Sukhatme. Experiments with a large heterogeneous mobile robot team: Exploration, mapping, deployment and detection. *Int.J.Rob.Res.*, 25 (5-6):431–447, 2006.
- Harry Chia-Hung Hsu and Alan Liu. Multiagent-based multi-team formation control for mobile robots. *Journal of Intelligent and Robotic Systems*, 42(4):337–360, 04/01 2005.
- I.-A.F. Ihle, R. Skjetne, and T.I. Fossen. Nonlinear formation control of marine craft with experimental results. In *Decision and Control, 2004. CDC. 43rd IEEE Conf. on*, volume 1, pages 680–685, Dec. 2004.
- A.J. Ijspeert, A. Martinoli, A. Billard, and L. M. Gambardella. Collaboration through the Exploitation of Local Interactions in Autonomous Collective Robotics: The Stick Pulling Experiment. *Autonomous Robots*, 11(2):149–171, 2001.
- O. Khatib. Real-time obstacle avoidance for manipulators and mobile robots. In *Robotics and Automation. Proceedings. 1985 IEEE Int. Conf. on*, volume 2, pages 500–505, 1985.
- Y. Koren and J. Borenstein. Potential field methods and their inherent limitations for mobile robot navigation. In *IEEE Int. Conf. on Robotics and Automation*, pages 1398–1404, 1991.
- Arvind Krishnamurthy and Robert Preis. Satellite formation, a mobile sensor network in space. *Parallel and Distributed Processing Symposium, Int.*, 13:243a, 2005.
- B.H. Krogh. A generalized potential field approach to obstacle avoidance control. In *Int. Robotics Research Conf.*, 1984.
- C. Ronald Kube and Hong Zhang. Collective robotic intelligence. In *Second Int. Conf. on Simulation of Adaptive behaviour*, pages 460–468, 1992.

- T. Laue and T. Rofer. A behaviour architecture for autonomous mobile robots based on potential fields. In *In 8th Int. Workshop on RoboCup 2004 (Robot World Cup Soccer Games and Conf.s), Lecture Notes in Artificial Intelligence, Lecture Notes in Computer Science*, pages 122–133. Springer, 2004.
- J. R. T. Lawton, R. W. Beard, and B. J. Young. A decentralized approach to formation maneuvers. *Robotics and Automation, IEEE Trans. on*, 19(6):933–941, 2003.
- Geunho Lee and Nak Young Chong. Decentralized formation control for a team of anonymous mobile robots. *The 6th Asian Control*, July 2006.
- Geunho Lee and Nak Young Chong. Self-configurable mobile robot swarms with hole repair capability. *Intelligent Robots and Systems, 2008. IROS 2008. IEEE/RSJ Int. Conf. on*, pages 1403–1408, 2008.
- Justin Lee, Svetha Venkatesh, and Mohan Kumar. Formation of a geometric pattern with a mobile wireless sensor network. *Journal of Robotic System*, 21(10):517–530, March 2004.
- M. Lemay, F. Michaud, D. Letourneau, and J. M Valin. Autonomous initialization of robot formations. *Robotics and Automation, 2004. Proceedings. ICRA '04. 2004 IEEE Int. Conf. on*, 3: 3018–3023, 2004.
- N. E. Leonard and E. Fiorelli. Virtual leaders, artificial potentials and coordinated control of groups. *Decision and Control, 2001. Proceedings of the 40th IEEE Conf. on*, 3:2968–2973, 2001.
- M. Anthony Lewis and Kar-Han Tan. High precision formation control of mobile robots using virtual structures. *Auton. Robots*, 4(4):387–403, 1997.
- Yangmin Li and Xin Chen. Leader-formation navigation with sensor constraints. *Information Acquisition, 2005 IEEE Int. Conf. on*, page 6 pp., 2005.
- Zhiyun Lin, Mireille Broucke, and Bruce Francis. Local control strategies for groups of mobile autonomous agents. *IEEE Trans. on Automatic Control*, 49:622–629, 2004.
- Y. Liu and K. M. Passino. Cohesive behaviours of multiagent systems with information flow constraints. *Automatic Control, IEEE Trans. on*, 51(11):1734–1748, 2006.
- T. Lochmatter, P. Roudit, C. Cianci, N. Correll, J. Jacot, and A. Martinoli. SwisTrack - A Flexible Open Source Tracking Software for Multi-Agent Systems. In *Proceedings of the IEEE/RSJ 2008 International Conference on Intelligent Robots and Systems (IROS 2008)*, pages 4004–4010. IEEE, 2008.

- Chou-Yaun Mai and Feng-Li Lian. Analysis of formation control and communication pattern in multi-robot systems. *SICE-ICASE, 2006. Int. Joint Conf.*, pages 640–645, 2006.
- M. Mataric. behaviour-based control: Examples from navigation, learning, and group behaviour, 1997.
- M. J. Mataric, M. Nilsson, and K. T. Simsarin. Cooperative multi-robot box-pushing. *Intelligent Robots and Systems 95. 'Human Robot Interaction and Cooperative Robots', Proceedings. 1995 IEEE/RSJ Int. Conf. on*, 3; 3:556–561, 1995.
- Maja J Mataric. Issues and approaches in design of collective autonomous agents. *Robotics and Autonomous Systems*, 16:321–331, 1994.
- P. Maxim, S. Hettiarachchi, William Spears, Diana F. Spears, Jerry C. Hamann, T. Kunkel, and C. Speiser. Trilateration localization for multi-robot teams. *Int. Conf. on Informatics in Control, Automation and Robotics*, 2008.
- S. Monteiro, M. Vaz, and E. Bicho. Attractor dynamics generates robot formation: from theory to implementation. In *Robotics and Automation, 2004. Proceedings. ICRA '04. 2004 IEEE Int. Conf. on*, volume 3, pages 2582–2586, 26 2004.
- A. Muhammad and M. Egerstedt. Topology and complexity of formations. In *Proceedings of the 2nd Int. Workshop on the Mathematics and Algorithms of Social Insects*, pages 107–114, 2003.
- Abubakr Muhammad and Magnus Egerstedt. Connectivity graphs as models of local interactions. *Applied Mathematics and Computation*, 168(1):243–269, 2005.
- D.J. Naffin and G.S. Sukhatme. Negotiated formations. *Intelligent Autonomous Systems 8*, pages 181–190, 2004.
- D.J. Naffin, M. Akar, and G.S. Sukhatme. Lateral and longitudinal stability for decentralized formation control. *Distributed Autonomous Robotic Systems 6*, pages 443–452, 2007.
- A. Naghsh, J. Saez-Pons, J. Penders, J. Gancet, E. Motard, L. Nomdedeu, J. Sales, E. Cervera, R. Marin, P. Sanz, and R. Sebastia. Remote and in-situ multirobot interaction for firefighters interventions under smoke condition. In *Telematics Applications (TA 2010). Second IFAC Symposium on*, 2010.
- L. Nomdedeu, J. Sales, E. Cervera, J. Alemany, R. Sebastia, J. Penders, and V. Gazi. An experiment on squad navigation of human and robots. In *Control, Automation, Robotics and Vision, 2008. ICARCV 2008. 10th Int. Conf. on*, pages 1212–1218, 2008.

- P. Ogren, E. Fiorelli, and N. E. Leonard. Cooperative control of mobile sensor networks: adaptive gradient climbing in a distributed environment. *Automatic Control, IEEE Trans. on*, 49(8): 1292–1302, 2004.
- Reza Olfati-Saber and Richard M. Murray. Distributed cooperative control of multiple vehicle formations using structural potential functions. In *in IFAC World Congress*, 2002.
- L. E. Parker. Current research in multirobot systems. *Journal of Artificial Life And Robotics*, 7 (1/2):1–5, 2003.
- L. E. Parker, B. Kannan, Xiaoquan Fu, and Yifan Tang. Heterogeneous mobile sensor net deployment using robot herding and line-of-sight formations, 2003.
- L. E. Parker, B. Kannan, Fang Tang, and M. Bailey. Tightly-coupled navigation assistance in heterogeneous multi-robot teams, 2004.
- Lynne E. Parker. Current state of the art in distributed autonomous mobile robotics. In *Distributed Autonomous Robotic Systems*, pages 3–12. Springer, 2000.
- J. Penders, L. Alboul, C. Roast, and E. Cervera. Robot swarming in the guardians project. In *In European Conference on Complex Systems*, 6, volume 6, 2007.
- Jacques Penders, Lyuba Alboul, Ulf Witkowski, Amir Naghsh, Joan Saez-Pons, Stefan Herbrechtsmeier, and Mohamed El Habbal. A robot swarm assisting a human fire-fighter. *Advanced Robotics*, 25(1-2):93–117, 2011.
- J.-B. Pomet, B. Thuilot, G. Bastin, and G. Campion. A hybrid strategy for the feedback stabilization of nonholonomic mobile robots. In *Robotics and Automation, 1992. Proceedings., 1992 IEEE Int. Conf. on*, volume 1, pages 129–134, May 1992.
- D.O. Popa, H.E. Stephanou, C. Helm, and A.C. Sanderson. Robotic deployment of sensor networks using potential fields. In *Robotics and Automation, 2004. Proceedings. ICRA '04. 2004 IEEE Int. Conf. on*, volume 1, pages 642–647, 26 2004.
- Manuel Espinosa Prieto. Multi robot 2d tracking by image color. Master’s thesis, Sheffield Hallam University, UK, 2009.
- John H. Reif and H. Wang. Social potential fields: A distributed behavioural control for autonomous robots. *Robotics and Autonomous Systems*, 27:171–194, 1999.
- I.M. Rekleitis, G. Dudek, and E.E. Milios. Multi-robot collaboration for robust exploration. In *Robotics and Automation, 2000. Proceedings. ICRA '00. IEEE Int. Conf. on*, volume 4, pages 3164–3169 vol.4, 2000.

- Craig W. Reynolds. Flocks, herds, and schools: A distributed behavioural model. *Computer Graphics*, 1987.
- E. Large S. Goldenstein and D. Metaxas. Non-linear dynamical system approach to behaviour modeling. *The Visual Computer*, 15(7):349–364, 1999.
- J. Saez-Pons, L. Alboul, J. Penders, and G. Veysel. Swarming in the guardians project. In *Robotics for Risky Interventions and Surveillance of the Environment (RISE08). EURON/IARP Int. Workshop on*, 2008.
- J. Saez-Pons, L. Alboul, J. Penders, and L. Nomdedeu. Multi-robot team formation control in the guardians project. *Industrial Robot: An Int. Journal*, 37(4):372–383, 2010.
- J. Saez-Pons, L. Alboul, and J. Penders. Experiments in cooperative human multi-robot navigation. *ICRA'11. Proceedings of the IEEE Int. Conf. on Robotics and Automation, 2011.*, 2011a.
- Joan Saez-Pons, Lyuba Alboul, Jacques Penders, and Leo Nomdedeu. Heterogeneous multi-agent system behaviour patterns for robotics applications. In *EURON/IARP Int. Workshop on Robotics for Risky Interventions and Surveillance of the Environment (RISE09)*, 2009.
- Joan Saez-Pons, Amir M. Naghsh, and Leo Nomdedeu. Cooperative navigation and integration of a human into multi-robot system. In *TAROS*, pages 382–383, 2011b.
- Jorge Sales, Ral Marn, Enric Cervera, Sergio Rodriguez, and Javier Prez. Multi-sensor person following in low-visibility scenarios. *Sensors*, 10(12):10953–10966, 2010.
- Pedro Santana, Jose Barata, Hildebrando Cruz, O Cruz, Antonio Mestre, Joao Lisboa, and Luis Flores. A multi-robot system for landmine detection. In *in Proceedings of the 10th IEEE Int. Conf. on Emerging Technologies and Factory Automation (ETFA 2005)*, pages 721–728, 2005.
- F.E. Schneider and D. Wildermuth. A potential field based approach to multi robot formation navigation. In *Robotics, Intelligent Systems and Signal Processing, 2003. Proceedings. 2003 IEEE Int. Conf. on*, volume 1, pages 680–685, 8-13 2003.
- D.A. Schoenwald, J.T. Feddema, and F.J. Opperl. Decentralized control of a collective of autonomous robotic vehicles. In *American Control Conf., 2001. Proceedings of the 2001*, volume 3, pages 2087–2092, 2001. doi: 10.1109/ACC.2001.946052.
- Hong Shi, Long Wang, and Tianguang Chu. Virtual leader approach to coordinated control of multiple mobile agents with asymmetric interactions, 2005.
- G.T. Sibley, M.H. Rahimi, and G.S. Sukhatme. Robomote: a tiny mobile robot platform for large-scale ad-hoc sensor networks. In *Robotics and Automation, 2002. Proceedings. ICRA '02. IEEE Int. Conf. on*, volume 2, pages 1143–1148, 2002.

- Peng Song and V. Kumar. A potential field based approach to multi-robot manipulation. In *Robotics and Automation, 2002. Proceedings. ICRA '02. IEEE Int. Conf. on*, volume 2, pages 1217–1222, 2002.
- W. M. Spears, D. F. Spears, R. Heil, W. Kerr, and S. Hettiarachchi. An overview of physicomimetics. In *Lecture Notes in Computer Science State of the Art Series*, 2005.
- D.J. Stilwell and B.E. Bishop. Platoons of underwater vehicles. *Control Systems Magazine, IEEE*, 20(6):45–52, Dec 2000.
- K. Sugihara and I. Suzuki. Distributed motion coordination of multiple mobile robots. In *Intelligent Control, 1990. Proceedings., 5th IEEE Int. Symposium on*, volume 1, pages 138–143, sep 1990.
- K. Sugihara and I. Suzuki. Distributed algorithms for formation of geometric patterns with many mobile robots. *Journal of Robotic Systems*, 13(3):127–139, 1998.
- Jindong Tan and Ning Xi. Integration of sensing, computation, communication and cooperation for distributed mobile sensor networks. In *Robotics, Intelligent Systems and Signal Processing, 2003. Proceedings. 2003 IEEE Int. Conf. on*, volume 1, pages 54–59, 8-13 2003.
- Jindong Tan, Ning Xi, Weihua Sheng, and Jizhong Xiao. Modeling multiple robot systems for area coverage and cooperation. In *Robotics and Automation, 2004. Proceedings. ICRA '04. 2004 IEEE Int. Conf. on*, volume 3, pages 2568 – 2573 Vol.3, 26 2004.
- H.G. Tanner and A. Kumar. Formation stabilization of multiple agents using decentralized navigation functions, 2005.
- H.G. Tanner, G.J. Pappas, and V. Kumar. Leader-to-formation stability. *Robotics and Automation, IEEE Trans. on*, 20(3):443–455, june 2004.
- D. Vail and M. Veloso. Dynamic multi-robot coordination, 2003.
- ZhiDong Wang, E. Nakano, and T. Takahashi. Solving function distribution and behaviour design problem for cooperative object handling by multiple mobile robots. *Systems, Man and Cybernetics, Part A: Systems and Humans, IEEE Trans. on*, 33(5):537–549, Sept. 2003a.
- Zhigang Wang, MengChu Zhou, and N. Ansari. Ad-hoc robot wireless communication. In *Systems, Man and Cybernetics, 2003. IEEE Int. Conf. on*, volume 4, pages 4045–4050, Oct. 2003b.
- Barry Brian Werger and Maja J. Matarić. From insect to internet: Situated control for networked robot teams. *Annals of Mathematics and Artificial Intelligence*, 31(1-4):173–197, 2001.

- R. Wiegand, Mitchell Potter, Donald Sofge, and William Spears. A generalized graph-based method for engineering swarm solutions to multiagent problems. *Parallel Problem Solving from Nature - PPSN IX*, pages 741–750, 2006.
- Alan F. T. Winfield and Julien Nembrini. Safety in numbers: fault-tolerance in robot swarms. *Int. Journal of Modelling, Identification and Control*, 1(1):30–37, jan 2006.
- Li Xiang, M. F. Ercan, Zhou Yi, and Yu Fai Fung. Algorithm for swarm robot flocking behaviour. *Autonomous Robots and Agents, 2009. ICARA 2009. 4th Int. Conf. on*, pages 161–165, 2009.
- S. Yamada and J. Saito. Adaptive action selection without explicit communication for multirobot box-pushing. *Systems, Man, and Cybernetics, Part C: Applications and Reviews, IEEE Transactions on*, 31(3):398–404, Aug 2001.
- D. Zarzhitsky, D.F. Spears, and W.M. Spears. Swarms for chemical plume tracing. In *Swarm Intelligence Symposium, 2005. SIS 2005. Proceedings 2005 IEEE*, pages 249–256, June 2005.